

# **NOAA Atlas NESDIS 3**



## **WORLD OCEAN ATLAS 1994 VOLUME 3: SALINITY**

Washington, D.C.  
April 1994

**U.S. DEPARTMENT OF COMMERCE**  
**National Oceanic and Atmospheric Administration**  
National Environmental Satellite, Data, and Information Service

# **NOAA Atlas NESDIS 3**



## **WORLD OCEAN ATLAS 1994 VOLUME 3: SALINITY**

Sydney Levitus  
Russell Burgett  
Timothy P. Boyer  
National Oceanographic Data Center  
Ocean Climate Laboratory

Washington, D.C.  
April 1994

**U.S. DEPARTMENT OF COMMERCE**  
**Ronald H. Brown, Secretary**

**National Oceanic and Atmospheric Administration**  
**D. James Baker, Under Secretary**

National Environmental Satellite, Data, and Information Service  
Robert S. Winokur, Assistant Administrator

---

For sale by the U.S. Government Printing Office  
Superintendent of Documents, Mail Stop: SSOP, Washington, DC 20402-9328  
ISBN 0-16-043200-6

---

**National Oceanographic Data Center**  
**USER SERVICES**

This publication, as well as detailed information about NODC data holdings, products, and services, is available from the:

National Oceanographic Data Center  
User Services Branch  
NOAA/NESDIS E/OC21  
1825 Connecticut Avenue, NW  
Washington, DC 20235

Telephone: (202) 606-4549  
Fax: (202) 606-4586  
Omnet: NODC.WDCA  
Internet: [services@nodc.noaa.gov](mailto:services@nodc.noaa.gov)

# Contents

Preface .....	xi
Acknowledgements .....	xii
Abstract .....	1
1. Introduction .....	1
2. Data and data distribution .....	1
2.1 Data sources .....	2
2.2 Data quality control .....	2
2.2a Duplicate elimination .....	2
2.2b Range checking .....	3
2.2c Statistical checks .....	3
2.2d Subjective elimination of data .....	3
2.2e Representativeness of the data .....	3
2.2f Static stability check .....	4
3. Data processing procedures .....	4
3.1 Vertical interpolation to standard levels .....	4
3.2 Methods of analysis .....	5
3.2a Overview .....	5
3.2b Derivation of Barnes' (1964) weight function .....	6
3.2c Derivation of Barnes' (1964) response function .....	7
3.2d Derivation of Barnes' (1973) weight function .....	7
3.2e Choice of response function .....	8
3.2f First guess field determination .....	8
3.3 Choice of objective analysis procedures .....	9
3.4 Choice of spatial grid .....	10
4. Results .....	10
4.1 Annual mean salinity at standard levels .....	10
4.1a Explanation of standard level figures .....	10
4.1b Standard level analyses .....	10
4.2 Basin zonal averages .....	10
4.3 Basin mean profiles and volume means .....	10
5. Summary .....	11
6. Future work .....	11
7. References .....	12
8. Appendix A: Distribution of observations of salinity at all standard levels in the world ocean for the annual composition period .....	23
9. Appendix B: Annual salinity at standard levels in the world ocean .....	30

10. Appendix C: Global and basin zonal averages of annual mean salinity .....	51
11. Appendix D: Global and basin volume averages of annual mean salinity .....	55
12. Appendix E: Area and volume basin means .....	61
13. Appendix F: Seasonal distribution of observations of salinity at standard levels in the world ocean by seasons .....	68
14. Appendix G: Seasonal mean salinity at standard levels in the world ocean .....	76
15. Appendix H: Seasonal mean minus annual mean salinity at standard levels in the world ocean .....	84
16. Appendix I: Monthly distributions of salinity observations at the sea surface, 125, and 250m depth .....	88

## List of Tables

Table 1	Distribution with depth of the number of one-degree squares of ocean (Ocean ODSQS), the total number (N) of salinity observations, and the number of one-degree squares (ODSQS) containing observations of salinity.
Table 2	Acceptable distances for "inside" and "outside" values used in the Reiniger-Ross scheme for interpolating observed level data to standard levels.
Table 3	Response function of the objective analysis scheme as a function of wavelength.
Table 4	Basin identifiers and depths of "mutual exclusion" used in this study.

## List of Figures

- Figure 1 Time series of the number of salinity profiles as a function of year for each season.  
Figure 2 Time series of the number of salinity observations as a function of year A) at the sea surface  
B) at 1000 m C) at 2000 m.  
Figure 3 Distribution of salinity observations as a function of depth for the globe and the Northern and Southern Hemispheres.  
Figure 4 Division of world ocean into individual basins.

### APPENDIX A

- Figure A1 Annual distribution of salinity observations at the surface.  
Figure A2 Annual distribution of salinity observations at 30 m depth.  
Figure A3 Annual distribution of salinity observations at 50 m depth.  
Figure A4 Annual distribution of salinity observations at 75 m depth.  
Figure A5 Annual distribution of salinity observations at 100 m depth.  
Figure A6 Annual distribution of salinity observations at 125 m depth.  
Figure A7 Annual distribution of salinity observations at 150 m depth.  
Figure A8 Annual distribution of salinity observations at 250 m depth.  
Figure A9 Annual distribution of salinity observations at 400 m depth.  
Figure A10 Annual distribution of salinity observations at 500 m depth.  
Figure A11 Annual distribution of salinity observations at 700 m depth.  
Figure A12 Annual distribution of salinity observations at 900 m depth.  
Figure A13 Annual distribution of salinity observations at 1000 m depth.  
Figure A14 Annual distribution of salinity observations at 1200 m depth.  
Figure A15 Annual distribution of salinity observations at 1300 m depth.  
Figure A16 Annual distribution of salinity observations at 1500 m depth.  
Figure A17 Annual distribution of salinity observations at 1750 m depth.  
Figure A18 Annual distribution of salinity observations at 2000 m depth.  
Figure A19 Annual distribution of salinity observations at 2500 m depth.  
Figure A20 Annual distribution of salinity observations at 3000 m depth.  
Figure A21 Annual distribution of salinity observations at 4000 m depth.

### APPENDIX B

- Figure B1 Annual mean salinity (psu) at the surface.  
Figure B2 Annual mean salinity (psu) at 30 m depth.  
Figure B3 Annual mean salinity (psu) at 50 m depth.  
Figure B4 Annual mean salinity (psu) at 75 m depth.  
Figure B5 Annual mean salinity (psu) at 100 m depth.  
Figure B6 Annual mean salinity (psu) at 125 m depth.  
Figure B7 Annual mean salinity (psu) at 150 m depth.  
Figure B8 Annual mean salinity (psu) at 250 m depth.  
Figure B9 Annual mean salinity (psu) at 400 m depth.  
Figure B10 Annual mean salinity (psu) at 500 m depth.  
Figure B11 Annual mean salinity (psu) at 700 m depth.  
Figure B12 Annual mean salinity (psu) at 900 m depth.  
Figure B13 Annual mean salinity (psu) at 1000 m depth.  
Figure B14 Annual mean salinity (psu) at 1200 m depth.  
Figure B15 Annual mean salinity (psu) at 1300 m depth.  
Figure B16 Annual mean salinity (psu) at 1500 m depth.



Figure B17 Annual mean salinity (psu) at 1750 m depth.  
 Figure B18 Annual mean salinity (psu) at 2000 m depth.  
 Figure B19 Annual mean salinity (psu) at 2500 m depth.  
 Figure B20 Annual mean salinity (psu) at 3000 m depth.  
 Figure B21 Annual mean salinity (psu) at 4000 m depth.

## APPENDIX C

Figure C1 Annual global zonal average (by one-degree squares) of salinity (psu).  
 Figure C2 Annual Pacific zonal average (by one-degree squares) of salinity (psu).  
 Figure C3 Annual Atlantic zonal average (by one-degree squares) of salinity (psu).  
 Figure C4 Annual Indian zonal average (by one-degree squares) of salinity (psu).

## APPENDIX D

Figure D1a Annual global salinity (psu) basin means (0-1000 m).  
 Figure D1b Annual global salinity (psu) basin means (0-5500 m).  
 Figure D2a Annual Pacific salinity (psu) basin means (0-1000 m).  
 Figure D2b Annual Pacific salinity (psu) basin means (0-5500 m).  
 Figure D3a Annual Atlantic salinity (psu) basin means (0-1000 m).  
 Figure D3b Annual Atlantic salinity (psu) basin means (0-5500 m).  
 Figure D4a Annual Indian salinity (psu) basin means (0-1000 m).  
 Figure D4b Annual Indian salinity (psu) basin means (0-5500 m).  
 Table D1a Annual salinity (psu) basin means and standard errors for the world ocean and Pacific Ocean as a function of depth.  
 Table D1b Annual salinity (psu) basin means and standard errors for the Atlantic Ocean and Indian Ocean as a function of depth.

## APPENDIX E

Table E1 Area, volume, and percent volume contribution of each standard level to total basin volume mean, for the world ocean as a function of depth.  
 Table E2 Area, volume, and percent volume contribution of each standard level to total basin volume mean, for the Pacific Ocean as a function of depth.  
 Table E3 Area, volume, and percent volume contribution of each standard level to total basin volume mean, for the Atlantic Ocean as a function of depth.  
 Table E4 Area, volume, and percent volume contribution of each standard level to total basin volume mean, for the Indian ocean as a function of depth.  
 Table E5a Number of independent points ( $N_i$ ) used in the standard error computations for the world ocean and Pacific Ocean.  
 Table E5b Number of independent points ( $N_i$ ) used in the standard error computations for the Atlantic Ocean and Indian Ocean.  
 Table E6 Volume means of salinity for the major ocean basins and the volume of each basin.

## APPENDIX F

Figure F1 Winter (Jan.-Mar.) distribution of salinity observations at the sea surface.  
 Figure F2 Winter (Jan.-Mar.) distribution of salinity observations at 50 m depth.  
 Figure F3 Winter (Jan.-Mar.) distribution of salinity observations at 75 m depth.  
 Figure F4 Winter (Jan.-Mar.) distribution of salinity observations at 100 m depth.  
 Figure F5 Winter (Jan.-Mar.) distribution of salinity observations at 125 m depth.  
 Figure F6 Winter (Jan.-Mar.) distribution of salinity observations at 150 m depth.

- Figure F7 Spring (Apr.-Jun.) distribution of salinity observations at the sea surface.  
 Figure F8 Spring (Apr.-Jun.) distribution of salinity observations at 50 m depth.  
 Figure F9 Spring (Apr.-Jun.) distribution of salinity observations at 75 m depth.  
 Figure F10 Spring (Apr.-Jun.) distribution of salinity observations at 100 m depth.  
 Figure F11 Spring (Apr.-Jun.) distribution of salinity observations at 125 m depth.  
 Figure F12 Spring (Apr.-Jun.) distribution of salinity observations at 150 m depth .
- Figure F13 Summer (Jul.-Sep.) distribution of salinity observations at the sea surface.  
 Figure F14 Summer (Jul.-Sep.) distribution of salinity observations at 50 m depth.  
 Figure F15 Summer (Jul.-Sep.) distribution of salinity observations at 75 m depth.  
 Figure F16 Summer (Jul.-Sep.) distribution of salinity observations at 100 m depth.  
 Figure F17 Summer (Jul.-Sep.) distribution of salinity observations at 125 m depth.  
 Figure F18 Summer (Jul.-Sep.) distribution of salinity observations at 150 m depth.
- Figure F19 Fall (Oct.-Dec.) distribution of salinity observations at the sea surface.  
 Figure F20 Fall (Oct.-Dec.) distribution of salinity observations at 50 m depth.  
 Figure F21 Fall (Oct.-Dec.) distribution of salinity observations at 75 m depth.  
 Figure F22 Fall (Oct.-Dec.) distribution of salinity observations at 100 m depth.  
 Figure F23 Fall (Oct.-Dec.) distribution of salinity observations at 125 m depth.  
 Figure F24 Fall (Oct.-Dec.) distribution of salinity observations at 150 m depth.

## APPENDIX G

- Figure G1 Winter (Jan.-Mar.) mean salinity (psu) at the sea surface.  
 Figure G2 Winter (Jan.-Mar.) mean salinity (psu) at 50 m depth.  
 Figure G3 Winter (Jan.-Mar.) mean salinity (psu) at 75 m depth.  
 Figure G4 Winter (Jan.-Mar.) mean salinity (psu) at 100 m depth.  
 Figure G5 Winter (Jan.-Mar.) mean salinity (psu) at 125 m depth.  
 Figure G6 Winter (Jan.-Mar.) mean salinity (psu) at 150 m depth..
- Figure G7 Spring (Apr.-Jun.) mean salinity (psu) at the sea surface.  
 Figure G8 Spring (Apr.-Jun.) mean salinity (psu) at 50 m depth.  
 Figure G9 Spring (Apr.-Jun.) mean salinity (psu) at 75 m depth.  
 Figure G10 Spring (Apr.-Jun.) mean salinity (psu) at 100 m depth.  
 Figure G11 Spring (Apr.-Jun.) mean salinity (psu) at 125 m depth.  
 Figure G12 Spring (Apr.-Jun.) mean salinity (psu) at 150 m depth.
- Figure G13 Summer (Jul.-Sep.) mean salinity (psu) at the sea surface.  
 Figure G14 Summer (Jul.-Sep.) mean salinity (psu) at 50 m depth.  
 Figure G15 Summer (Jul.-Sep.) mean salinity (psu) at 75 m depth.  
 Figure G16 Summer (Jul.-Sep.) mean salinity (psu) at 100 m depth.  
 Figure G17 Summer (Jul.-Sep.) mean salinity (psu) at 125 m depth.  
 Figure G18 Summer (Jul.-Sep.) mean salinity (psu) at 150 m depth.
- Figure G19 Fall (Oct.-Dec.) mean salinity (psu) at the sea surface.  
 Figure G20 Fall (Oct.-Dec.) mean salinity (psu) at 50 m depth.  
 Figure G21 Fall (Oct.-Dec.) mean salinity (psu) at 75 m depth.  
 Figure G22 Fall (Oct.-Dec.) mean salinity (psu) at 100 m depth.  
 Figure G23 Fall (Oct.-Dec.) mean salinity (psu) at 125 m depth.  
 Figure G24 Fall (Oct.-Dec.) mean salinity (psu) at 150 m depth.

## APPENDIX H

- Figure H1 Winter (Jan.-Mar.) minus annual mean salinity (psu) at the sea surface.  
Figure H2 Winter (Jan.-Mar.) minus annual mean salinity (psu) at 50 m depth.  
Figure H3 Winter (Jan.-Mar.) minus annual mean salinity (psu) at 100 m depth.
- Figure H4 Spring (Apr.-Jun.) minus annual mean salinity (psu) at the sea surface.  
Figure H5 Spring (Apr.-Jun.) minus annual mean salinity (psu) at 50 m depth.  
Figure H6 Spring (Apr.-Jun.) minus annual mean salinity (psu) at 100 m depth.
- Figure H7 Summer (Jul.-Sep.) mean minus annual salinity (psu) at the sea surface.  
Figure H8 Summer (Jul.-Sep.) mean minus annual salinity (psu) at 50 m depth.  
Figure H9 Summer (Jul.-Sep.) mean minus annual salinity (psu) at 100 m depth.
- Figure H10 Fall (Oct.-Dec.) mean minus annual salinity (psu) at the sea surface.  
Figure H11 Fall (Oct.-Dec.) mean minus annual salinity (psu) at 50 m depth.  
Figure H12 Fall (Oct.-Dec.) mean minus annual salinity (psu) at 100 m depth.

## APPENDIX I

- Fig. I1 January distribution of salinity observations at the surface.  
Fig. I2 January distribution of salinity observations at 125 m depth.  
Fig. I3 January distribution of salinity observations at 250 m depth.  
Fig. I4 February distribution of salinity observations at the surface.  
Fig. I5 February distribution of salinity observations at 125 m depth.  
Fig. I6 February distribution of salinity observations at 250 m depth.  
Fig. I7 March distribution of salinity observations at the surface.  
Fig. I8 March distribution of salinity observations at 125 m depth.  
Fig. I9 March distribution of salinity observations at 250 m depth.  
Fig. I10 April distribution of salinity observations at the surface.  
Fig. I11 April distribution of salinity observations at 125 m depth.  
Fig. I12 April distribution of salinity observations at 250 m depth.  
Fig. I13 May distribution of salinity observations at the surface.  
Fig. I14 May distribution of salinity observations at 125 m depth.  
Fig. I15 May distribution of salinity observations at 250 m depth.  
Fig. I16 June distribution of salinity observations at the surface.  
Fig. I17 June distribution of salinity observations at 125 m depth.  
Fig. I18 June distribution of salinity observations at 250 m depth.  
Fig. I19 July distribution of salinity observations at the surface.  
Fig. I20 July distribution of salinity observations at 125 m depth.  
Fig. I21 July distribution of salinity observations at 250 m depth.  
Fig. I22 August distribution of salinity observations at the surface.  
Fig. I23 August distribution of salinity observations at 125 m depth.  
Fig. I24 August distribution of salinity observations at 250 m depth.  
Fig. I25 September distribution of salinity observations at the surface.  
Fig. I26 September distribution of salinity observations at 125 m depth.  
Fig. I27 September distribution of salinity observations at 250 m depth.  
Fig. I28 October distribution of salinity observations at the surface.  
Fig. I29 October distribution of salinity observations at 125 m depth.  
Fig. I30 October distribution of salinity observations at 250 m depth.  
Fig. I31 November distribution of salinity observations at the surface.  
Fig. I32 November distribution of salinity observations at 125 m depth.  
Fig. I33 November distribution of salinity observations at 250 m depth.

- Fig. I34      December distribution of salinity observations at the surface.  
Fig. I35      December distribution of salinity of observation at 125 m depth.  
Fig. I36      December distribution of salinity of observations at 250 m depth.

## Preface

This atlas continues and extends an earlier work entitled *Climatological Atlas of the World Ocean* (Levitus, 1982). This earlier work has proven to be of great utility to the international oceanographic, climate research, and operational communities. In particular, the objectively analyzed fields of temperature and salinity have been used in a variety of ways. These include use as boundary and/or initial conditions in numerical ocean circulation models, for verification of numerical simulations of the ocean, as a form of "sea truth" for satellite measurements such as altimetric observations of sea surface height, and for planning oceanographic expeditions. We have expanded this earlier work to include chemical parameters such as phosphate, nitrate, and silicate because: 1) our belief that a comprehensive set of objectively analyzed parameter fields describing the state of the ocean, based on all existing oceanographic data, should be available as a matter of course to the international research community and 2) the immediate, compelling need for such analyses to study the role of biogeochemical cycles in determining how the earth's climate system works. For example, it is well known that the amount of carbon dioxide in the earth's atmosphere is expected to double during the next century. Regardless of one's scientific and/or political view of a possible "enhanced greenhouse warming" due to the increase of carbon dioxide, it is a necessity that the international scientific community have access to the most complete historical oceanographic data bases to study this problem, as well as other scientific and environmental problems.

The production of global analyses of oceanographic data is a major undertaking. Such work benefits from the input of many individuals and organizations. We have tried to structure the data sets and analyses that constitute this atlas in such a way as to encourage feedback from experts around the world who have knowledge that can improve future atlases. The production of works like this atlas series is becoming easier because of advances in computer hardware and software. These include: 1) the development of relatively inexpensive but powerful workstations that can be dedicated to data processing and analysis and 2) the development of high resolution printers and interactive graphics software that minimize the need for expensive, time consuming manual drafting and photographic processing. Because of the substantial increase in the historical oceanographic data bases expected over the next several years, the Ocean Climate Laboratory plans to update and expand this atlas series on a relatively frequent basis that will be determined by the accession of significant amounts of new data. We plan to publish volumes that focus on derived quantities, higher resolution analyses, and additional parameters such as chlorophyll, primary production, and plankton taxa and biomass.

The objective analyses in this atlas, and data on which they are based, are being made available internationally without restriction on various magnetic media as well as CD-ROMs. This is to insure the widest possible distribution.

In each acknowledgement section of this atlas series we have expressed our view that such series is only possible through international cooperation of scientists, data managers, and scientific administrators throughout the international community. I would also like to thank my co-authors, colleagues, and staff from the Ocean Climate Laboratory of NODC for their dedication to the project leading to publication of this atlas series. Their integrity and thoroughness have made possible this multi-volume atlas series. Oceanography is a field of increasing specialization, and it is my belief that the development of national and international oceanographic data archives is best performed by scientists who are actively working with the historical data. Margarita Conkright and Timothy Boyer receive my particular thanks.

Sydney Levitus  
Director, Ocean Climate Laboratory  
National Oceanographic Data Center  
Washington, D.C.  
March, 1994

## Acknowledgements

The establishment of a research group at the National Oceanographic Data Center to focus on the preparation of research quality oceanographic data sets and their objective analyses sets has been made possible by a grant from the NOAA Climate and Global Change Program. Substantial amounts of historical oceanographic data used in this study were located and digitized (Data Archaeology and Rescue projects) with funding from the NOAA Climate and Global Change Program, the NOAA Environmental Services Data and Information Management Program, the National Science Foundation, and the Office of Naval Research.

The work described in this atlas was made possible by scientists, technicians, ships' crew, data managers, and science administrators from the international scientific community. This atlas represents the results of several different research/data management projects of the NODC Ocean Climate Laboratory at the National Oceanographic Data Center (NODC), Washington, D.C. The products in this atlas are all based on the master oceanographic data archives maintained by NODC/WDC-A as well as data acquired as a result of the NODC Data Archaeology and Rescue (NODAR) project and the IODE/IOC Global Oceanographic Data Archaeology and Rescue (GODAR) project. These archives and data sets exist because scientists of the international scientific community have submitted their data to national and regional data centers. In turn these centers have submitted data to the World Data Center system established under the International Council of Scientific Unions and the Intergovernmental Oceanographic Commission. This atlas and similar works would not exist without these international efforts. In particular we would like to thank data managers at these centers and the administrators and staff of these international organizations. The archiving of oceanographic data at international data centers means that the substantial expenditures in human and capital resources devoted to oceanographic measurement programs will be fully exploited, both for present and future scientific studies.

Although many data managers from the international community have been instrumental in the building of global oceanographic data bases we would like to thank in particular Harry Dooley of the International Council for Exploration of the Sea, Osamu Yamada, Director of the Japanese Oceanographic Data Center, Yuri Sychev of the Russian National Oceanographic Data Center, Hou Wen-Feng of the Chinese National Oceanographic Data Center, Shin Tani formerly of the Japanese Oceanographic Data Center, and Ronald Wilson of the Marine Environmental Data Service, Canada.

Jeff Burney provided excellent system administration and programming support. Daphne Johnson provided invaluable assistance in unpacking numerous data sets used in this project and preparing figures. Robert Gelfeld was instrumental in the acquisition of numerous data sets as part of the NODAR and GODAR Projects. Margarita Conkright provided assistance in the preparation of figures and of this atlas in general. Grigory Isayev and Linda Stathoplos helped with technical editing of the manuscript. Our colleagues at NODC/WDC-A provided support for various data management projects related to this atlas. Jennifer Campbell helped in preparing the manuscript for publication. The support of Gregory Withee and Bruce Douglas, former and present directors of NODC is appreciated. Management support by Dave Goodrich of the NOAA Office of Global Programs is appreciated.

We also would like to thank Jim Carton and Dave Adamec for reviewing the manuscript version of this atlas and providing constructive comments.

The data sets and products represented by this atlas are distributed internationally without restriction in accordance with U.S. Climate and Global Change as well as ICSU/IOC data management policies in support of Global Change Research.

# WORLD OCEAN ATLAS, 1994: VOLUME 3, Salinity

*Sydney Levitus, Russell Burgett, and Timothy Boyer*  
National Oceanographic Data Center  
Washington, D.C.

## ABSTRACT

This atlas contains maps of salinity at selected standard levels of the world ocean on a one-degree grid. Maps for all-data annual and seasonal compositing periods are presented. The fields used to generate these maps were computed by objective analysis of historical data. Data distribution maps are presented for various compositing periods. Basin zonal averages and basin volume averages are computed from these objectively analyzed fields and presented in the form of figures and tables.

## 1. INTRODUCTION

The format of this atlas, as well as some of the text, follow Levitus (1982). This atlas is an analysis of all historical salinity data available from the National Oceanographic Data Center (NODC), Washington, D.C., plus data gathered as a result of two data management projects: the NODC Oceanographic Data Archaeology and Rescue (NODAR) project and the Intergovernmental Oceanographic Commission (IOC) Global Oceanographic Data Archaeology and Rescue (GODAR) project. Data used here have been analyzed in a consistent, objective manner on a one-degree latitude-longitude grid at standard oceanographic analysis levels between the surface and ocean bottom or to a maximum depth of 5500m. The procedures used are similar, but not identical to, the analyses presented by Levitus (1982). Annual, seasonal, and monthly analyses have been computed for salinity. The present analyses and statistical information are primarily intended for use in the study of the role of the world ocean as part of the earth's climate system.

Objective analyses shown in this atlas are limited by the nature of the data base (non-synoptic, scattered in space)

and characteristics of the objective analysis techniques, and the grid used. These limitations and characteristics will be discussed below.

With the additional data made available since Levitus (1982), we have now been able to expand this earlier work to include monthly analyses of salinity. However, even with these additional data, we are still hampered in a number of ways by a lack of data. Because of the lack of data, we are forced to examine the annual cycle by compositing all data regardless of the year of observation. In some areas, quality control is made difficult by the limited number of data. Data may exist in an area for only one season, thus precluding any representative annual analysis. In some areas there may be a reasonable spatial distribution of data points on which to base an analysis, but there may be only a few (perhaps only one) datum in each one-degree square.

## 2. DATA AND DATA DISTRIBUTION

Data sources and quality control procedures are described

below. Because quality control procedures are so important, a technical report has been prepared fully describing these procedures (Boyer and Levitus, 1994).

## 2.1 Data sources

The Station Data and S/CTD used in this project were obtained from the National Oceanographic Data Center (NODC), Washington, D.C. and represent all the data available in the Oceanographic Station Data (SD) file and S/CTD file as of the first quarter of 1993 (NODC, 1993), plus data gathered as a result of the NODAR and GODAR projects (Levitus *et al.*, 1994a) that have not yet been archived in the NODC digital archives. In addition, the collection of international oceanographic profiles that comprise the Hydrographic Atlas of the Southern Ocean developed by Olbers *et al.* (1992) at the Alfred Wegener Institute for Polar and Marine Research were included. S/CTD that are received at coarse vertical resolution are often placed in the Station Data file. We have transferred these data to the S/CTD file.

Figures 1-3 and Table 1 show the global distributions of salinity measurements as a function of time at selected depths. Shown in Figure 3 are the number of observed data points that occur in the depth range centered around each standard level. The depth range for the sea surface is 0-5 m. At all other standard levels, the depth range is defined as the region between the midpoints of the standard level being considered and the adjacent standard levels above and below. Appendix A shows the geographic distribution of historical salinity observations as a function of depth. Appendix F shows the distribution of historical salinity observations as a function of depth for individual seasons.

One must understand our terms "standard level data" and "observed level data" to understand the various data distribution and summary figures and tables we present in this atlas. We refer to the actual measured value of an oceanographic parameter *in situ* as an "observation," and to the depth at which such a measurement was made as "observed level depth." We may refer to such data as "observed level data." Before the advent of oceanographic instrumentation that measure at high frequencies in the vertical, oceanographers often attempted to make measurements at selected "standard levels" in the water column. Sverdrup *et al.* (1942) presented the suggestions of the International Association of Physical Oceanography (IAPSO) as to which depths oceanographic measurements should be made or interpolated to for analysis. Different nations or institutions have "supersets" of standard level

observation (e.g. NODC, 1993). For many purposes, including here, observed level data are interpolated to standard observation levels, if they do not occur exactly at a standard observation level. In contrast to Levitus (1982), we have used counts of "observed level values" wherever possible when summarizing the historical data used in this atlas. The distinction may seem minor, but in fact the criteria used to determine whether observed level data are suitable for use in interpolating to standard levels are not trivial. For example, one does not wish to use an observed level value at 5000 m depth to determine an interpolated standard level value at 20 m depth. Section 3.1 discusses this further.

## 2.2 Data quality control

Quality control of the data is a major task whose difficulty is directly related to lack of data (in some areas) upon which to base statistical checks. Consequently certain empirical criteria were applied, and as part of the last processing step, subjective judgment was used. Individual data, and in some cases entire profiles or cruises, have been flagged because these data produced features that were judged to be non-representative or in error. As part of our work, we will make available both observed level profiles as well as standard level profiles with various quality control flags applied. Our knowledge of the variability of the world ocean now includes a greater appreciation and understanding of the ubiquity of eddies, rings, and lenses in some parts of the world ocean as well as interannual and interdecadal variability of water mass properties. Therefore, we have simply flagged data, not eliminated them. Thus individual investigators can make their own decision regarding the representativeness or correctness of the data. Investigators studying the distribution of features such as eddies will be interested in those data that we may regard as unrepresentative for our purpose here.

### 2.2a Duplicate elimination

Because data are received from many sources, all data files were checked for the presence of exact replicates. Approximately 20,000 Station Data profiles in the NODC Station Data File were found to be exact replicates of other profiles in this file. All but one profile from each set of replicate profiles were eliminated as the first step of our processing. All data sets used that were not part of the NODC Station Data file were checked for duplicates against the NODC Station Data file.



### **2.2b Range checking**

Range checking was performed on all data as a first error check to eliminate the relatively few data that seemed to be grossly in error. Range checks were prepared for individual regions of the world ocean in contrast to Levitus' (1982) use of one range check for the entire world ocean for each parameter. Future work will include ranges for different basins by individual seasons. Boyer and Levitus (1994) detail the quality control procedures and include tables showing the ranges we selected for each basin

### **2.2c Statistical checks**

Statistical checks were performed to eliminate outliers as follows. All data for each parameter (irrespective of seasons), at each standard level, were averaged by five-degree squares to produce a record of the number of observations, mean, and standard deviation in each square. Statistics were computed for each compositing period; annual and each of the four seasons. Below 50 m depth, a three-standard-deviation criterion was used to flag data and eliminate individual observations from further use in our objective analyses. Above 50 m depth, a five-standard-deviation criterion was used in five-degree squares that contained any land area. In selected five degrees squares that came close to land areas, a four standard-deviation check was used. In all other squares a three-standard-deviation criterion was used with the following exceptions. For those data that occurred at or deeper than the standard level depth in the one-degree square in which the profile was observed, a four standard deviation criteria was used. For those data in a one-degree square that were measured at a depth deeper than the depth of any adjacent one-degree square, a four-standard-deviation check was used.

The reason for the weaker criterion in coastal and near-coastal regions is the exceptionally large variability in the coastal five-degree square statistics for some parameters. Frequency distributions of some parameters in some coastal regions are observed to be skewed or bimodal. Thus to avoid eliminating possibly good data in highly variable environments, the standard deviation criteria were weakened.

The total number of salinity measurements in each cast, as well as the total number of observations exceeding the criterion, were recorded. If more than two observations in a cast were found to exceed the standard deviation criterion, then the entire cast was eliminated. This check was imposed after tests indicated that surface data from

particular casts (which upon inspection appeared to be erroneous) were being eliminated but deeper data were not. Other situations were found where erroneous data from the deeper portion of a cast were eliminated, while near-surface data from the same cast were not eliminated because of larger natural variability in surface layers. One reason for this was the decrease of the number of observations with depth and the resulting change in sample statistics. The standard-deviation check was applied twice to the data set for each compositing period. Individual flags were set for each of these periods.

In summary, first the five-degree square statistics were computed, and the elimination procedure described above was used to provide a preliminary data set. Next, new five-degree-square statistics were computed from this preliminary data set and used with the same statistical check to produce a new, "clean" data set. The reason for applying the statistical check twice was to eliminate, in the first round, any grossly erroneous or non-representative data from the data set that would artificially increase the variances. The second check then should be more effective in eliminating smaller, but probably still erroneous or non-representative observations.

### **2.2d Subjective elimination of data**

The data were averaged by one-degree squares for input to the objective analysis program. After initial objective analyses were computed, the input set of one-degree means still contained suspicious data contributing to unrealistic distributions, yielding intense bull's-eyes or gradients. Examination of these features indicated that some of them were due to particular oceanographic cruises. In such cases data from an entire cruise were eliminated from further use by setting a flag on each profile from the cruise.

### **2.2e Representativeness of the data**

Another quality control issue is data representativeness. The general paucity of data forces us to composite all historical data to produce "climatological" fields. In a given one-degree square, there may be data from a month or season of one particular year, while in the same or a nearby square there may be data from an entirely different year. If there is large interannual variability in a region where scattered sampling in time has occurred, then one can expect the analysis to reflect this. Because the observations are scattered non-randomly with respect to time, except for a few limited areas, the results cannot, in a strict sense, be considered a true long-term climatological average.

We present smoothed analyses of historical means, based (in certain areas) on relatively few observations. We believe, however, that useful information about the oceans can be gained through our procedures and that the large-scale features are representative of the real ocean. We believe that, if a hypothetical global synoptic set of ocean data (temperature, salinity, or oxygen) existed, and one were to smooth this data to the same degree as we have smoothed the historical means overall, the large-scale features would be similar to our results. Some differences would certainly occur because of interannual to decadal-scale variability. As more data are added to the historical archives, we will be able to evaluate this variability on basin and gyre scales following the studies of Levitus (1989a,b,c; 1990) and Levitus *et al.* (1994b).

To clarify discussions of the amount of available data, quality control techniques, and representativeness of the data, the reader should examine in detail the maps showing the distribution of data (Appendices A and F). These maps are provided to give the reader a quick, simple way of examining the historical data distributions. Basically, the data diminish in number with increasing depth and latitude. In the upper ocean, the all-data annual mean distributions are quite good for defining large-scale features, but for the seasonal periods, the data base for some regions is inadequate. With respect to the deep ocean, in some areas the distribution of observations may be adequate for some diagnostic computations but inadequate for other purposes. Obviously if an isolated deep basin or some region of the deep ocean has only one observation, then no horizontal gradient computations are meaningful. However useful information is provided by the observation in the computation of other quantities (e.g., a volumetric mean over a major ocean basin).

### 2.2f Static stability check

Each hydrographic cast was checked for static stability as defined by Hesselberg and Sverdrup (1914). Neumann and Pierson (1966, p. 139) review this definition. The computation is a "local" one in the sense that adiabatic displacements between adjacent temperature-salinity measurements in the vertical are considered rather than displacements to the sea surface. Lynn and Reid (1968) discuss the reasons for use of the local stability computation. The procedure for computation follows that used by Lynn and Reid (1968) and is given by

$$E = \lim_{\partial z \rightarrow 0} \rho_0 \delta \rho / \partial z$$

in which  $\rho_0 = 1.02 \text{ g cm}^{-3}$ . As noted by Lynn and Reid, the term "is the individual density gradient defined by vertical displacement of a water parcel (as opposed to the geometric density gradient). For discrete samples the density difference ( $\delta \rho$ ) between two samples is taken after one is adiabatically displaced to the depth of the other". For the results at any standard level ( $k$ ), the computation was performed by displacing parcels at the next deeper standard level ( $k+1$ ) to level  $k$ . Instabilities have been reported over large areas of the tropical oceans. Levitus (1982) described the density inversions reported by Schubert (1935) from the results of the Meteor Expedition. It appears that the inversions reported are so large that they should not be considered real. Another report describing density inversions is that of Spilhaus *et al.* (1950) who reported inversions along the U.S. eastern continental shelf. They reported inversions that could not be explained in terms of measurement or sampling errors. They presented evidence that indicates that the inversions might be due to tidal currents.

The actual procedure for using stability checks to eliminate sets of data points was as follows. To a depth of 30m, inversions in excess of  $3 \times 10^{-5} \text{ g cm}^{-3}$  were eliminated, and below this depth down to the 400 m level, inversions in excess of  $2 \times 10^{-5} \text{ g cm}^{-3}$  were eliminated. Below 400 m any inversion was eliminated. To eliminate an inversion both temperature and salinity were flagged and eliminated from further use at both standard levels involved in the computation. In the actual processing a count was kept of the number of inversions in each cast. If a cast had two or more unacceptable inversions, as defined above, then the entire cast was eliminated from further use.

## 3. DATA PROCESSING PROCEDURES

### 3.1 Vertical interpolation to standard levels

Vertical interpolation of observed level data to standard levels followed procedures in UNESCO (1991). These procedures are in part based on the work of Reiniger and Ross (1968). Four observed level values surrounding the standard level values were used, two values from above the standard level and two values below the standard level. Paired parabolas were generated via Lagrangian interpolation. A reference curve was fitted to the four data points and used to define unacceptable interpolations caused by "overshooting" in the interpolation. When a spurious extremum could not be eliminated using this technique, linear interpolation was used. When there were

too few data points above or below the standard level to apply the Reiniger and Ross technique, we used a three-point Lagrangian interpolation. If three points were not available (either two above and one below or vice-versa), we used linear interpolation. In the event that an observation occurred exactly at the depth of a standard level, then a direct substitution was made. Table 2 provides the range of acceptable distances for which observed level data could be used for interpolation to a standard level. The criteria were a function of depth. The criteria for the "outside" points were the same as used by NODC in their three-point Lagrangian interpolation and by Levitus (1982). The criteria for the "inner" points was much more restrictive and resulted in fewer standard level data values compared to the NODC and Levitus (1982) criteria. Future criteria might depend on the geographic location of the profile as well as the time of year.

The data summaries in Table 1 and all other such counts represent the observed level data. These are counts of observed level data that occur within a depth interval around each standard level. This differs from the statistics presented by Levitus (1982) who presented counts of interpolated standard level data.

### 3.2 Methods of analysis

#### 3.2a Overview

An objective analysis scheme of the type described by Barnes (1973) was used to produce the fields shown in this atlas. This scheme had its origins in the work of Cressman (1959) and Barnes (1964). The Barnes (1973) scheme requires only one "correction" to the first guess field at each grid point in comparison to the successive correction method of Cressman and Barnes (1964). For completeness we derive the weight function and response function per Barnes (1964) and then per Barnes (1973).

Inputs to the analysis scheme were observed one-degree square means of data at standard levels (for whatever period and parameter being analyzed), and a first-guess value for each square. For instance, one-degree square means for our annual analysis were computed using all available data regardless of date of observation. For July, we used all historical July data regardless of year of observation.

Analysis was the same for all standard depth levels. Each one-degree square value was defined as being representative of its square. The 360x180 gridpoints are located at the intersection of half-degree lines of latitude and longitude. An influence radius was then specified. At

those grid points where there was an observed mean value, the difference between the mean and the first-guess field was computed. Next, a correction to the first-guess value at all gridpoints was computed as a distance-weighted mean of all gridpoint difference values that lie within the area around the gridpoint defined by the influence radius. Mathematically, the correction factor derived by Barnes (1964) is given by the expression

$$C_{ij} = \frac{\sum_{s=1}^n W_s Q_s}{\sum_{s=1}^n W_s} \quad (1)$$

in which

$C_{ij}$  = the correction factor at gridpoint coordinates (i,j)

(i,j) = coordinates of a gridpoint in the east-west and north-south directions, respectively

n = the number of observations that fall within the area around the point i,j defined by the influence radius

$Q_s$  = the difference between the observed mean and the first guess at the  $S^{\text{th}}$  point in the influence area

$W_s$  =  $\exp(-E r^2 R^{-2})$  for  $r < R$

$W_s$  = 0 for  $r > R$

r = distance of the observation from the gridpoint

R = influence radius

E = 4

The derivation of the weight function,  $W_s$ , will be presented in the following section. At each gridpoint we computed an analyzed value  $G_{ij}$  as the sum of the first guess,  $F_{ij}$  and the correction  $C_{ij}$ . The expression for this is

$$G_{ij} = F_{ij} + C_{ij} \quad (2)$$

If there were no data points within the area defined by the influence radius, then the correction was zero, the first-guess field was left unchanged, and the analyzed value was simply the first-guess value. This correction procedure was applied at all gridpoints to produce an

analyzed field. The resulting field was first smoothed with a median filter (Tukey, 1974; Rabiner *et al.*, 1975) and then smoothed with a five-point smoother of the type described by Shuman (1957).

The analysis scheme is based on the work of several researchers analyzing meteorological data. Berghorsson and Doos (1955) computed corrections to a first-guess field using various techniques: one assumed that the difference between a first-guess value and an analyzed value at a gridpoint was the same as the difference between an observation and a first-guess value at a nearby observing station. All the observed differences in an area surrounding the gridpoint were then averaged and added to the gridpoint first guess value to produce an analyzed value. Cressman (1959) applied a distance-related weight function to each observation used in the correction in order to give more weight to observations that occur closest to the gridpoint. In addition, Cressman introduced the method of performing several iterations of the analysis scheme using the analysis produced in each iteration as the first-guess field for the next iteration. He also suggested starting the analysis with a relatively large influence radius and decreasing it with successive iterations so as to analyze smaller scale phenomena with each pass.

Sasaki (1960) introduced a weight function that was specifically related to the density of observations, and Barnes (1964, 1973) extended the work of Sasaki. The weight function of Barnes (1973) has been used here. The derivation of the weight function we used which we present for completeness, follows the work of Barnes (1973).

The objective analysis scheme we used is in common use by the meso scale meteorological community. Several studies of objective analysis techniques have been made. Achtemeier (1987) examined the "concept of varying influence radii for a successive corrections objective analysis scheme." Seaman (1983) compared the "objective analysis accuracies of statistical interpolation and successive correction schemes." Smith and Leslie (1984) performed an "error determination of a successive correction type objective analysis scheme." Smith *et al.* (1986) made "a comparison of errors in objectively analyzed fields for uniform and non-uniform station distribution."

### 3.2b Derivation of Barnes' (1964) weight function

The principle upon which Barnes' (1964) weight function is derived is that "the two-dimensional distribution of an

atmospheric variable can be represented by the summation of an infinite number of independent harmonic waves, that is, by a Fourier integral representation". If  $f(x,y)$  is the variable, then in polar coordinates  $(r,\theta)$ , a smoothed or filtered function  $g(x,y)$  can be defined:

$$g(x,y) = \frac{1}{2\pi} \int_0^{2\pi} \int_0^{\infty} \eta f(x+r\cos\theta, y+r\sin\theta) d\left(\frac{r^2}{4K}\right) d\theta \quad (3)$$

in which  $r$  is the radial distance from a gridpoint whose coordinates are  $(x,y)$ . The weight function is defined as

$$\eta = \exp(-r^2/4K) \quad (4)$$

which resembles the Gaussian distribution. The shape of the weight function is determined by the value of  $K$ , which depends on the distribution of data. The determination of  $K$  follows. The weight function has the property that

$$\frac{1}{2\pi} \int_0^{2\pi} \int_0^{\infty} \eta d\left(\frac{r^2}{4K}\right) d\theta = 1. \quad (5)$$

This property is desirable because in the continuous case (3) the application of the weight function to the distribution  $f(x,y)$  will not change the mean of the distribution. However, in the discrete case (1), we only sum the contributions to within the distance  $R$ . This introduces an error in the evaluation of the filtered function, because the condition given by (5) does not apply. The error can be pre-determined and set to a reasonably small value in the following manner. If one carries out the integration in (5) with respect to  $\theta$ , the remaining integral can be rewritten as

$$\int_0^R \eta d\left(\frac{r^2}{4K}\right) + \int_R^{\infty} \eta d\left(\frac{r^2}{4K}\right) = 1. \quad (6)$$

Defining the second integral as  $\epsilon$  yields

$$\int_0^R \exp\left(-\frac{r^2}{4K}\right) d\left(\frac{r^2}{4K}\right) = 1 - \epsilon. \quad (7)$$

in which

$$\epsilon = \exp(-R^2/4K).$$

Levitus (1982) chose  $\epsilon = 0.02$ , which implies with respect to (6) the representation of 98 percent of the influence of any data around the gridpoint in the area defined by the influence radius,  $R$ . In terms of the weight function used in the evaluation of (1) this choice leads to a value of  $E=4$  since

$$E = R^2/4K = -\ln \epsilon.$$

The choice of  $\epsilon$  and the specification of  $R$  determine the shape of the weight function.

Barnes (1964) proposed using this scheme in an iterative fashion similar to Cressman (1959). Levitus (1982) used a four iteration scheme with a variable influence radius for each pass.

### 3.2c Derivation of Barnes' (1964) response function

It is desirable to know the response of a data set to the interpolation procedure applied to it. Following Barnes (1964) we let

$$f(x) = A \sin(ax) \quad (8)$$

in which  $a = 2\pi/\lambda$  with  $\lambda$  being the wavelength of a particular Fourier component, and substitute this function into equation (3) along with the expression for  $\hat{\eta}$  in equation (4). Then

$$g(x) = D (A \sin(ax)) = D f(x) \quad (9)$$

in which

$$D = \exp(-\pi^2 R^2 / 4\lambda^2).$$

$D$  is the response function for one application of the analysis. The phase of each Fourier component is not changed by the interpolation procedure. The results of an analysis pass are used as the first guess for the next analysis pass in an iterative fashion. The response function after  $N$  iterations as derived by Barnes (1964) is

$$g_N(x) = f(x) D \sum (1-D)^{N-1} \quad (10)$$

Equation (10) differs trivially from that given by Barnes. The difference is due to the fact that our first-guess field was defined as a zonal average, annual mean, or seasonal mean, whereas Barnes used the first application of the analysis as a first guess. Barnes (1964) also showed that applying the analysis scheme in an iterative fashion will result in convergence of the analyzed field to the observed data field. However, it is not desirable to approach the observed data too closely, because at least seven or eight gridpoints are needed to represent a Fourier component.

The response function given in (10) is useful in two ways: it is informative to know what Fourier components make up the analyses, and the computer programs used in generating the analyses can be checked for correctness by comparison with (10).

### 3.2d Derivation of Barnes' (1973) weight function

Barnes (1973) showed how a nearly equivalent analysis (with respect to the response function) could be performed with just one iteration, assuming a first guess field is provided. We use this one-pass scheme in our present analyses. Derivation of the weight function for this scheme is provided (below) after the derivation of the response function in the following section. Following Barnes (1973), equation (9) can be rewritten as

$$g_0(x,y) = D_0 f(x,y). \quad (11)$$

The subscript nought denotes the first pass through the data with weight function

$$\hat{\eta}_0 = \exp(-r^2/4K_0). \quad (12)$$

Using the results of the initial analysis as a first guess for the second iteration through the data, we add the residual field of the second pass analysis to the first guess provided by the first iteration. We write this as

$$g_1(x,y) = g_0(x,y) + [f(x,y) - g_0(x,y)] D_1 \quad (13)$$

where  $D_1$  is the response resulting from application of the weight function

$$\hat{r}_1 = \exp(-r^2/4k_1); \quad k_1 = \gamma k_0 \quad \text{and} \quad \gamma > 0 \quad (14)$$

$$D_1 = \exp(-a^2 k_1) = \exp(-a^2 \gamma k_0) = D_0^\gamma \quad (15)$$

Substituting (15) and (11) into (13) yields

$$g_1(x,y) = f(x,y) D_0 (1 + D_0^{\gamma-1} - D_0^\gamma) \quad (16)$$

The new response function is

$$D' = D_0 (1 + D_0^{\gamma-1} - D_0^\gamma) \quad (17)$$

The value  $k_1 = \gamma k_0$  is chosen to produce a desired response function. In our analyses a value of  $k_1 = 0.8$  was used. This choice leads to the response function given in Table 3.

There are several advantages of a one-pass interpolation analysis. The saving of computer time is an obvious advantage. A more important advantage is that statistical analysis of the analyzed fields becomes much simpler.

### 3.2e Choice of response function

The distribution of observations (see appendices) at different depths and for the different averaging periods, not regular in space or by season. At one extreme, regions exist in which every one-degree square contains data and no interpolation needs to be performed. At the other extreme are regions in which few data exist. Thus with variable data spacing the average separation distance between gridpoints containing data is a function of geographical position and averaging period. However, if we computed and used a different average separation distance for each parameter at each depth and each averaging period, we would be generating analyses in which the wavelengths of observed phenomena might differ from one depth level to another and from one season

to another. We chose instead to use a fixed influence radius of 555 km which allows us to analyze each parameter at every depth and season in exactly the same way.

Inspection of (1) shows that the difference between the analyzed field and the first guess at any gridpoint is proportional to the sum of the weighted differences between the observed mean and first-guess at all gridpoints containing data within the influence area.

The reason for using the five-point smoother and the median smoother is that our data are not evenly distributed in space. As the analysis moves from regions containing data to regions devoid of data, small-scale discontinuities may develop. The five-point and median smoothers are used to eliminate these discontinuities. The five-point smoother does not affect the phase of the waves in the data.

At gridpoints where no observed data points fall within the influence area, one could expand the influence radius until some minimum number of data points were found. We did not use this procedure, because it implies an analysis with different maximum length scales in different regions, and we wish to minimize such differences.

The response function for the analyses presented in this atlas is given in Table 3. The response function represents the smoothing inherent in the objective analysis described above plus the effects of one application of the five-point smoother and one application of a five-point median smoother.

### 3.2f First guess field determination

There are gaps in the data coverage and, in some parts of the world ocean, there exist adjacent basins whose water mass properties are individually nearly homogeneous but have distinct basin-to-basin differences. Spurious features can be created when an influence area extends over two basins of this nature. Our choice of first-guess field attempts to minimize the creation of these features.

To provide a first guess field for the annual analysis at any standard level, we first zonally averaged the observed data in each one-degree latitude belt by individual ocean basins. In the work of Levitus (1982), the Mediterranean and Red Seas were treated as individual basins and the Venezuela Basin and the Sulu Sea were treated as individual basins below their sill depths. The Norwegian Sea and Arctic Ocean were treated separately below the sill depth of the

Greenland-Iceland-Shetland ridge. In the present work, additional basins have also been defined.

To avoid the problem of the influence region extending across land or sills to adjacent basins, the objective analysis program uses basin "identifiers" to avoid the use of data from adjacent basins. Table 4 lists these basins and the depth at which no exchange of information between basins is allowed during the objective analysis of data, i.e., "depths of mutual exclusion." Some regions are nearly, but not completely, isolated topographically. Because some of these nearly isolated basins have water mass properties that are different from surrounding basins, we have chosen to treat these as isolated basins as well. Not all such basins have been identified because of the complicated structure of the sea floor.

The zonal average computed for every one-degree belt in every individual ocean basin was used as the first guess for all one-degree squares in the belt. The reason for computing a separate first guess in each individual basin can be explained with the aid of equations (1) and (2). We have at any grid point  $(i,j)$  an analyzed value as defined by

$$G_{ij} = F_{ij} + \frac{\sum_{s=1}^n (W_s Q_s)}{\sum_{s=1}^n (W_s)} \quad (18)$$

For simplicity, we discuss the case in which only one observed data point falls within the influence area. The coordinates of this point will be denoted by  $i',j'$  on our grid. If we let  $OB_{ij}$  denote the observed one-degree square mean at this point then (18) becomes

$$G_{ij} = F_{ij} + (OB_{i',j'} - FG_{i',j'}) \quad (19)$$

Thus for this case the difference between the analyzed point and the first guess at point  $(i,j)$  is assumed to equal the first-guess at the point  $(i',j')$ . If the observed mean at a gridpoint is equal to the first-guess at that gridpoint, then the correction is zero, and this gridpoint will affect no other gridpoint. For situations where we have adjacent basins with individually nearly homogeneous properties (those not identified in Table 4), then defining a separate first-guess field for each basin means that the observed means in each basin are closer to their first-guess field than if this separation of basins had not been performed. Thus when the influence area extends across basins the

corrections are relatively small.

Iteration provided first guess fields for seasonal and monthly analyses. Annual analyses were used as first-guess fields for each of the four seasonal analyses. For salinity, a new annual analysis was computed as the mean of the four seasonal analyses, and then used as the first guess in a reanalysis of seasonal salinity data. This procedure produces slightly smoother annual means. More importantly we recognize that fairly large data-void regions exist, in some cases to such an extent that a seasonal or monthly analysis in these regions is not meaningful. We are interested in computing integral quantities such as salinity storage that are deviations from annual means. Geographic distribution of observations for the all-data annual periods (see appendices) is excellent for upper layers of the ocean. By using an all-data annual mean, first-guess field regions where data exists for only one season or month will show no contribution to the annual cycle. By contrast, if we used a zonal average for each season or month, then, in those latitudes where gaps exist, the first-guess field would be heavily biased by the few data points that exist. If these were anomalous data in some way, an entire basin wide belt might be affected.

One advantage of producing "global" fields for a particular compositing period (even though some regions are data void) is that such analyses can be modified by investigators for use in modelling studies. For example, England (1992) noted that the salinity distribution produced by Levitus (1982) for the Antarctic is too low (due to a lack of winter data for the Southern Hemisphere) to allow for the formation of Antarctic Intermediate Water in an ocean general circulation model. By increasing the salinity of the "observed" field the model was able to produce this water mass.

### 3.3 Choice of objective analysis procedures

Optimum interpolation (Gandin, 1963) has been used by some investigators to objectively analyze oceanographic data. We recognize the power of this technique but have not used it to produce analyzed fields. As described by Gandin (1963), optimum interpolation is used to analyze synoptic data using statistics based on historical data. In particular, second-order statistics such as correlation functions are used to estimate the distribution of first order parameters such as means. We attempt to map most fields in this atlas based on relatively sparse data sets. By necessity we must composite all data regardless of year of observation, to have enough data to produce a global, hemispheric, or regional analysis for a particular month,

season, or even yearly. Because of the paucity of data, we prefer not to use an analysis scheme that is based on second order statistics. In addition, as Gandin has also noted, there are two limiting cases associated with optimum interpolation. The first is when a data distribution is dense. In this case the choice of interpolation scheme makes little difference. The second case is when data are sparse. In this case an analyses scheme based on second order statistics is of questionable value. For additional information on objective analysis procedures, see Thiebaut and Pedder (1987) and Daley (1991).

### 3.4 Choice of spatial grid

We use the one-degree grid of Levitus (1982) which is based on the ocean topography defined by Smith *et al.*, (1966) as our spatial grid. We desire to build a set of climatological analyses that are identical in all respects for all parameters including relatively data sparse parameters such as nutrients. This provides investigators with a consistent set of analyses to work with. As more data are received at NODC/WDC-A, we will be able to produce higher resolution climatologies for certain parameters.

## 4. RESULTS

### 4.1 Annual mean salinity parameters at standard levels

#### 4.1a Explanation of standard level figures

All figures showing standard level analyses in this atlas series use similar symbols for displaying information. Continents are indicated as solid - black areas. Ocean areas shallower than the standard depth level being displayed are gray. Negative regions are dot stippled. Gridpoints for which there were less than three one-degree-square values available to "correct the first guess" are indicated by an X. Dashed lines represent non-standard contours. "H" and "L" indicate locations of the absolute maximum and minimum of the entire field. All figures were computer drafted. As a result some contours are not labelled. For clarity we use dark lines for every fourth or fifth contour in the standard level fields.

#### 4.1b Standard level analyses

Global distributions of annual mean salinity, at standard analysis levels are presented in Appendix B. Seasonal analyses are presented in Appendix G. Seasonal mean

minus annual mean difference fields of these parameters are presented in Appendix H.

### 4.2 Basin zonal averages

Basin zonal averages were computed using the definition of basins as shown in Fig. 4. Appendix C shows basin zonal averages of salinity.

### 4.3 Basin mean profiles and volume means

Area-weighted basin means of salinity parameters have been computed for the world ocean for each of the major ocean basin and for the northern and southern hemisphere portions of these basins and are presented as a function of depth in Appendices D. These means and associated standard errors are also presented in tabular form in the same appendices. The area and volume of each standard level over which the means are computed is given in Appendix E. The percentage contribution that each standard level contributes to the volume of each basin is given, as well as the number of independent points used in the standard error computation. Basin volume-weighted means and the total volume in each basin are also presented in Appendix E. Of course one can construct and display the basin-wide averages in a number of ways to serve various purposes. The tabulations allow users to graph the information and perform computations in any desired format.

The formula for defining an area weighted mean of some parameter  $X$  over the  $N$  ocean one-degree squares in a particular region or basin is

$$\bar{X}_N = \frac{\sum_{n=1}^N X_n A_n}{\sum_{n=1}^N A_n} \quad (20)$$

in which  $X_n$  represents the value of the parameter at the  $n^{\text{th}}$  one-degree square of the region, and  $A_n$  represents the area of the  $n^{\text{th}}$  one-degree square in the region. Computation of volume means uses formula (20) with the volume  $V_n$  replacing the area element  $A_n$ . The volume of a one-degree square box at any particular standard level is defined as follows. Excluding the sea surface and deepest standard level occurring at any one-degree square water column, the depth range  $\Delta z_k$ , through which a volume is computed for any standard level (denoted by  $k$ ), is given as

$$\Delta z_k = 0.5 [z_{k+1} - z_{k-1}] \quad (21)$$



in which  $z_{k+1}$  is the depth of the first standard level deeper than standard level  $k$ , and  $z_{k-1}$  is the depth of the first standard level shallower than standard level  $k$ . The volume of the sea surface standard level is taken over the 0-5 m depth interval. The depth range through which a volume is computed for the deepest standard level is given as

$$\Delta z_k = 0.5 [z_k - z_{k-1}] . \quad (22)$$

The standard error (S.E.) of each basin mean is computed as follows. The area-weighted root-mean-square deviation of all gridpoint values is computed (denoted as  $\sigma$ ). The total area of the standard level within the basin is computed and divided by the area defined by the influence radius of the objective analysis. This area is given as  $\pi R^2$  in which  $R=555$  km. The quotient yields a value,  $N_I$ , which is used as the number of independent points in estimating the standard error as

$$S.E. = \sigma / (N_I)^{1/2} .$$

## 5. SUMMARY

In the preceding sections we have described the results of a project to objectively analyze all historical salinity data archived at the National Oceanographic Data Center, Washington, D.C., plus additional data gathered as a result of the NODC and IOC data archaeology and rescue projects, that have not yet been incorporated into the NODC archive.

One advantage of the analysis techniques used in this atlas is that we know the amount of smoothing by objective analyses as given by the response function in Table 3. We believe this to be an important parameter in constructing and describing a climatology of any geophysical parameter. Particularly when computing anomalies from a standard climatology, it is important that the synoptic field be smoothed to the same extent as the climatology, to prevent generation of spurious anomalies simply through differences in smoothing. A second reason is that purely diagnostic computations require a minimum of seven or eight gridpoints to represent any Fourier component with accuracy. Higher order derivatives will require more smoothing.

We have attempted to create objectively analyzed fields and data sets that can be used as a "black box." We emphasize that some quality control procedures used are subjective. For those users who wish to make their own choices, all the data used in our analyses are available both at standard depth levels as well as observed depth levels. The results presented in this atlas show some features that are suspect and may be due to nonrepresentative or incorrect data that were not eliminated by the quality control techniques used. Although we have attempted to eliminate as many of these features as possible some obviously remain. Some may eventually turn out not to be artifacts but rather to represent real features, as yet undescribed.

## 6. FUTURE WORK

The acquisition of additional salinity data will allow for a more detailed description of the seasonal and monthly cycles. Our analyses will be updated when justified by additional observations.

## References

- Achtemeier, G. L., 1987: On the concept of varying influence radii for a successive corrections objective analysis. *Monthly Weather Review*, 11, 1761-1771.
- Barnes, S. L., 1964: A technique for maximizing details in numerical weather map analysis. *J. App. Meteor.*, 3, 396-409.
- \_\_\_\_\_, 1973: Mesoscale objective map analysis using weighted time series observations. *NOAA Technical Memorandum ERL NSSL-62*, 60 pp.
- Bergthorsson, P., and B. Doos, 1955: Numerical Weather map analysis. *Tellus*, 7, 329-340.
- Boyer, T., and S. Levitus, 1994: Quality control of historical temperature, salinity, and oxygen data. *NOAA Technical Report NESDIS* In preparation.
- Churgin, J., 1992: *Proceedings of the Ocean Climate Data Workshop*. Unpublished manuscript. Available from Users Services Branch, NODC, E/OC2, Universal Bldg., 1825 Connecticut Ave., NW, Washington, DC.
- Cressman, G. P., 1959: An operational objective analysis scheme. *Mon. Wea. Rev.*, 87, 329-340.
- Daley, R., 1991: *Atmospheric Data Analysis*. Cambridge University Press, Cambridge, 457 pp.
- England, M.H., 1992: On the formation of Antarctic Intermediate and Bottom Water in Ocean general circulation models. *J. Phys. Oceanogr.*, 22, 918- 926.
- Gandin, L.S., 1963: *Objective Analysis of Meteorological fields*. Gidrometeorol Izdat, Leningrad (translation by Israel program for Scientific Translations, Jerusalem, 1966, 242 pp.
- Hesselberg, T., and H. U. Sverdrup, 1914: Die Stabilitätsverhältnisse des Seewassers bei Vertikalen Verschiebungen. *Aarb. Bergen Mus.*, No. 14, 17 pp.
- Levitus, S., 1982: *Climatological Atlas of the World Ocean*, NOAA Professional Paper No. 13, U.S. Gov. Printing Office, 173 pp.
- Levitus, S., 1989a: Interpentadal Variability of Temperature and Salinity at Intermediate Depths of the North Atlantic Ocean, 1970-74 Versus 1955-59. *J. of Geophys. Res.-Oceans*, 94, 6091-6131.
- Levitus, S., 1989b: Interpentadal Variability of Salinity in the Upper 150 m of the North Atlantic Ocean, 1970-74 versus 1955-59. *J. of Geophys. Res.-Oceans*, 94, 9679-9685.
- Levitus, S., 1989c: Interpentadal Variability of Temperature and Salinity in the Deep North Atlantic, 1970-74 versus 1955-59. *J. of Geophys. Res.-Oceans*, 94, 16125-16131.
- Levitus, S., 1990: Interpentadal Variability of Steric Sea Level and Geopotential Thickness of the North Atlantic Ocean, 1970-74 versus 1955-59. *J. of Geophys. Res.-Oceans*, 95, 5233-5238.
- Levitus, S., R. Gelfeld, T. Boyer, and D. Johnson, 1994a: *Results of the NODC Oceanographic Data Archaeology and Rescue Projects*. Key to Oceanographic Records Documentation No. 19, NODC, Washington, D.C. , 73 pp.

- Levitus, S., J. Antonov, X. Zhou, H. Dooley, K. Selemenov, and V. Tereschenkov, 1994b: Decadal-Scale Variability of the North Atlantic Ocean. Accepted by National Academy of Sciences Press, Natural Climate Variability on decade-to-century time scales.
- Lynn, and J. L. Reid, 1968: Characteristics and Circulation of Deep and Abyssal Waters. *Deep Sea Research.*, 15, 577-598.
- NODC, 1993: *NODC User's Guide*. National Oceanic and Atmospheric Administration, Washington, D.C.
- Neumann, G. and W. J. Pierson, 1966: *Principles of Physical Oceanography*. Prentice Hall Inc., Englewood Cliffs, N.J., 545 pp.
- Muromtsev, A.M., 1958: *The Principal Hydrological Features of the Pacific Ocean*. Main Administration of the Hydrometeorological Service of the USSR Council of Ministers, State Oceanographic Institute, (Published for National Science Foundation, Washington, D.C. by the Israel Program for Scientific Translations, Jerusalem, 1963, 417 pp.)
- Olbers, D., V. Gouretzki, G. Seib, J. Schroeter, 1992: *The Hydrographic Atlas of the Southern Ocean*, Alfred-Wegener-Institute for Polar and Marine Research, Bremerhaven, 17 pp., 82 plates.
- Rabiner, L. R., M. R. Sambur, and C. E. Schmidt, 1975: *Applications of a nonlinear smoothing algorithm to speech processing*, *IEEE Trans. on Acoustics, Speech and Signal Processing*, Vol. Assp-23, 552-557.
- Reiniger, R.F., and C.F. Ross, 1968: A method of interpolation with application to oceanographic data. *Deep-Sea Res.*, 9, 185-193.
- Sasaki, Y., 1960: An objective analysis for determining initial conditions for the primitive equations. Ref. 60-1 6T, Atmospheric Research Lab., Univ. of Oklahoma Research Institute, Norman, 23 pp.
- Schubert, O. von, 1935: Die Stabilitätsverhältnisse im Atlantischen Ozean. *W'ss. Ergebn. dt. atlant. Exped Meteor 1925-1927*, 6(2), (1), 54 pp.
- Seaman, R. S., 1983. Objective Analysis accuracies of statistical interpolation and successive correction schemes. *Australian Meteor. Mag.*, 31, 225-240.
- Shuman, F. G., 1957: Numerical methods in weather prediction: II. Smoothing and filtering. *Mon. Wea. Rev.*, 85, 357-361.
- Smith, D. R., and F. Leslie, 1984: Error determination of a successive correction type objective analysis scheme. *Journal Atm. and Oceanic Tech.*, 1, 121-130.
- Smith, D.R., M.E. Pumphry, J.T. Snow, 1986: A comparison of errors in objectively analyzed fields for uniform and nonuniform station distribution, *J. Atm. and Oceanic Tech.* 3, 84-97.
- Smith, S. M, H. W. Menard, and G. Sharman, 1966: *Worldwide ocean depths and continental elevations*. SIO Ref. G5-8, Scripps Institution of Oceanography, Univ. of California, La Jolla, 17 pp.
- Spilhaus, A. F., A. Ehrlich, and A.R. Miller, 1950: Hydrostatic instability in the ocean. *Transactions Amer. Geophys. Union.*, 31(2).
- Sverdrup, H.U., M.W. Johnson, and R.H. Fleming, 1942: *The Oceans: Their physics, chemistry, and general biology*. Prentice Hall, 1060 pp.

Thiebaux, H.J., M.A. Pedder, 1987: *Spatial Objective Analysis: with applications in atmospheric science*. Academic Press, 299 pp.

Tukey, J. W., 1974: Nonlinear (nonsuperposable) methods for smoothing data, in "*Cong. Rec.*", 1974 EASCON, 673 pp.

UNESCO, 1991: *Processing of Oceanographic Station Data*. Imprimerie des Presses Unibversitaires de France, Imprimerie des Presses Universitaires de France, Vendome, 138 pp.

Table 1. Distribution with depth of the number of one-degree squares of ocean (Ocean ODSQS), the number (N) of salinity observations; and the number of one-degree squares (ODSQS) containing salinity observations.

Standard Level	Depth (m)	Ocean ODSQS	N	ODSQS
1	0	42164	1186507	29544
2	10	42054	1147880	29593
3	20	41936	1094177	29560
4	30	41809	1027197	29406
5	50	41244	927273	29041
6	75	40945	788306	28301
7	100	40327	698226	27810
8	125	40169	603376	27165
9	150	39858	574485	26975
10	200	39255	445383	25651
11	250	39058	476099	26439
12	300	38623	414442	25824
13	400	38272	309048	24177
14	500	37849	249658	22529
15	600	37579	156252	19462
16	700	37352	109738	17499
17	800	37059	93804	16257
18	900	36879	177247	21273
19	1000	36493	149911	19936
20	1100	36315	116611	18285
21	1200	36057	84847	16138
22	1300	35862	70431	15250
23	1400	35716	61161	13834
24	1500	35405	44112	12502
25	1750	34914	19529	8296
26	2000	33856	59196	14333
27	2500	32077	32827	11736
28	3000	29188	24724	9931
29	3500	25089	19173	8039
30	4000	19718	14463	6110
31	4500	12856	8758	4093
32	5000	6883	5118	2315
33	5500	1847	2513	1004

Table 2. Acceptable distances for "inside" and "outside" values used in the Reiniger-Ross scheme for interpolating observed level data to standard levels

Standard Levels	Standard Depths	Acceptable distances for inside values	Acceptable distances for outside values
1	0	5	200
2	10	50	200
3	20	50	200
4	30	50	200
5	50	50	200
6	75	50	200
7	100	50	200
8	125	50	200
9	150	50	200
10	200	50	200
11	250	100	200
12	300	100	200
13	400	100	200
14	500	100	400
15	600	100	400
16	700	100	400
17	800	100	400
18	900	200	400
19	1000	200	400
20	1100	200	400
21	1200	200	400
22	1300	200	1000
23	1400	200	1000
24	1500	200	1000
25	1750	200	1000
26	2000	1000	1000
27	2500	1000	1000
28	3000	1000	1000
29	3500	1000	1000
30	4000	1000	1000
31	4500	1000	1000
32	5000	1000	1000
33	5500	1000	1000

Table 3. Response function of the objective analysis scheme as a function of wavelength.

Wavelength*	Response Function
360 $\Delta X$	0.999
180 $\Delta X$	0.997
120 $\Delta X$	0.994
90 $\Delta X$	0.989
72 $\Delta X$	0.983
60 $\Delta X$	0.976
45 $\Delta X$	0.957
40 $\Delta X$	0.946
36 $\Delta X$	0.934
30 $\Delta X$	0.907
24 $\Delta X$	0.857
20 $\Delta X$	0.801
18 $\Delta X$	0.759
15 $\Delta X$	0.671
12 $\Delta X$	0.532
10 $\Delta X$	0.397
9 $\Delta X$	0.315
8 $\Delta X$	0.226
6 $\Delta X$	0.059
5 $\Delta X$	0.019
4 $\Delta X$	$2.23 \times 10^{-3}$
3 $\Delta X$	$1.90 \times 10^{-4}$
2 $\Delta X$	$5.30 \times 10^{-7}$

\* For  $\Delta X = 111$  km

Table 4. Basin identifiers and depths of "mutual exclusion" used in this study

Basin	Depth (m)	Basin	Depth (m)
Atlantic Ocean	---*	Pacific Ocean	---*
Indian Ocean	---*	Mediterranean Sea	---*
Baltic Sea	0	Black Sea	0
Red Sea	0	Persian Gulf	0
Hudson Bay	0	Southern Ocean	---*
Arctic Ocean (Bering)	0	Sea of Japan	125
Kara Sea	200	Sulu Sea	500
Arctic Ocean (Atlantic)	600	Baffin Bay	700
East Mediterranean	1000	West Mediterranean	1000
Sea of Oshkotsk	1300	Banda Sea	1400
Caribbean Sea	1400	Andaman Basin	2000
North Caribbean	2000	Gulf of Mexico	2000
Beaufort Sea	3000	South China Sea	3000
Barent Sea	3000	Celebes Sea	3000
Aleutian Basin	3000	Fiji Basin	3500
North American Basin	3500	West European Basin	3500
Southeast Indian Basin	3500	Coral Sea	3500
East Indian Ocean	3500	Central Indian Ocean	3500
Southwest Atlantic	3500	East South Atlantic	3500
Southeast Pacific	3500	Guatemala Basin	3500
East Caroline Basin	4000	Marianas Basin	4000
Phillipine Sea	4000	Arabian Sea	4000
Chile Basin	4000	Somali Basin	4000
Mascarine Basin	4500	Guinea Basin	4500
Croset Basin	4500	Brazil Basin	4500
Argentine Basin	4500	Tasman Sea	4500

\*Basins marked with a dash can interact with each other except certain areas such as the Isthmus of Panama



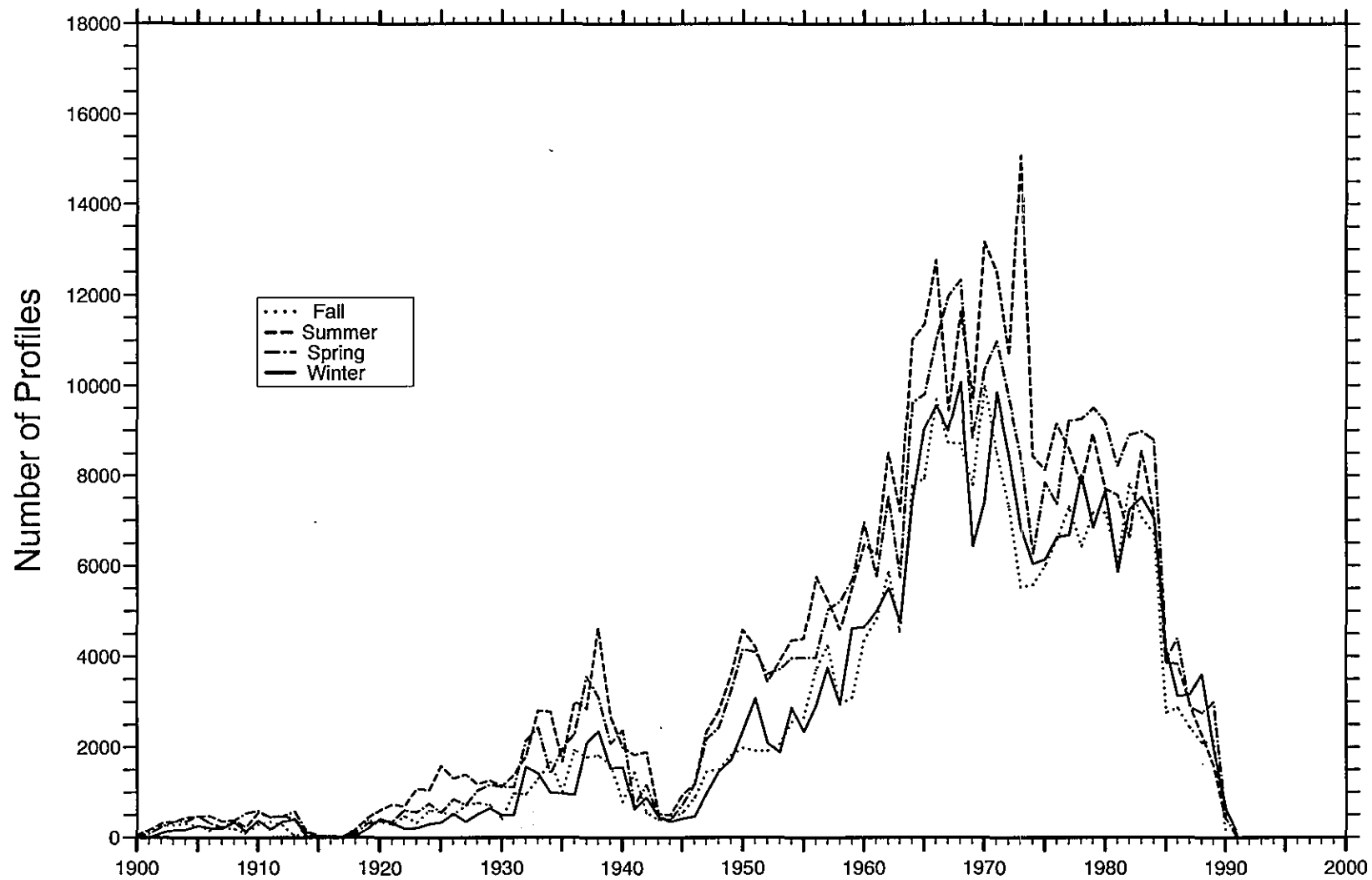


Figure 1. Time series of the number of salinity profiles as a function of year for each season.

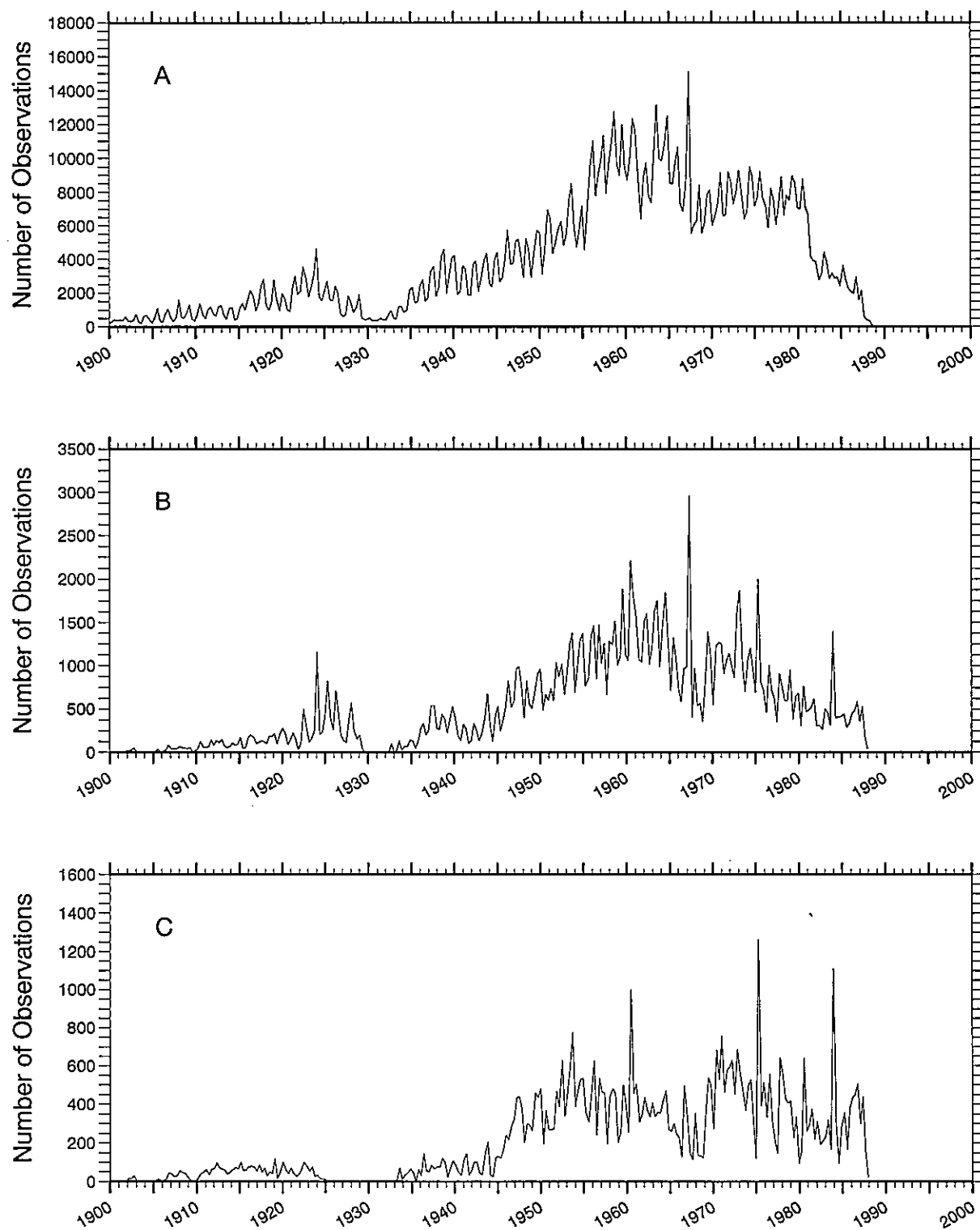
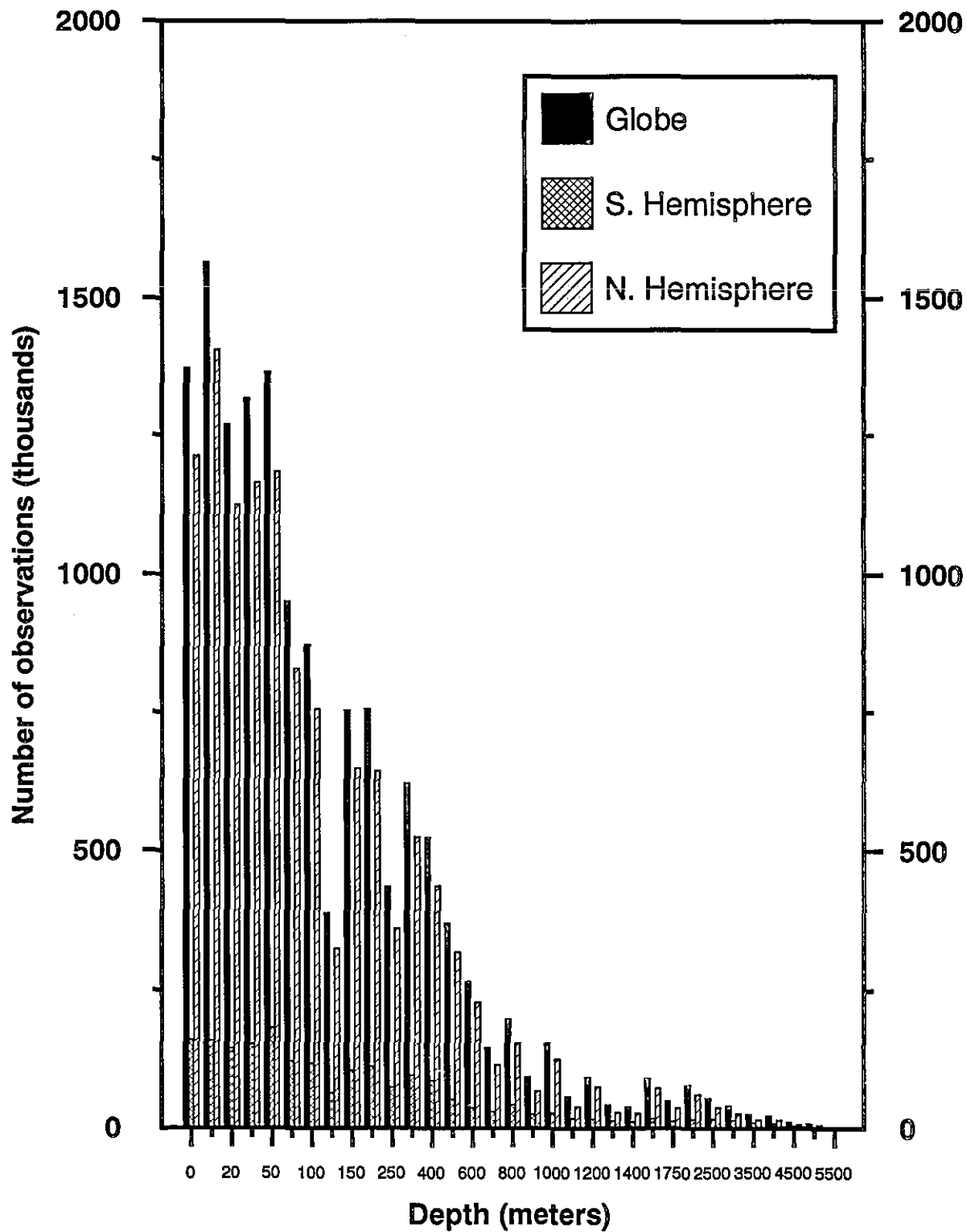


Figure 2. Time series of the number of salinity observations as a function of year A) at the sea surface, B) at 1000 m, C) at 2000 m.

**Fig. 3 Distribution of salinity observations as a function of depth for the globe and Northern and Southern Hemispheres**



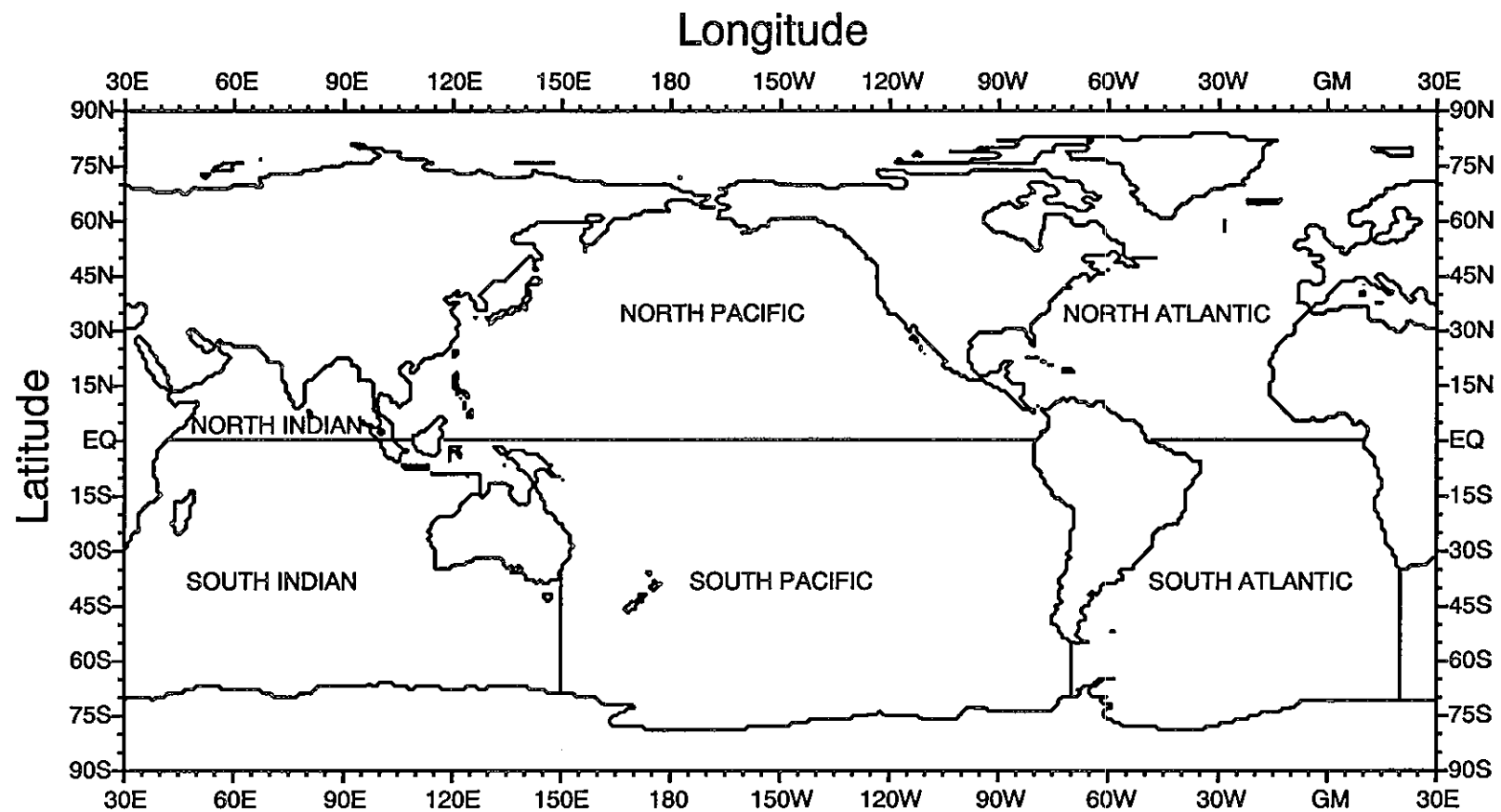


Fig 4. Division of world ocean into individual basins.

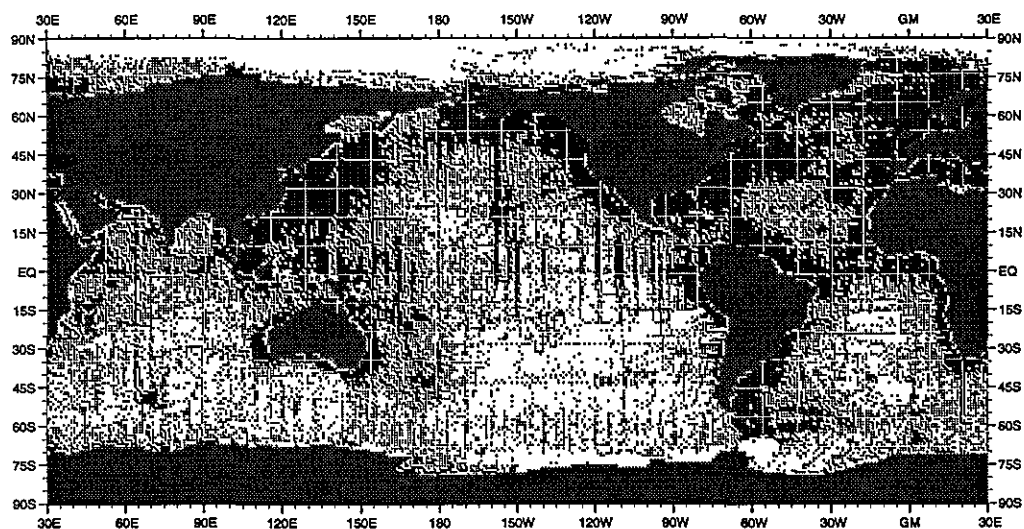


Fig. A1 Annual distribution of salinity observations at the surface

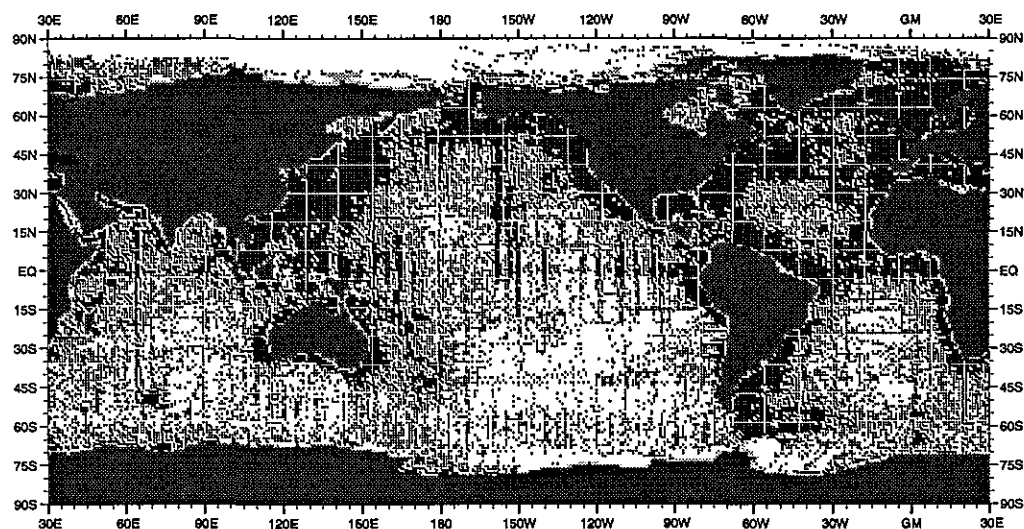


Fig. A2 Annual distribution of salinity observations at 30 m depth

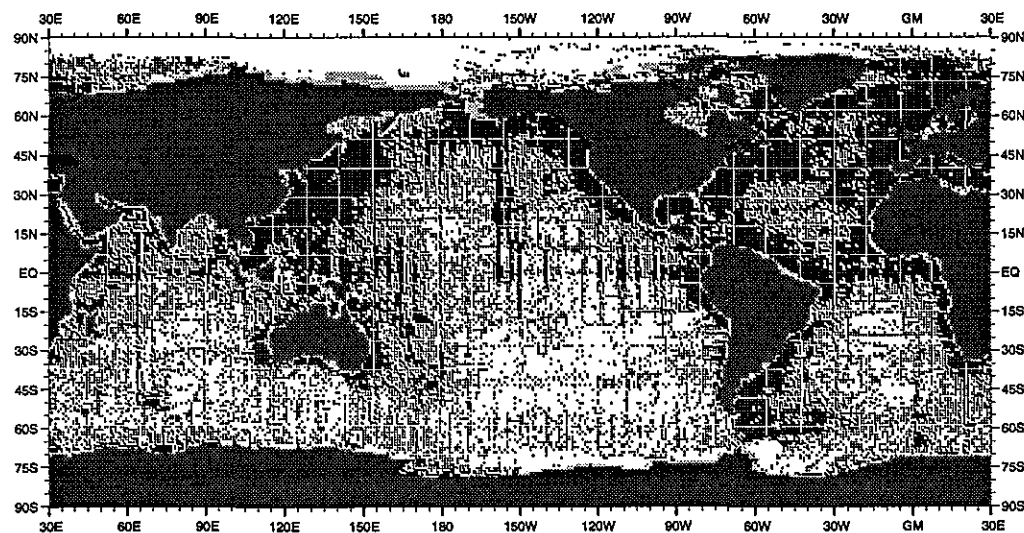


Fig. A3 Annual distribution of salinity observations at 50 m depth

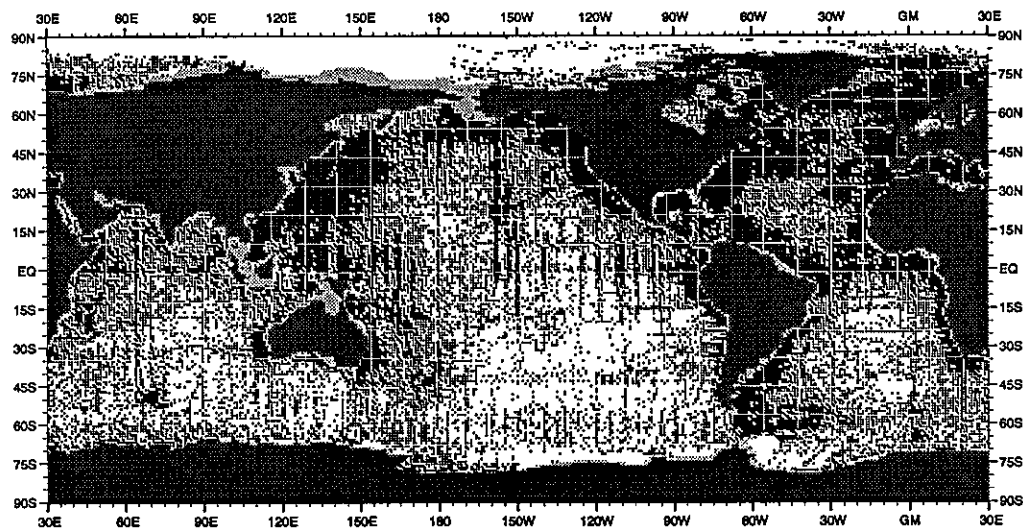


Fig. A4 Annual distribution of salinity observations at 75 m depth

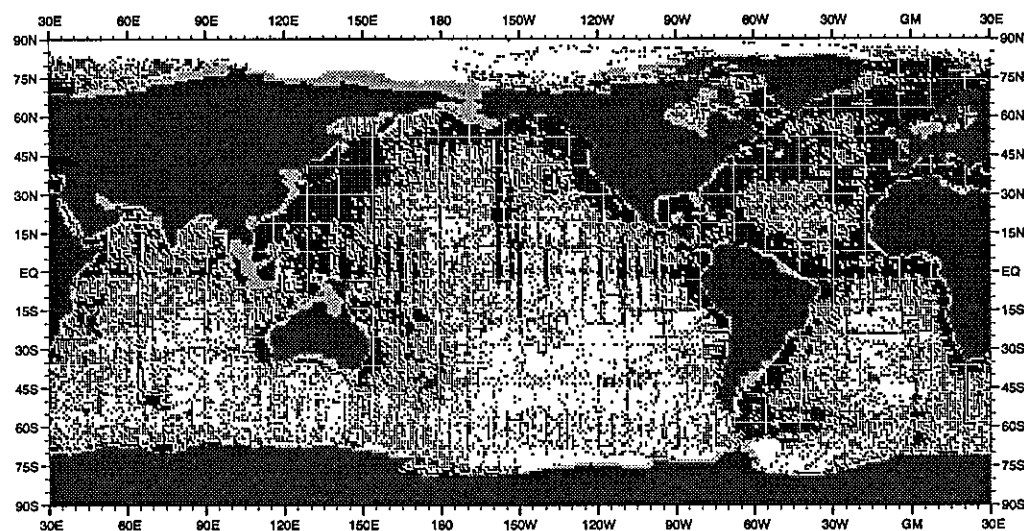


Fig. A5 Annual distribution of salinity observations at 100 m depth

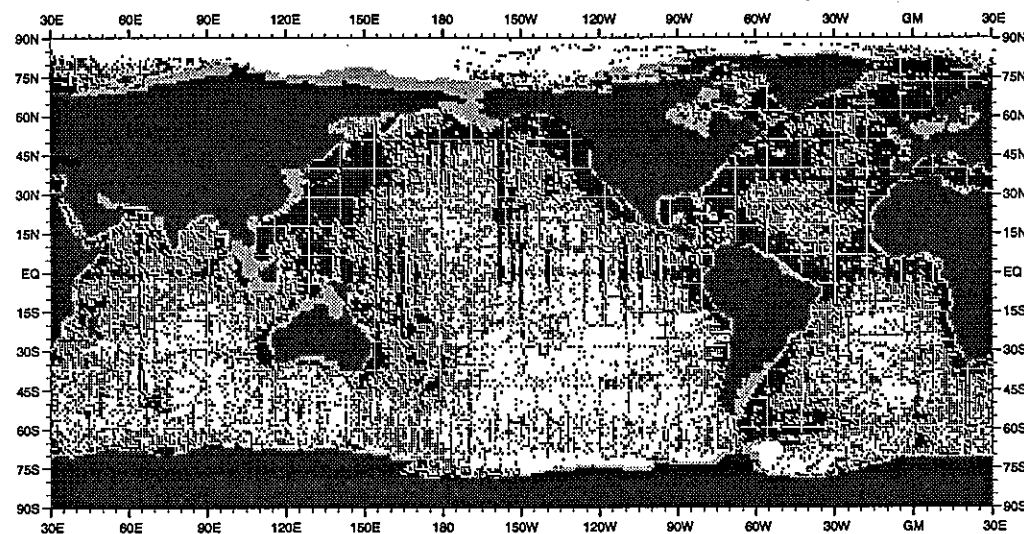


Fig. A6 Annual distribution of salinity observations at 125 m depth

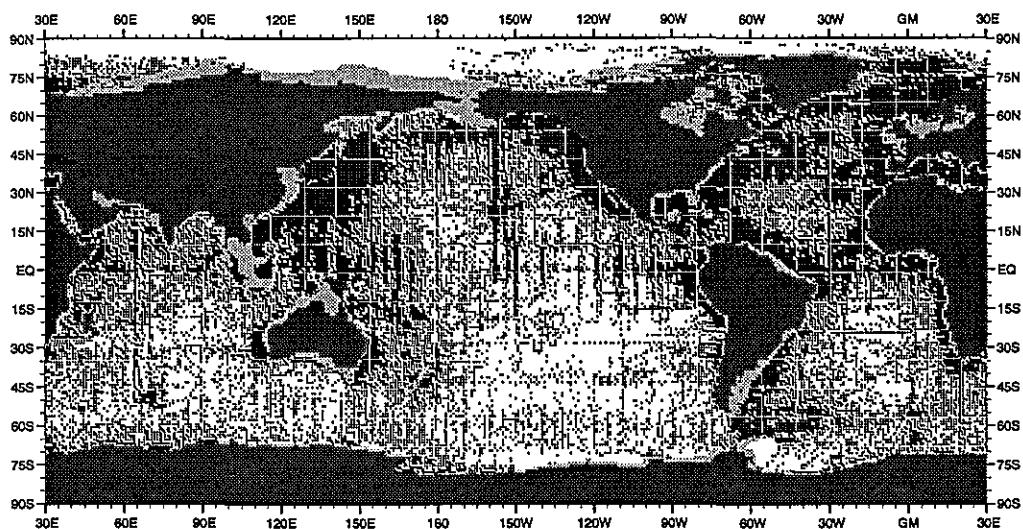


Fig. A7 Annual distribution of salinity observations at 150 m depth

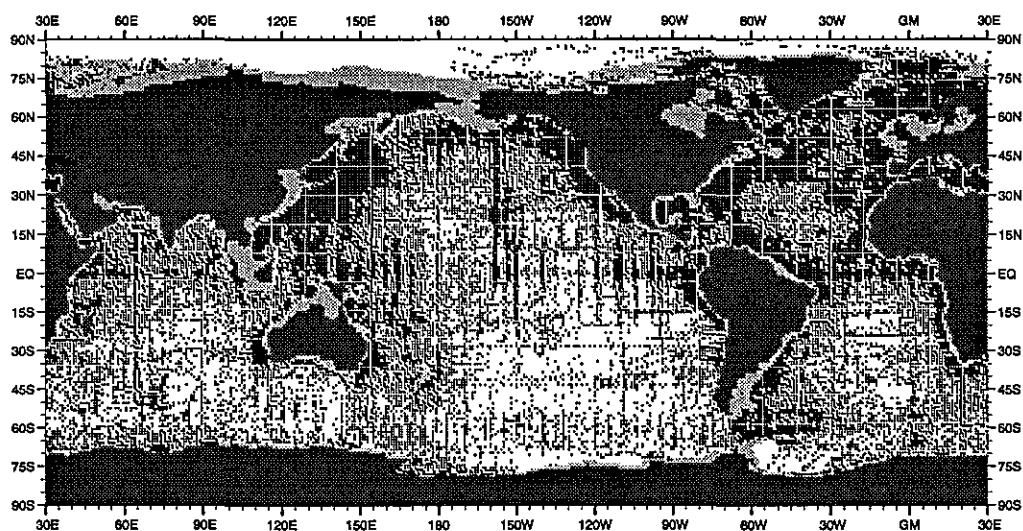


Fig. A8 Annual distribution of salinity observations at 250 m depth

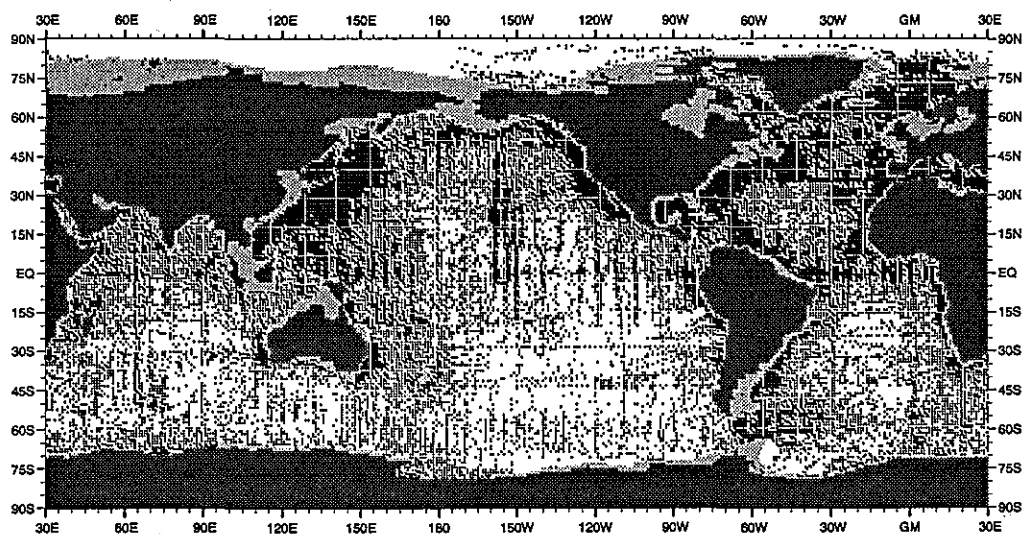


Fig. A9 Annual distribution of salinity observations at 400 m depth

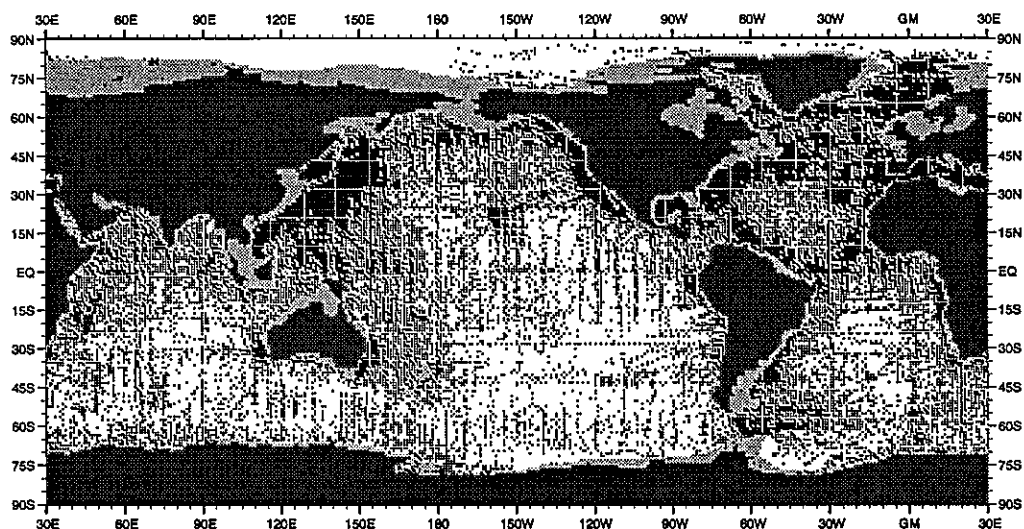


Fig. A10 Annual distribution of salinity observations at 500 m depth

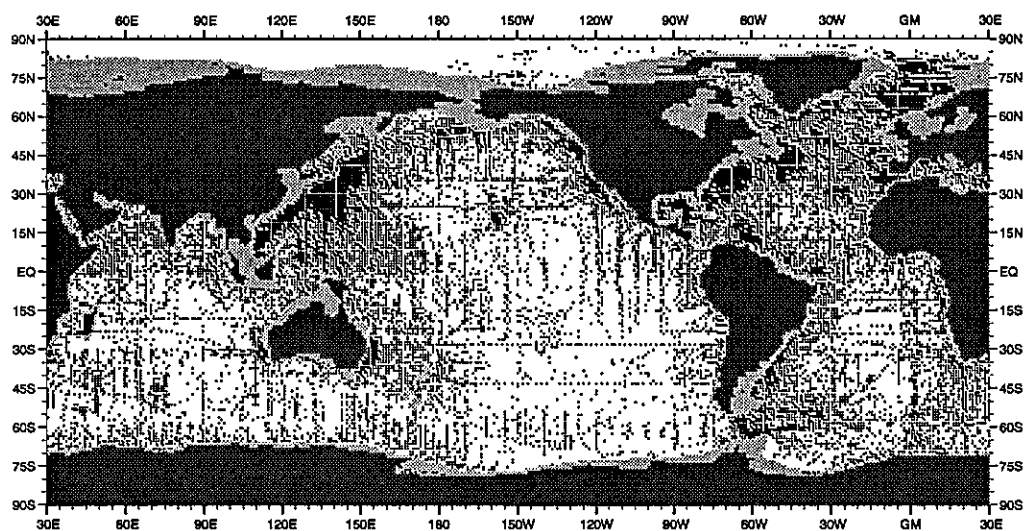


Fig. A11 Annual distribution of salinity observations at 700 m depth

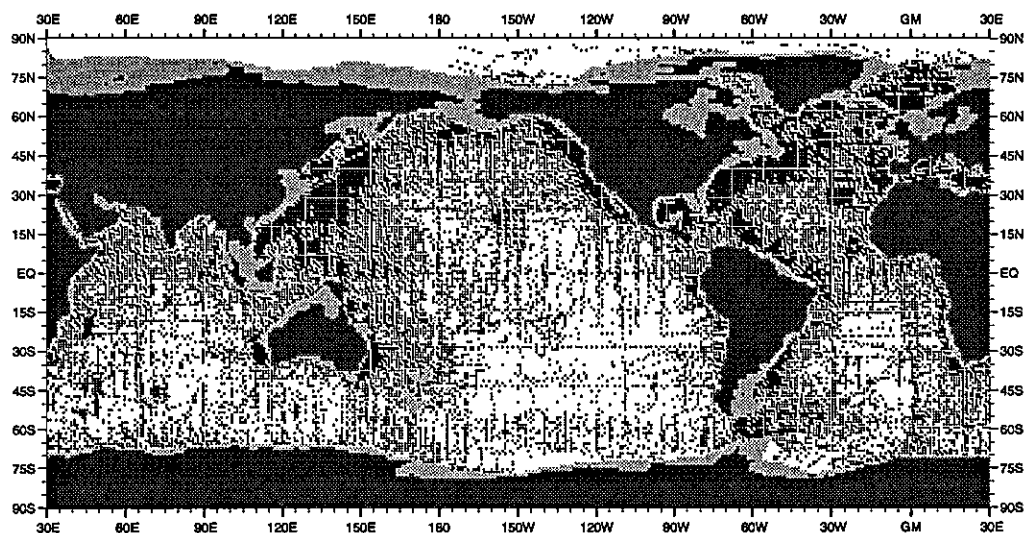


Fig. A12 Annual distribution of salinity observations at 900 m depth



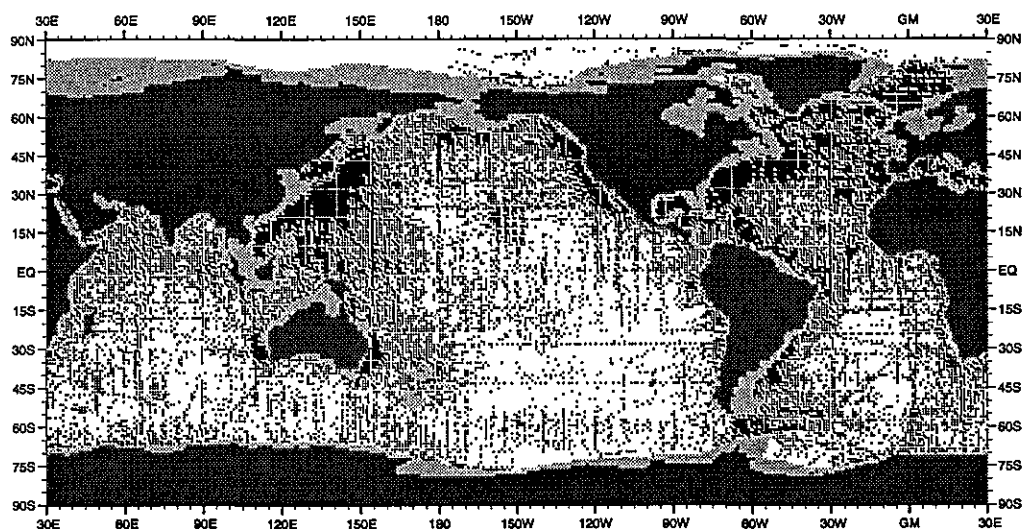


Fig. A13 Annual distribution of salinity observations at 1000 m depth

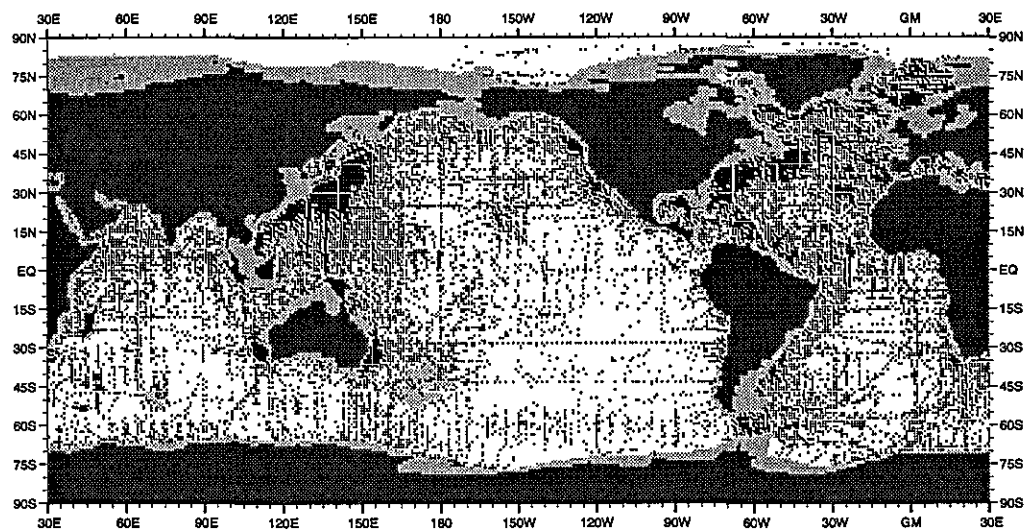


Fig. A14 Annual distribution of salinity observations at 1200 m depth

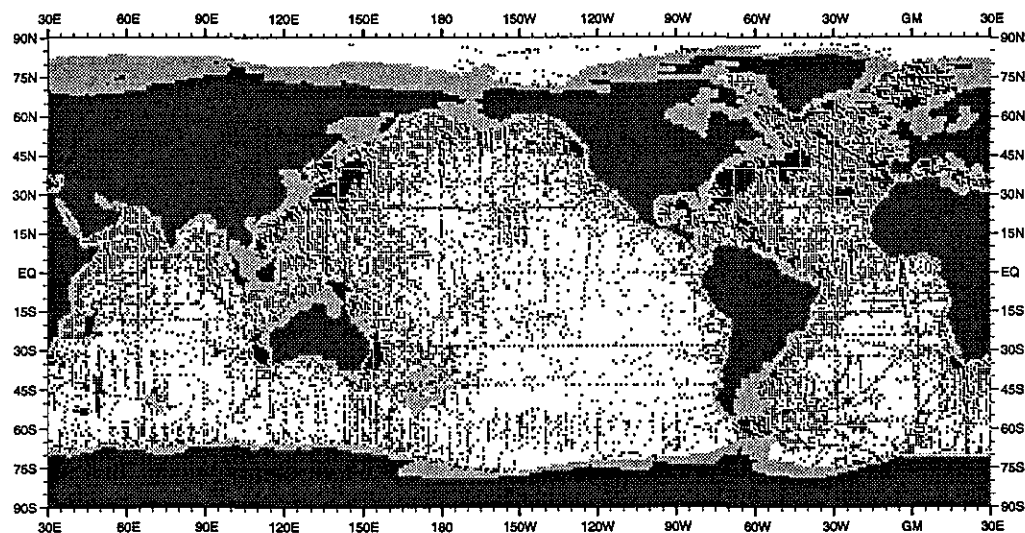


Fig. A15 Annual distribution of salinity observations at 1300 m depth

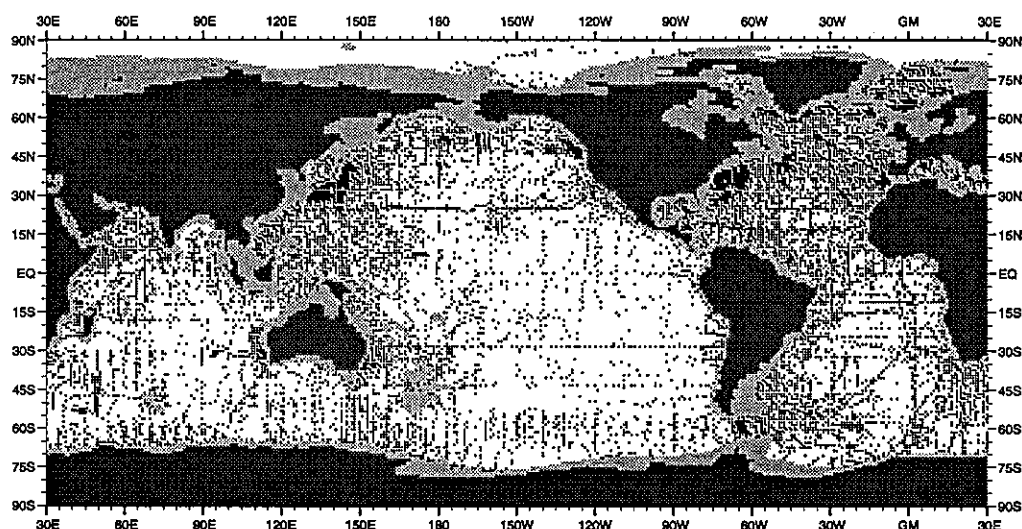


Fig. A16 Annual distribution of salinity observations at 1500 m depth

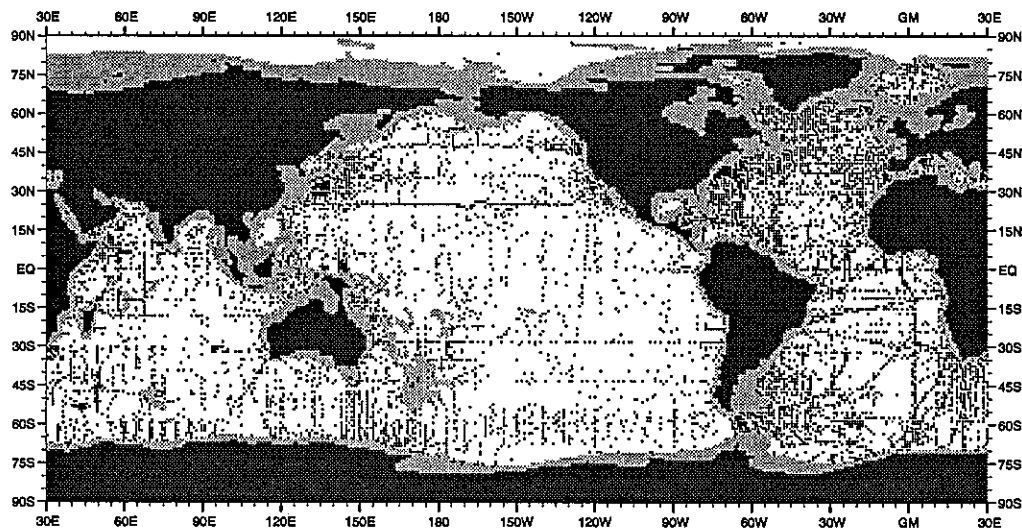


Fig. A17 Annual distribution of salinity observations at 1750 m depth

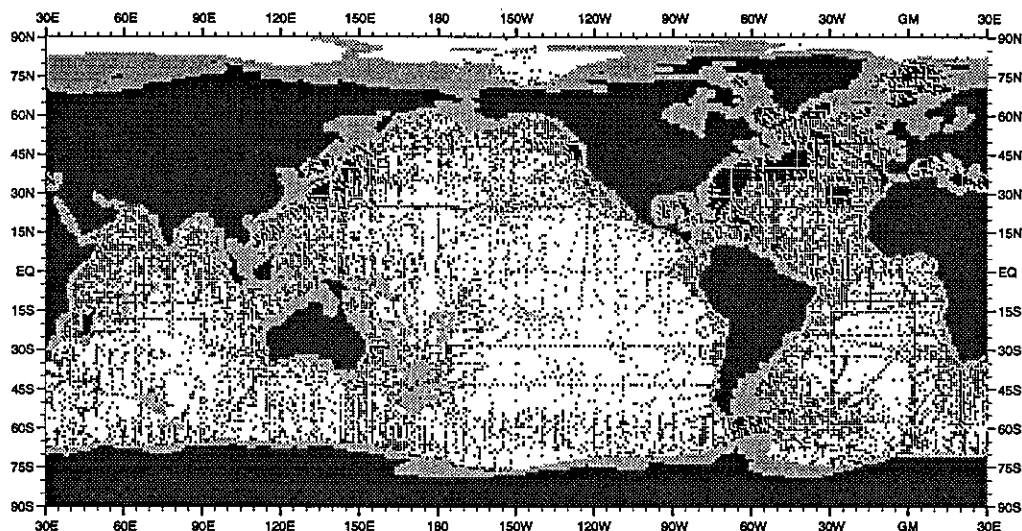


Fig. A18 Annual distribution of salinity observations at 2000 m depth

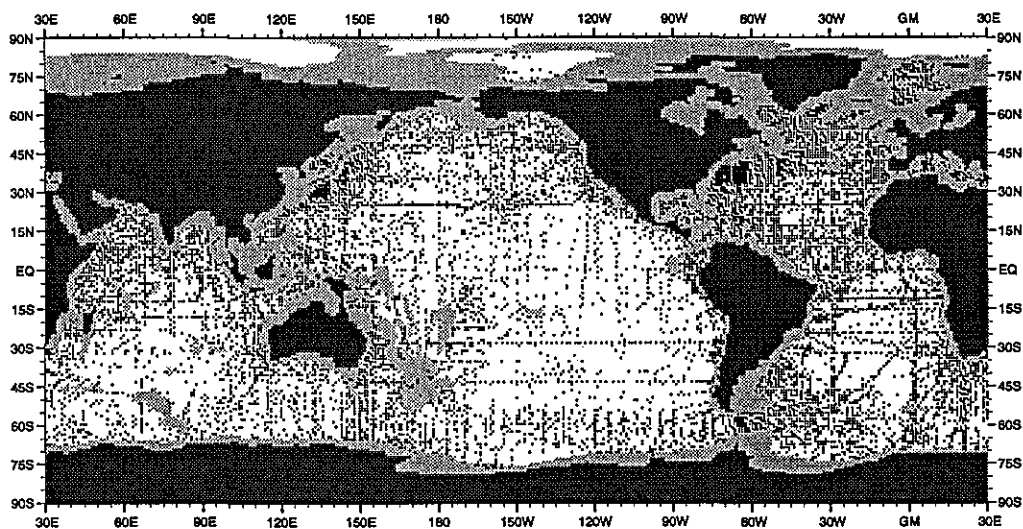


Fig. A19 Annual distribution of salinity observations at 2500 m depth

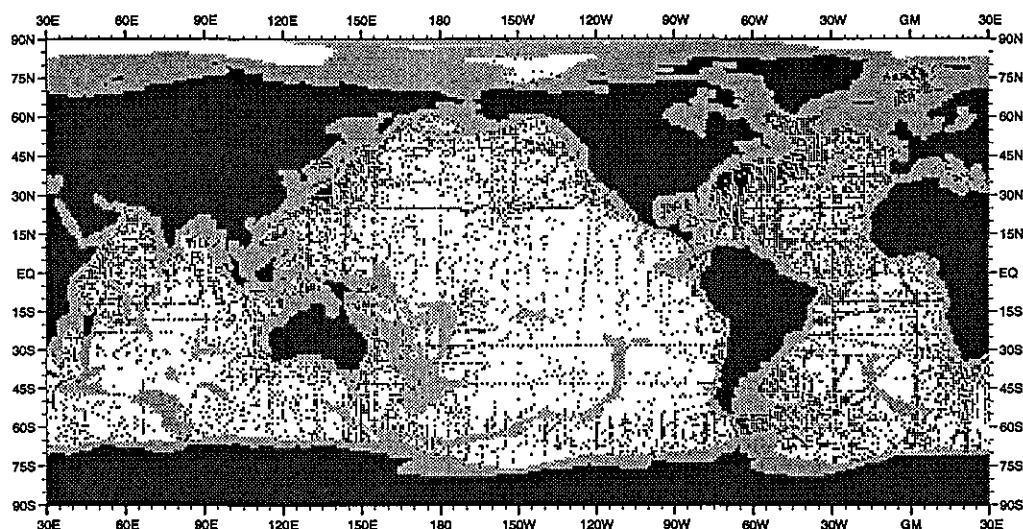


Fig. A20 Annual distribution of salinity observations at 3000 m depth

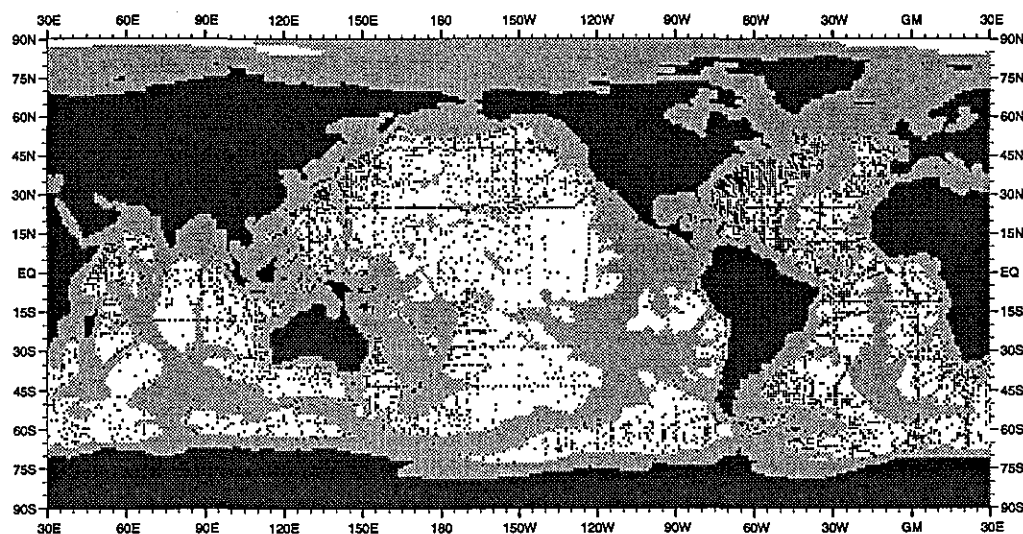


Fig. A21 Annual distribution of salinity observations at 4000 m depth

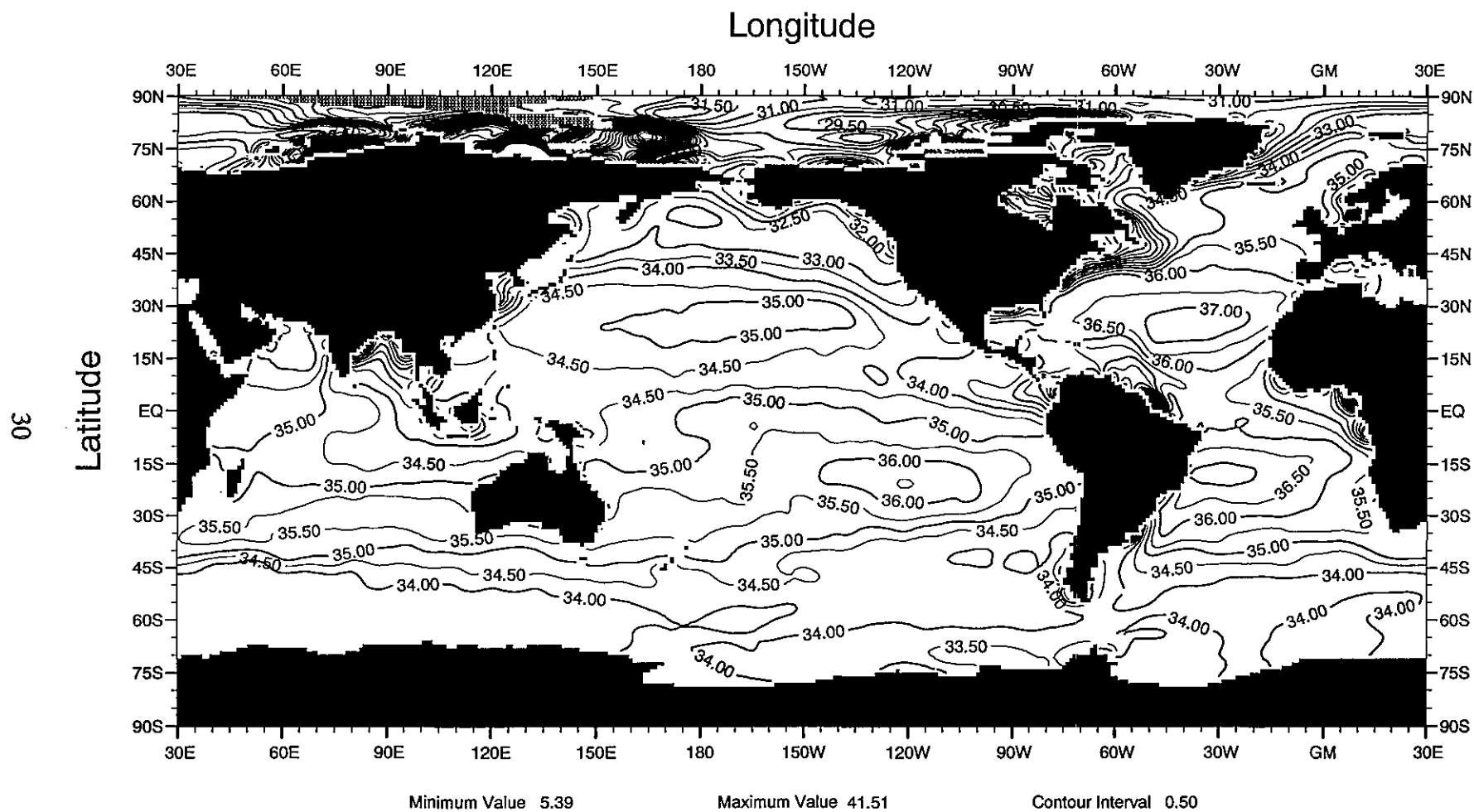


Fig. B1 Annual mean salinity (psu) at the surface

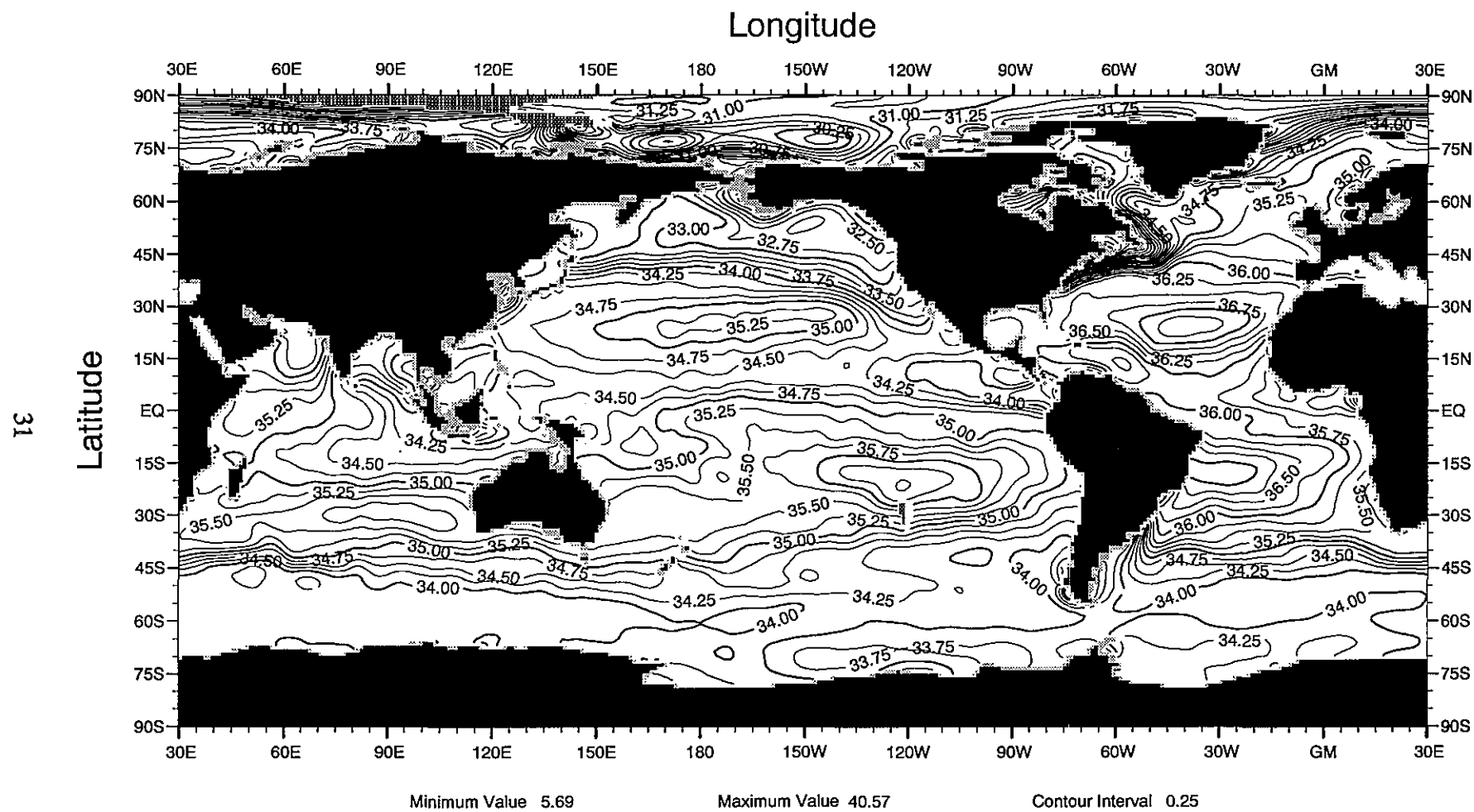


Fig. B2 Annual mean salinity (psu) at 30 m depth

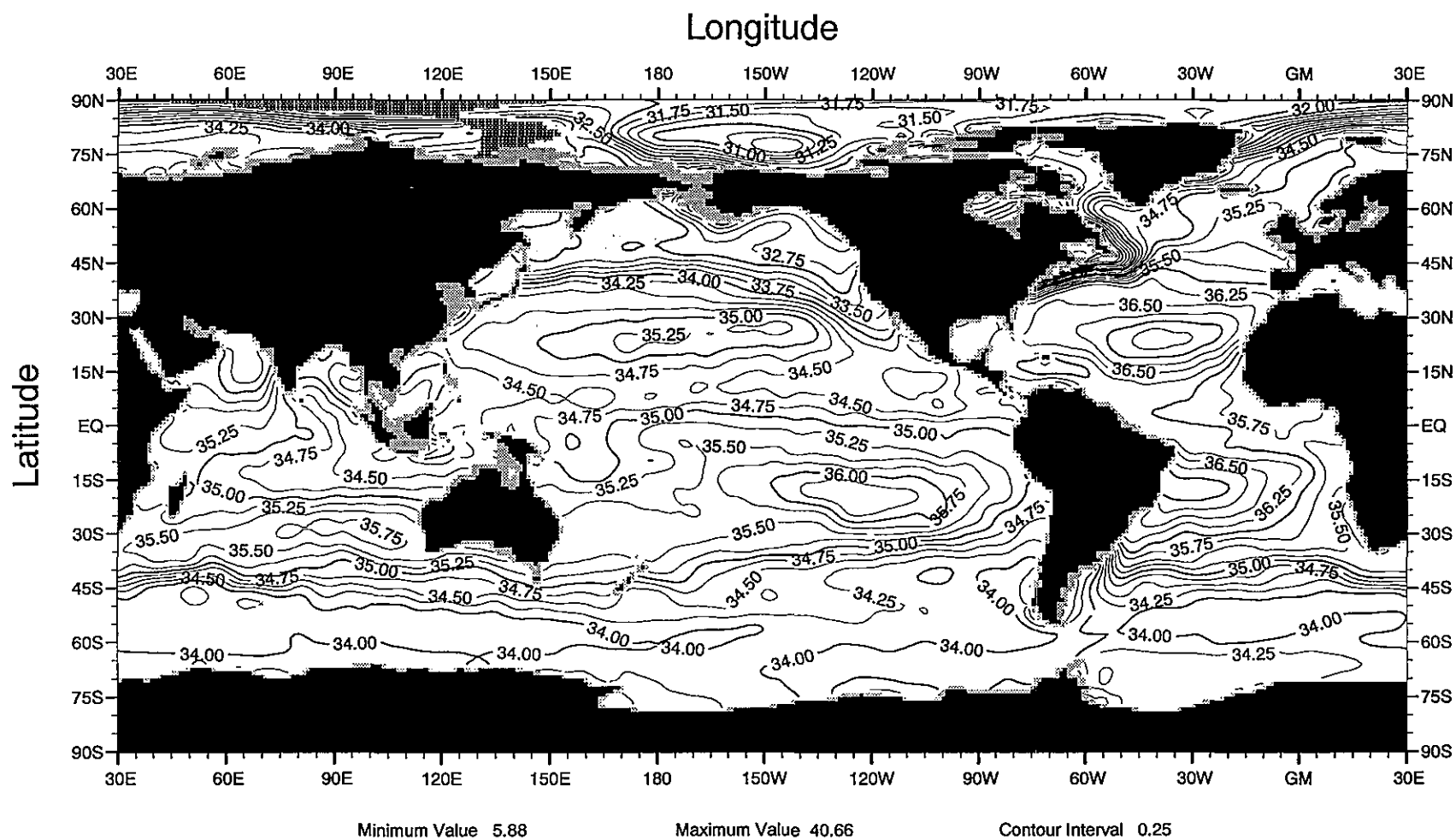


Fig. B3 Annual mean salinity (psu) at 50 m depth

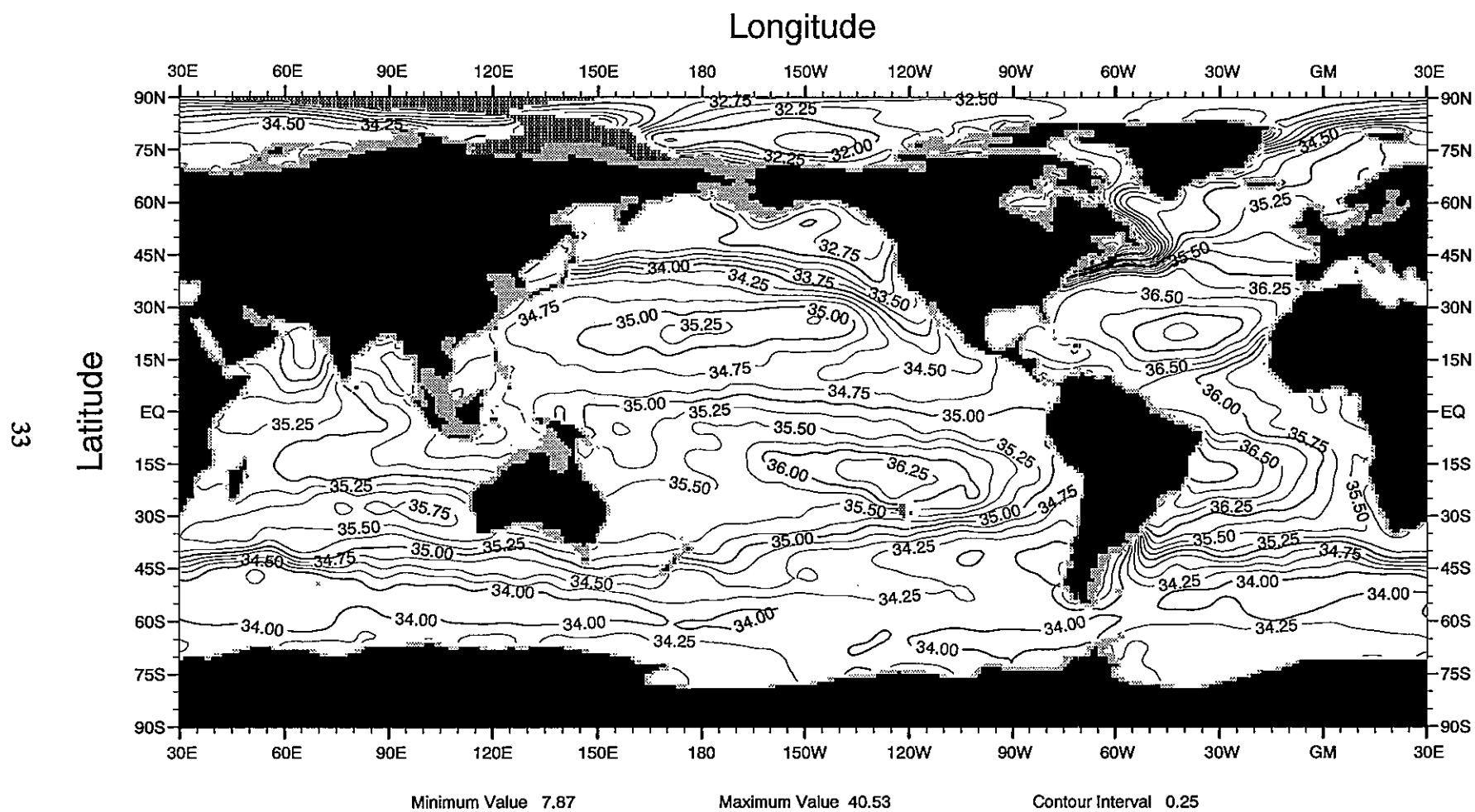


Fig. B4 Annual mean salinity (psu) at 75 m depth

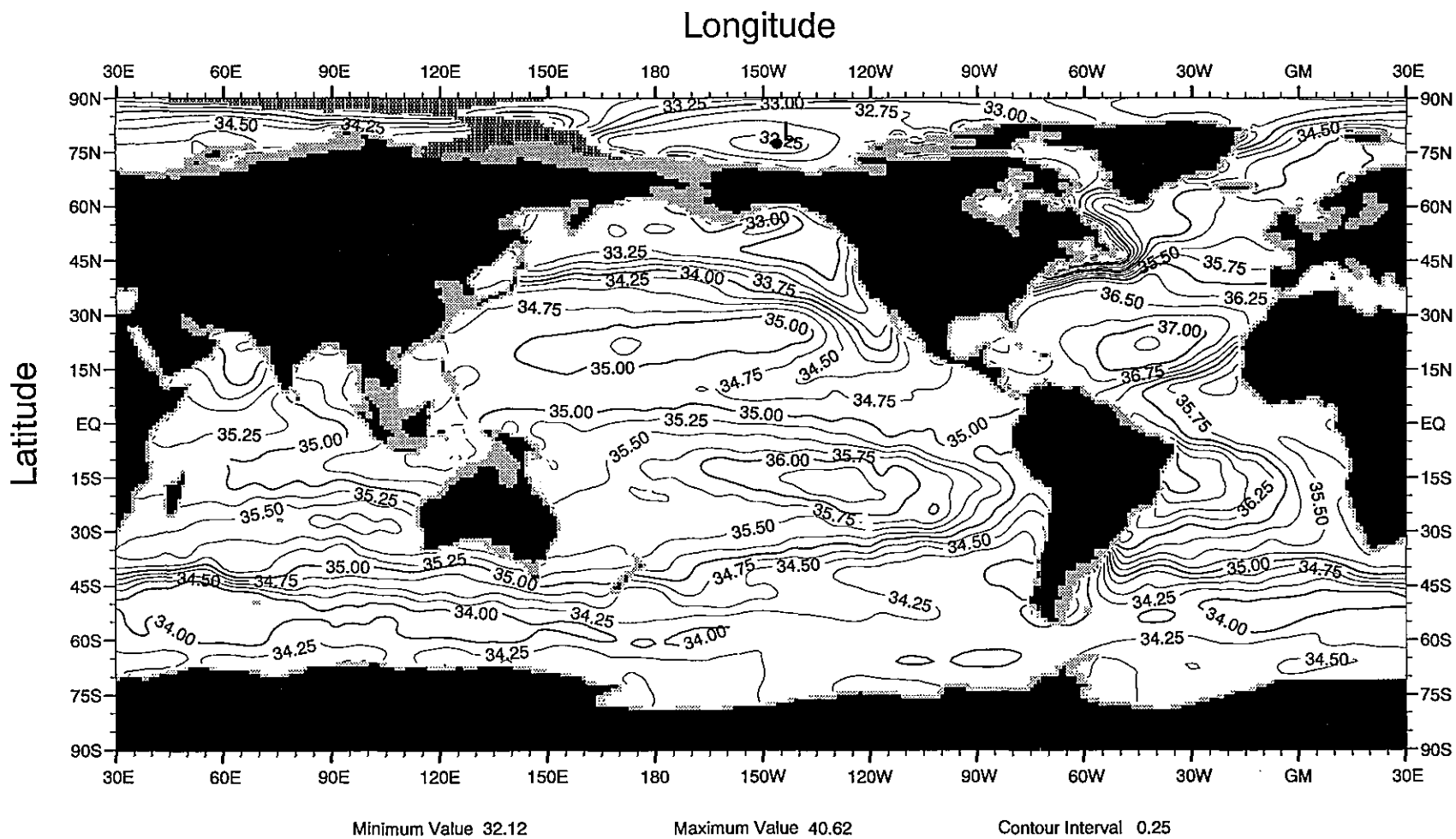


Fig. B5 Annual mean salinity (psu) at 100 m depth



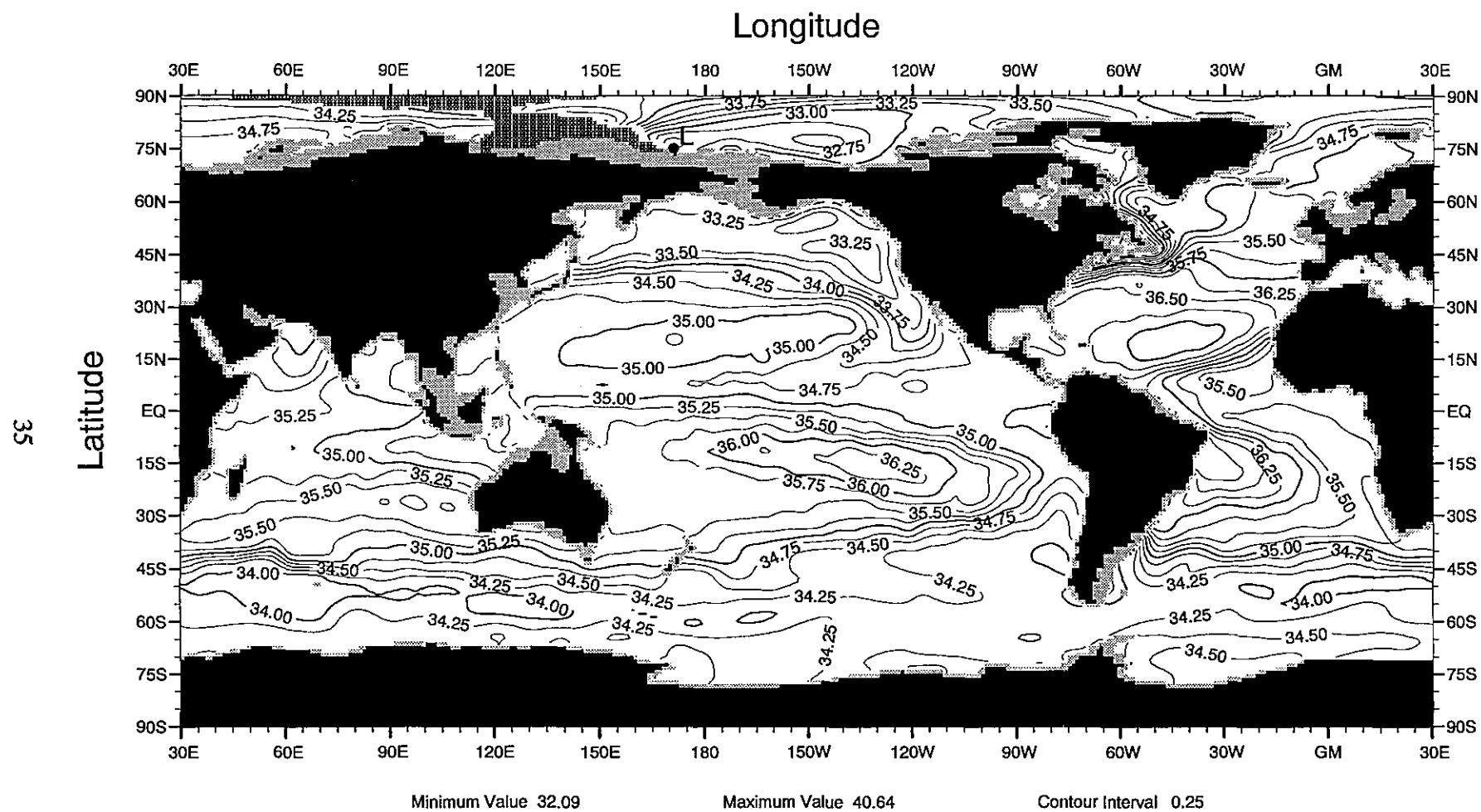


Fig. B6 Annual mean salinity (psu) at 125 m depth

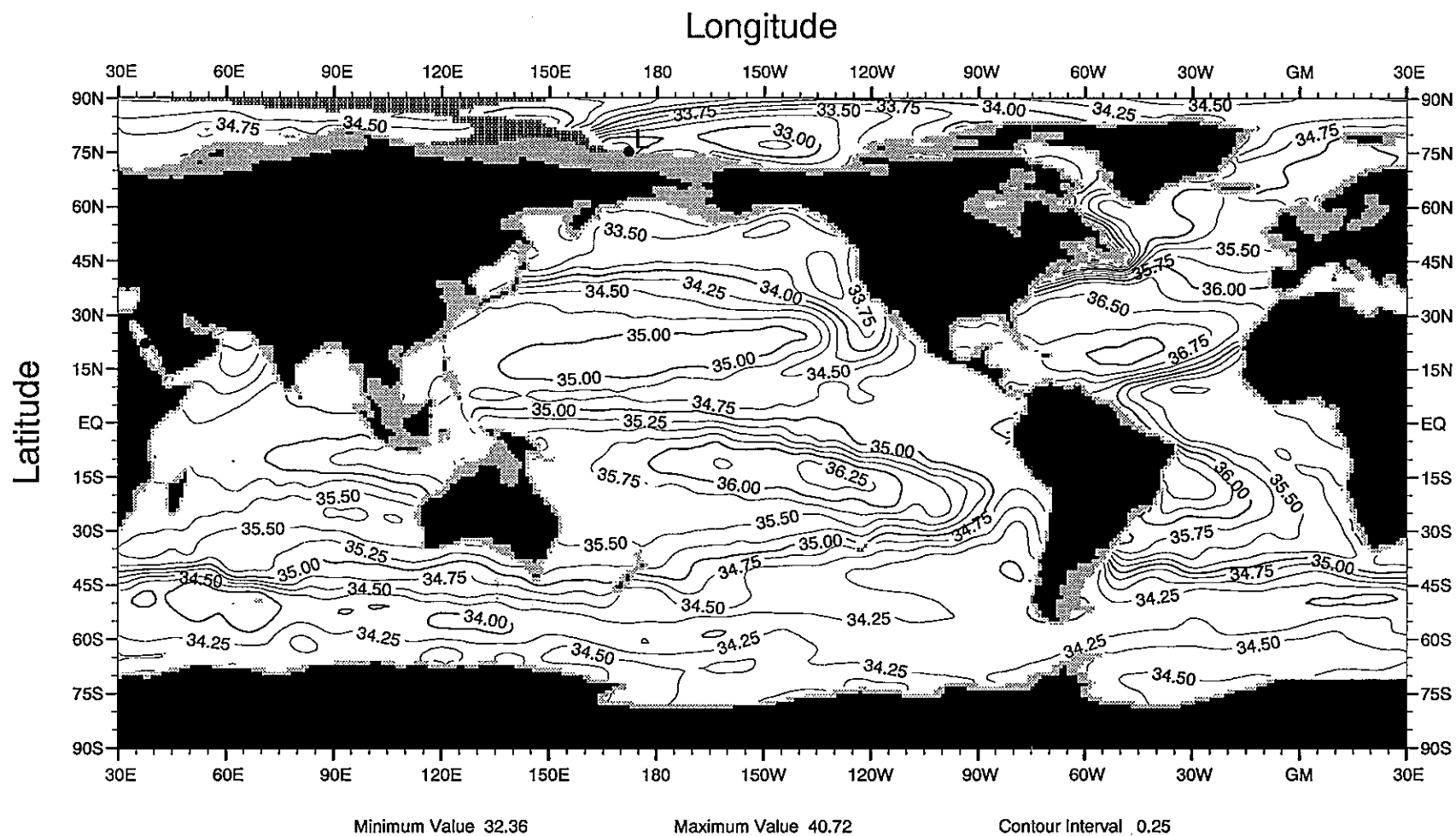


Fig. B7 Annual mean salinity (psu) at 150 m depth

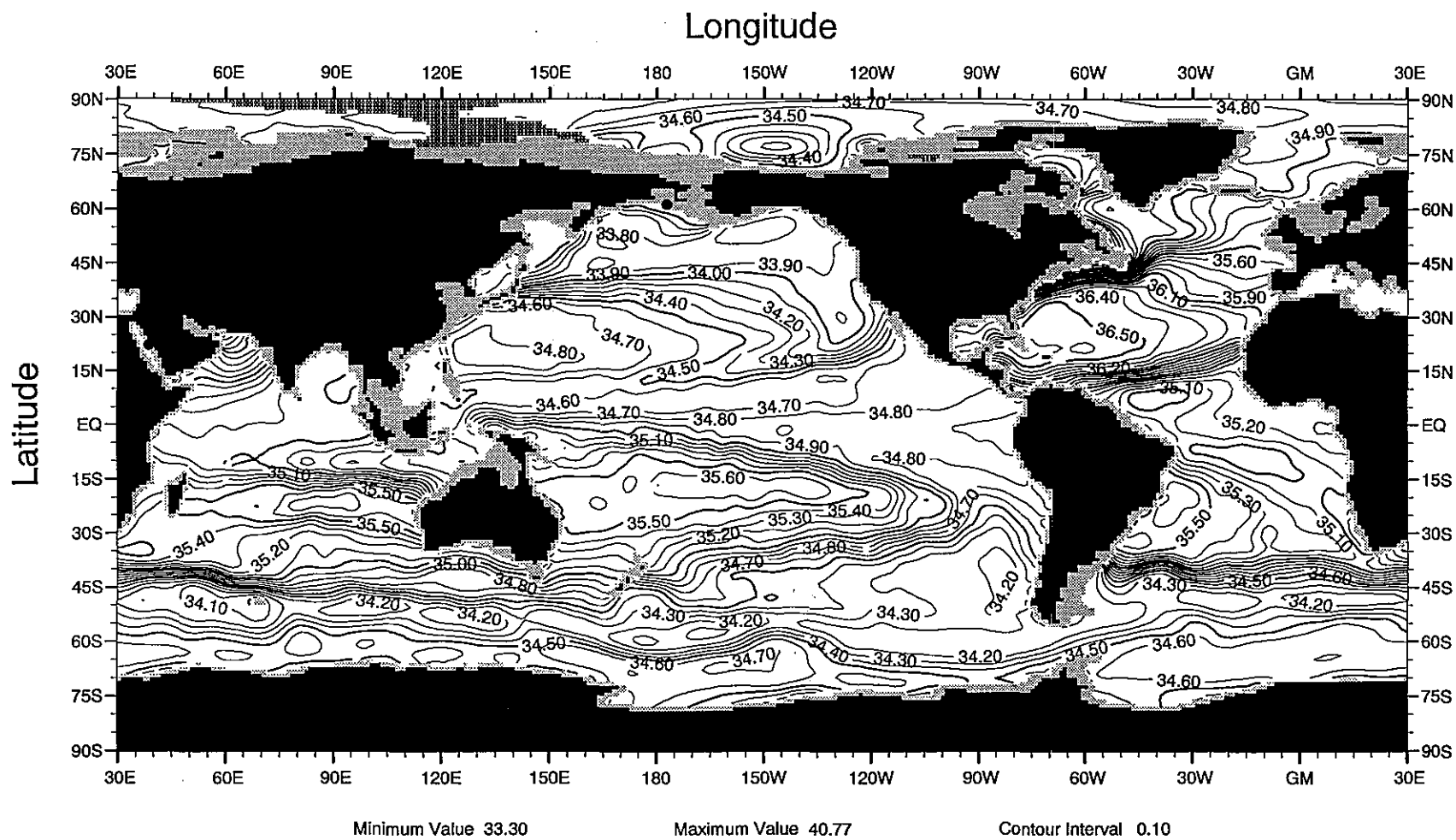


Fig. B8 Annual mean salinity (psu) at 250 m depth





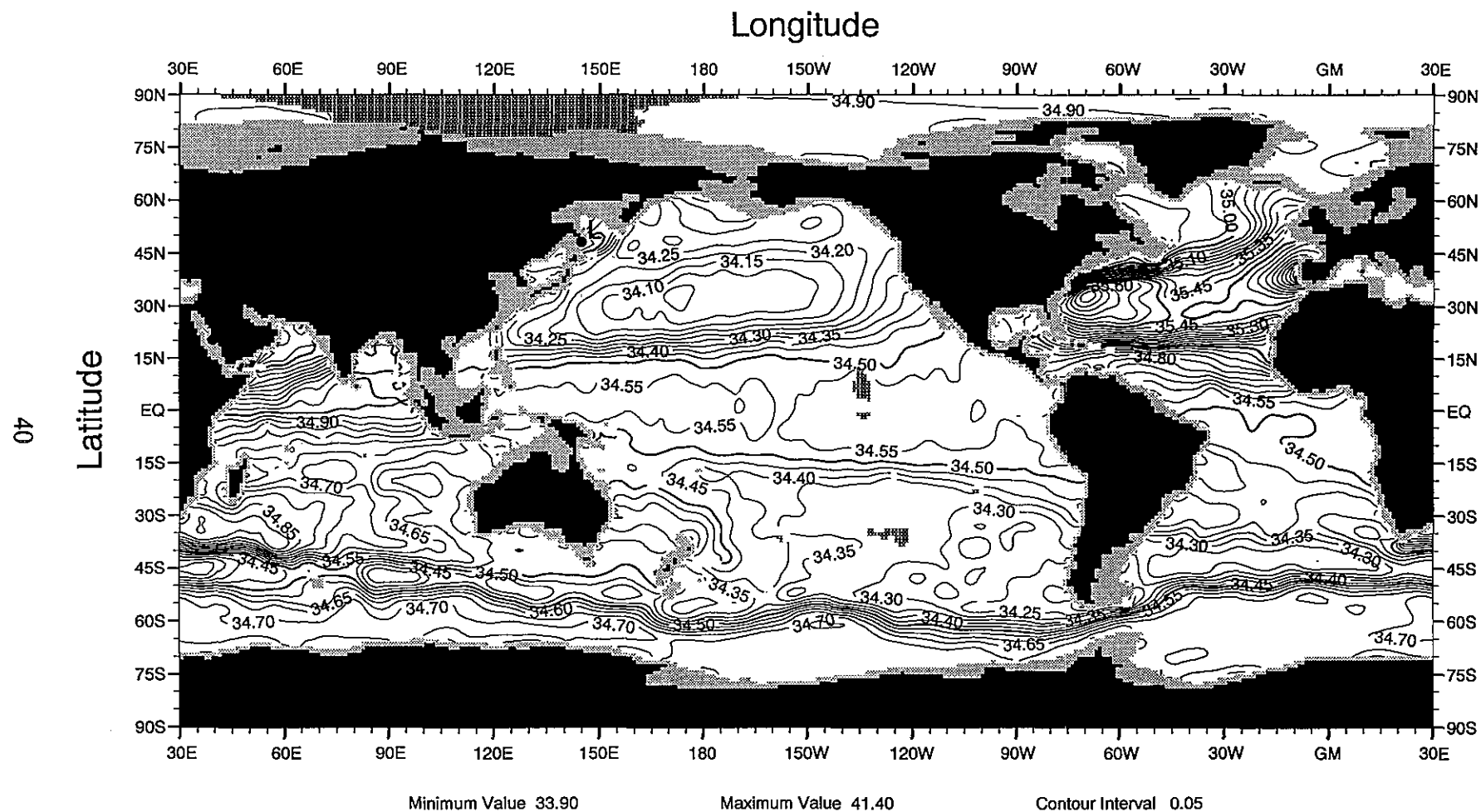


Fig. B11 Annual mean salinity (psu) at 700 m depth

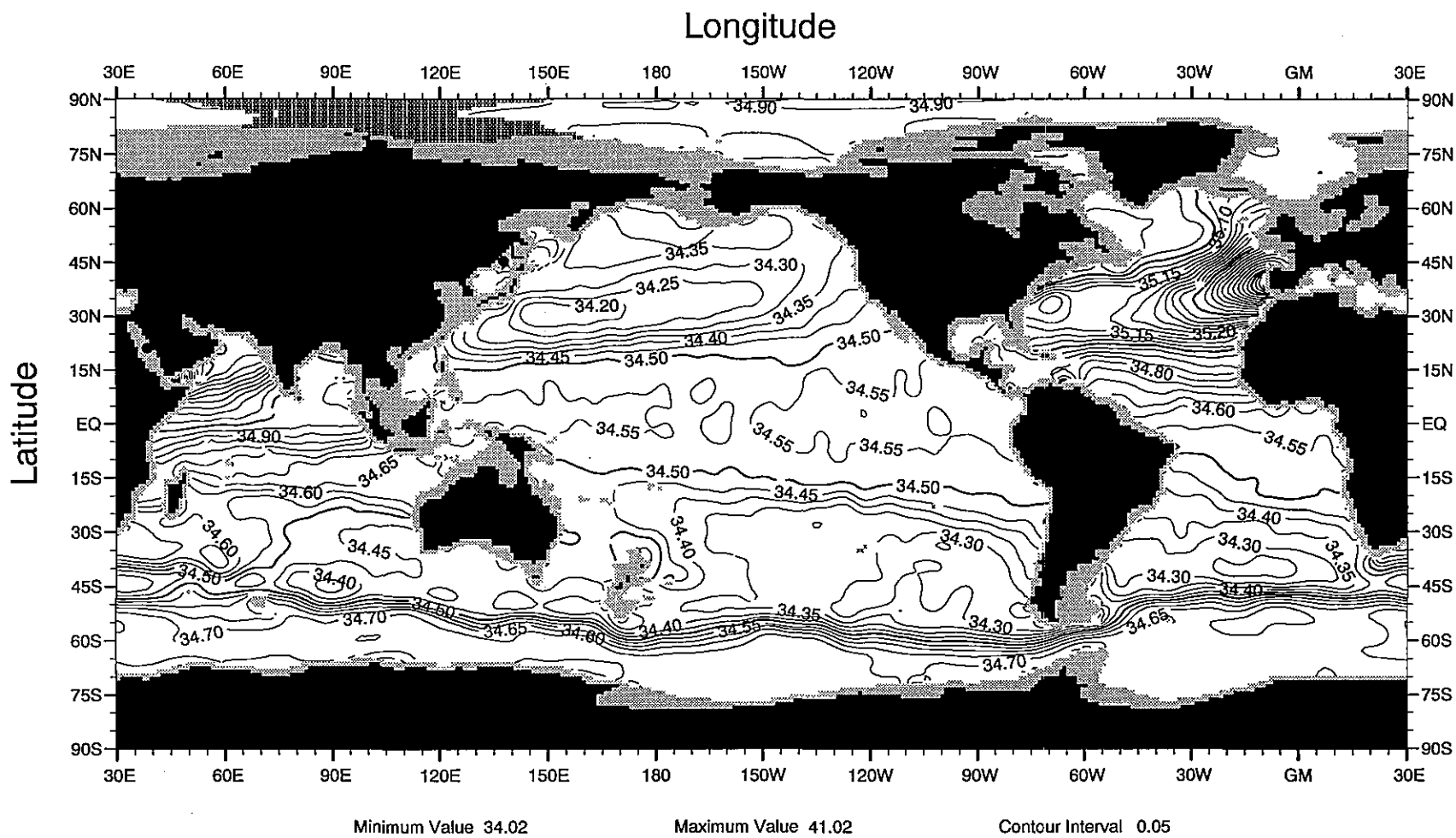
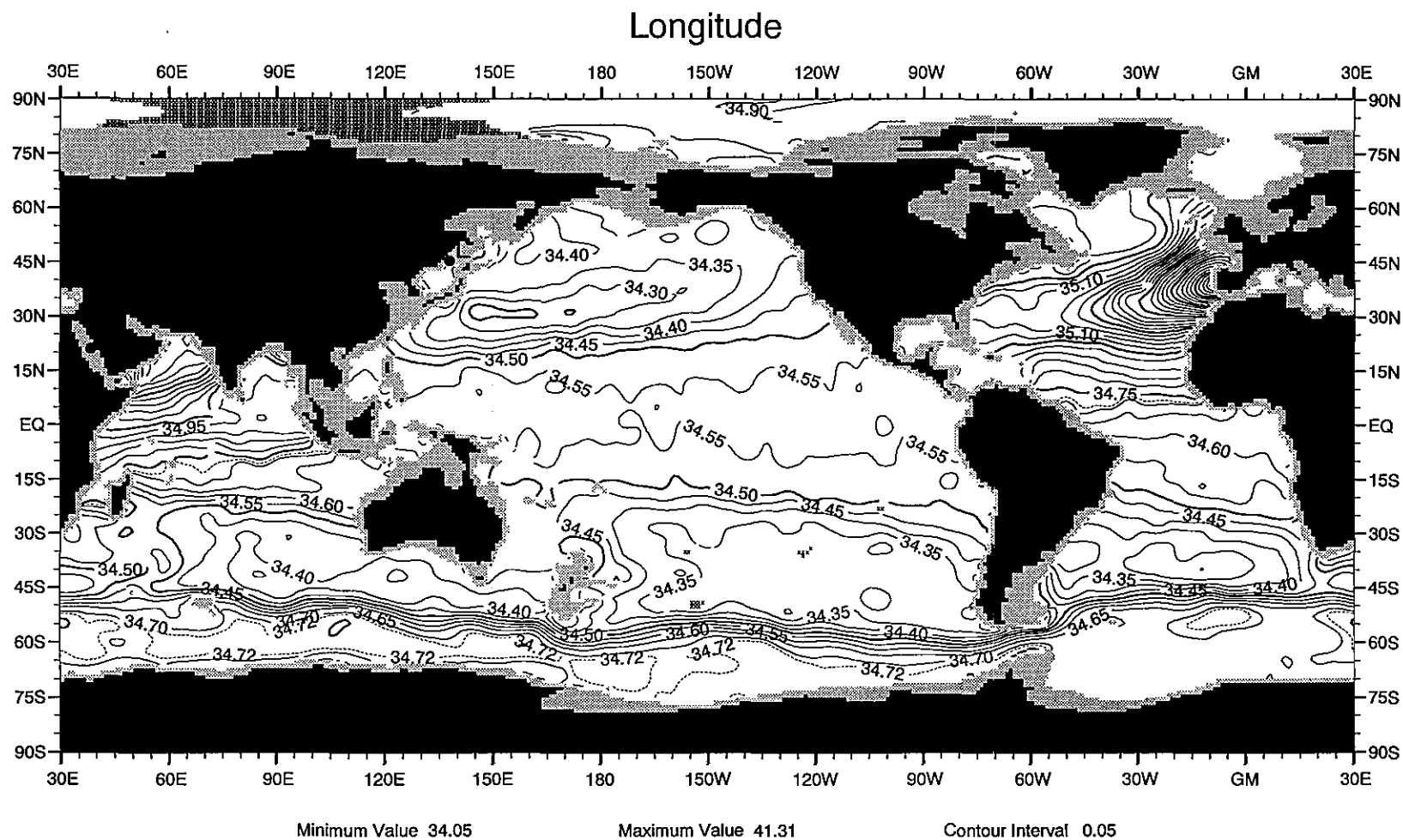


Fig. B12 Annual mean salinity (psu) at 900 m depth



**Fig. B13** Annual mean salinity (psu) at 1000 m depth



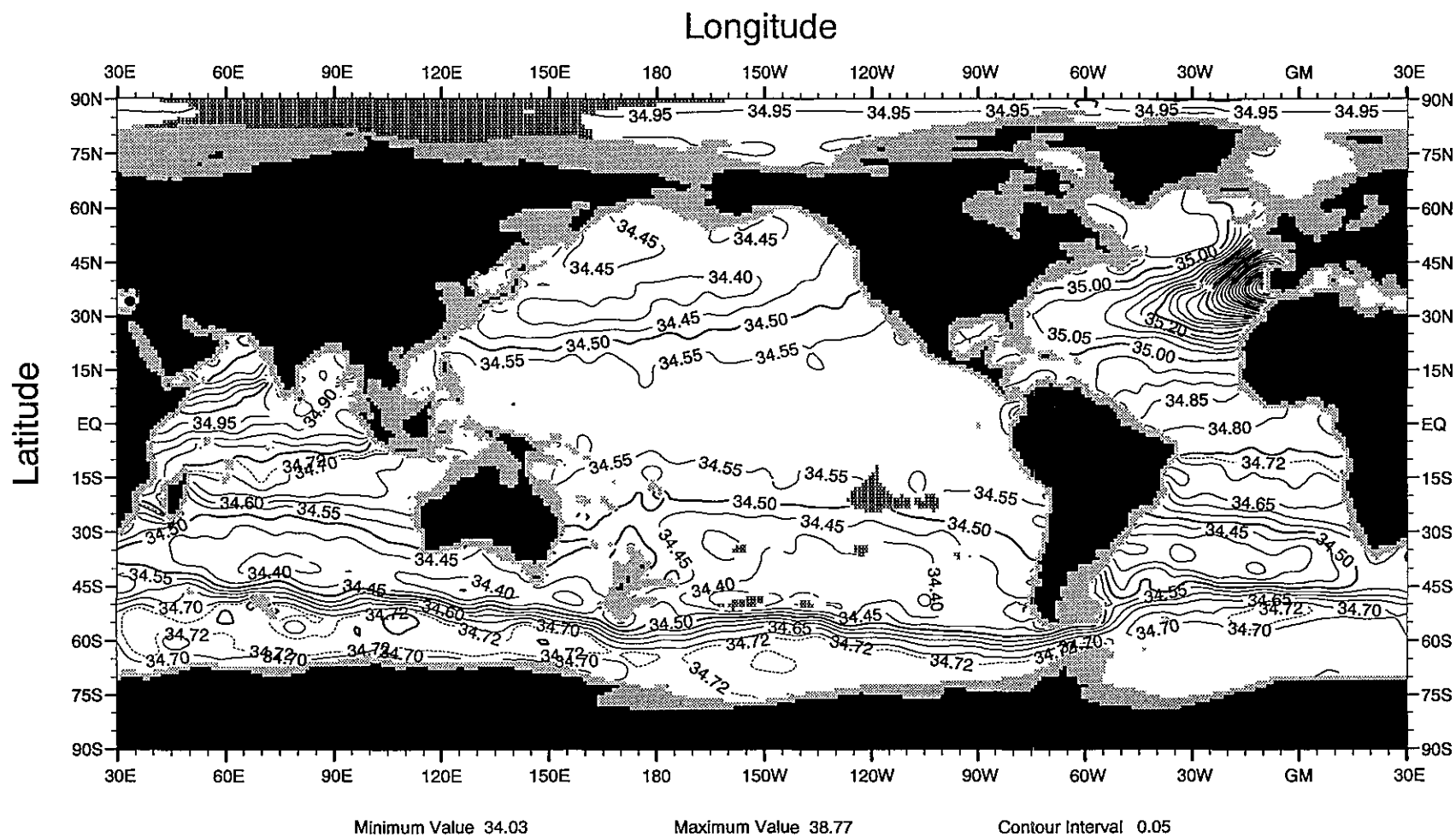


Fig. B14 Annual mean salinity (psu) at 1200 m depth

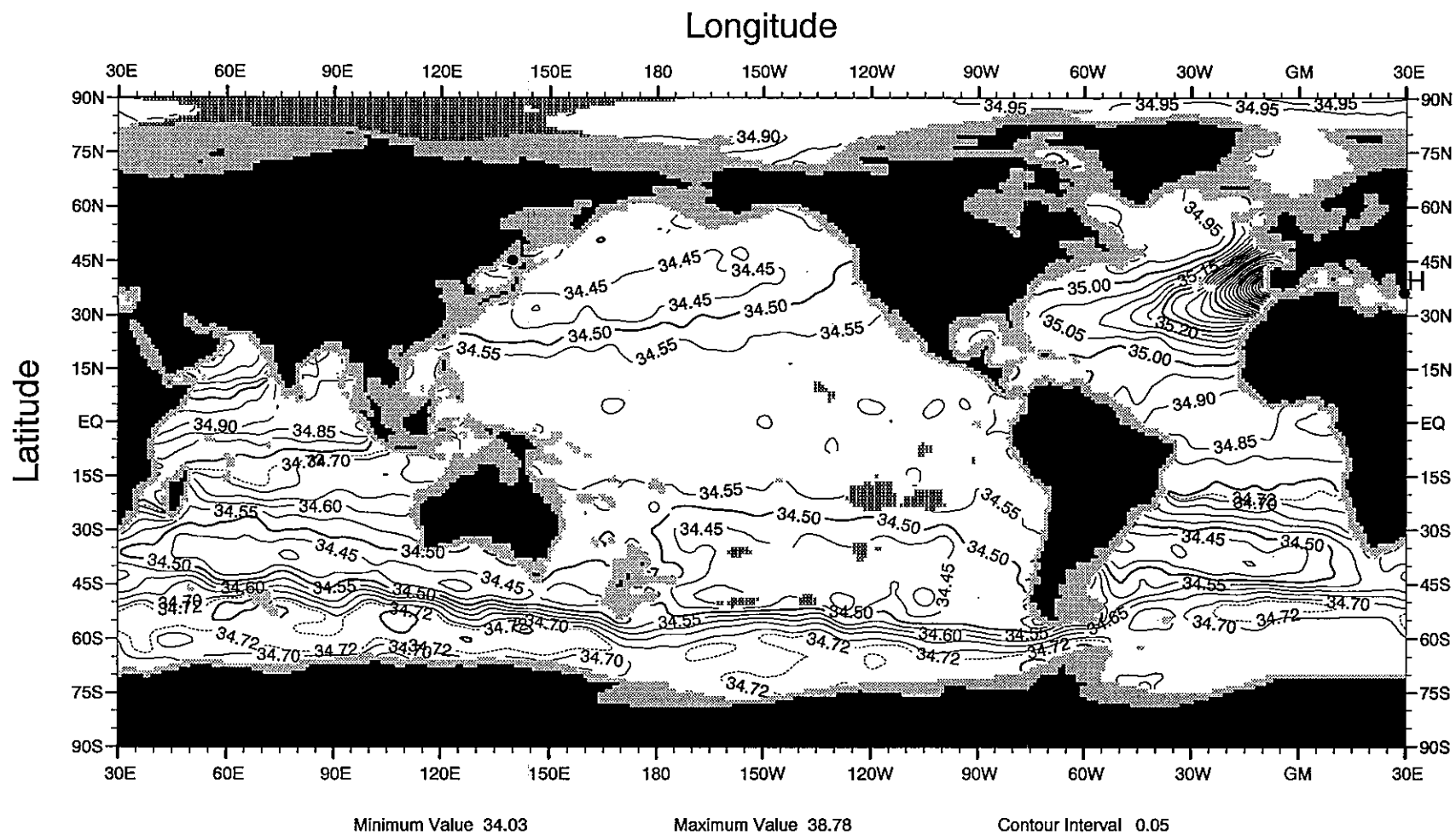


Fig. B15 Annual mean salinity (psu) at 1300 m depth

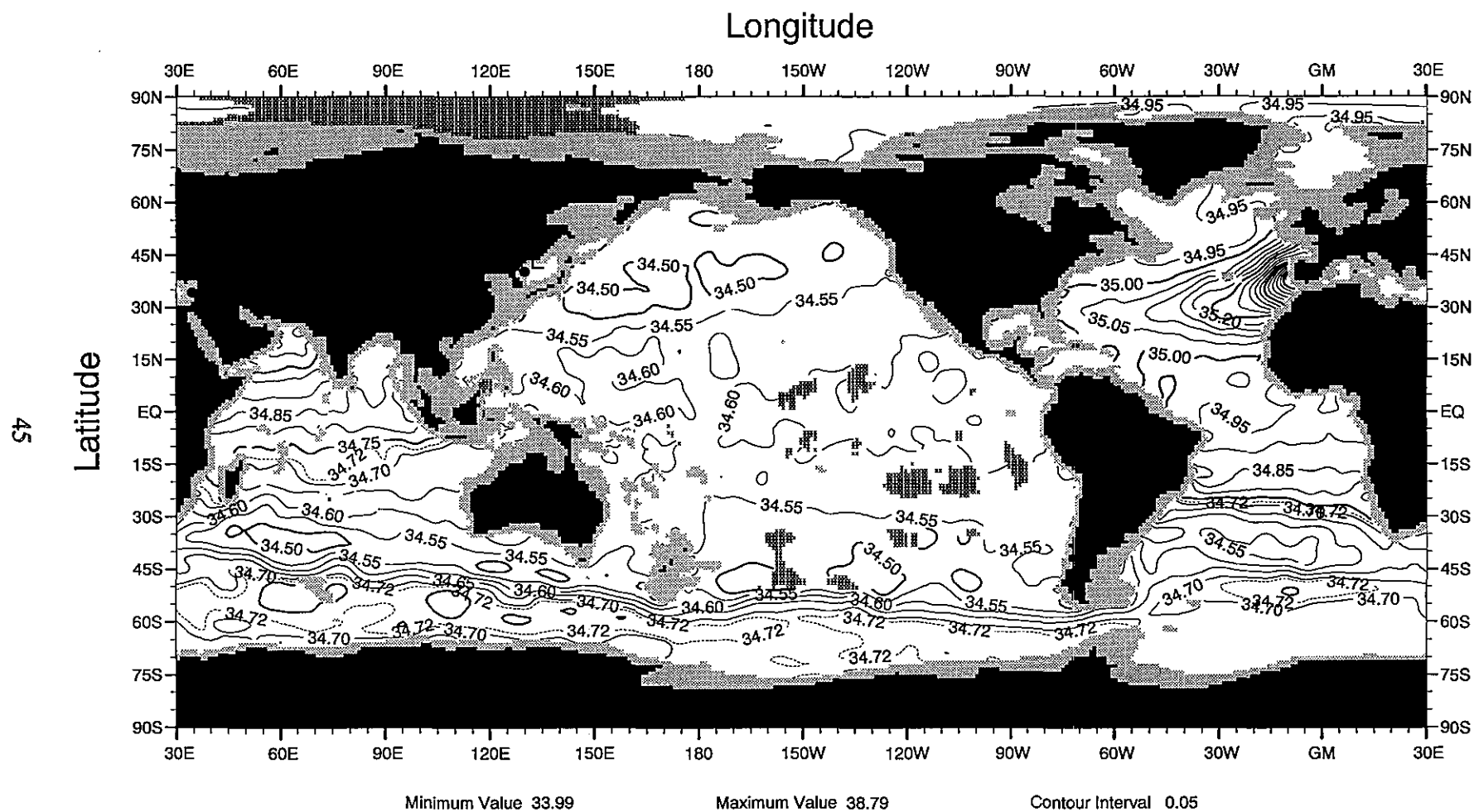


Fig. B16 Annual mean salinity (psu) at 1500 m depth

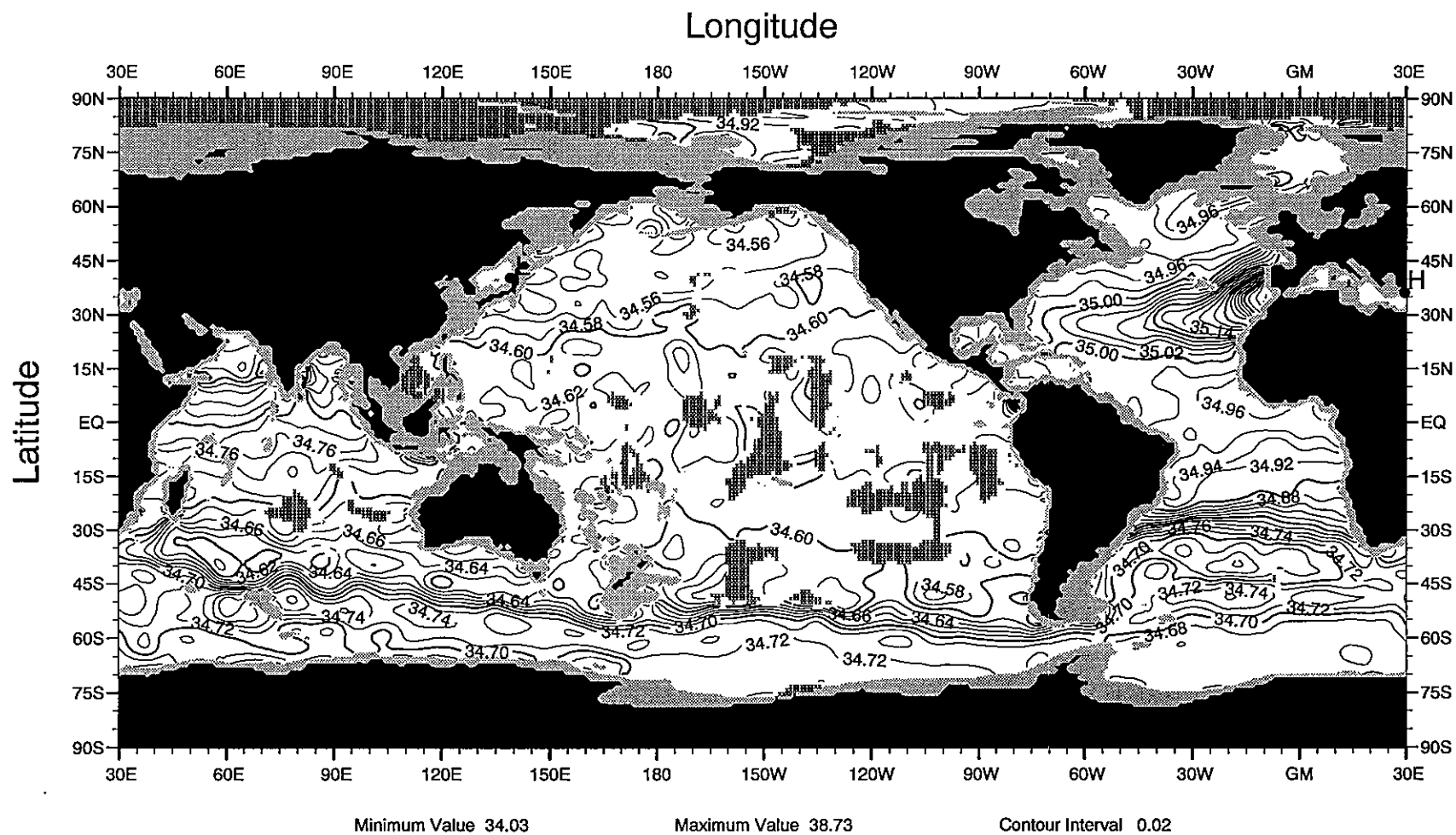


Fig. B17 Annual mean salinity (psu) at 1750 m depth

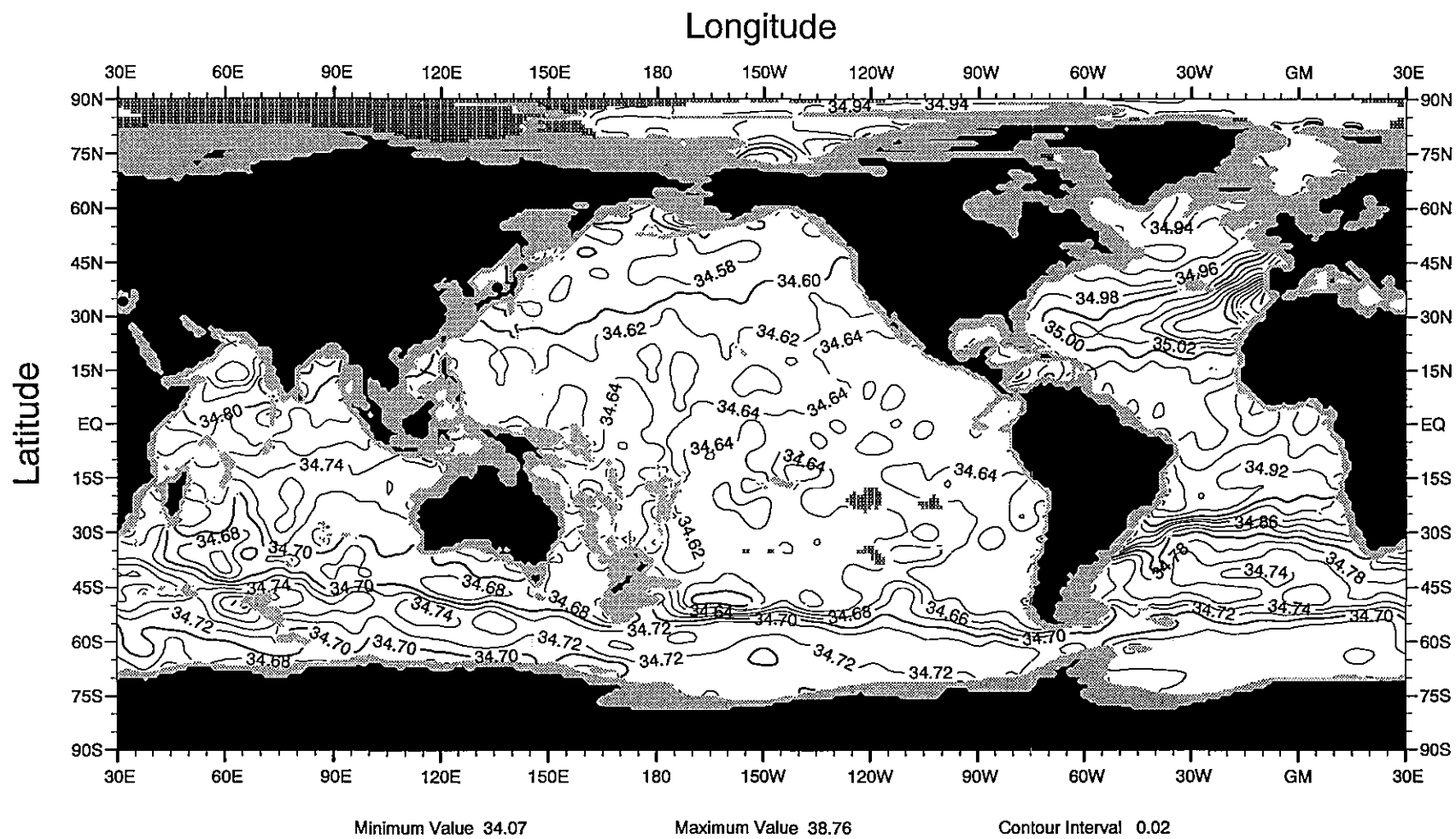


Fig. B18 Annual mean salinity (psu) at 2000 m depth

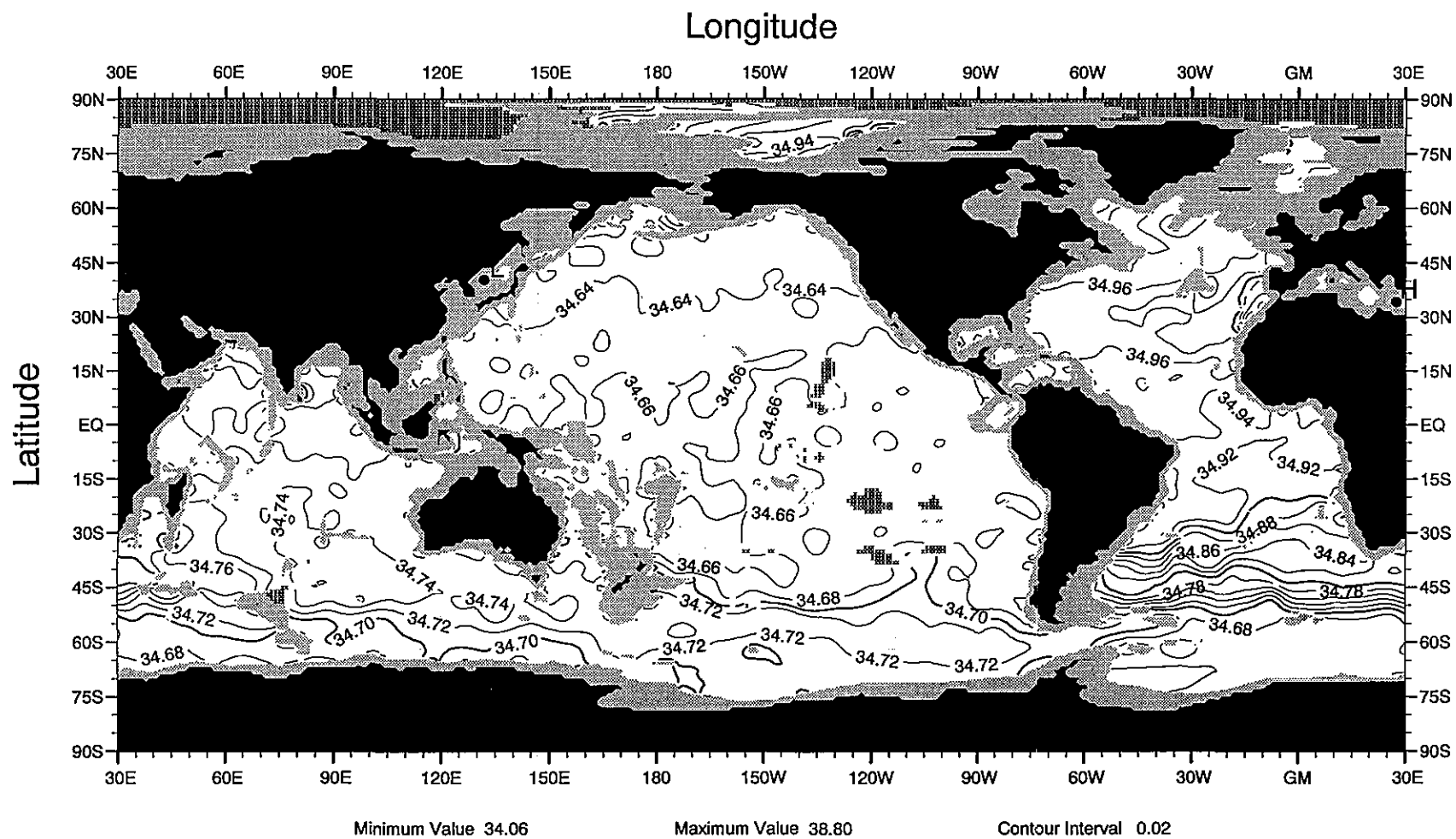


Fig. B19 Annual mean salinity (psu) at 2500 m depth

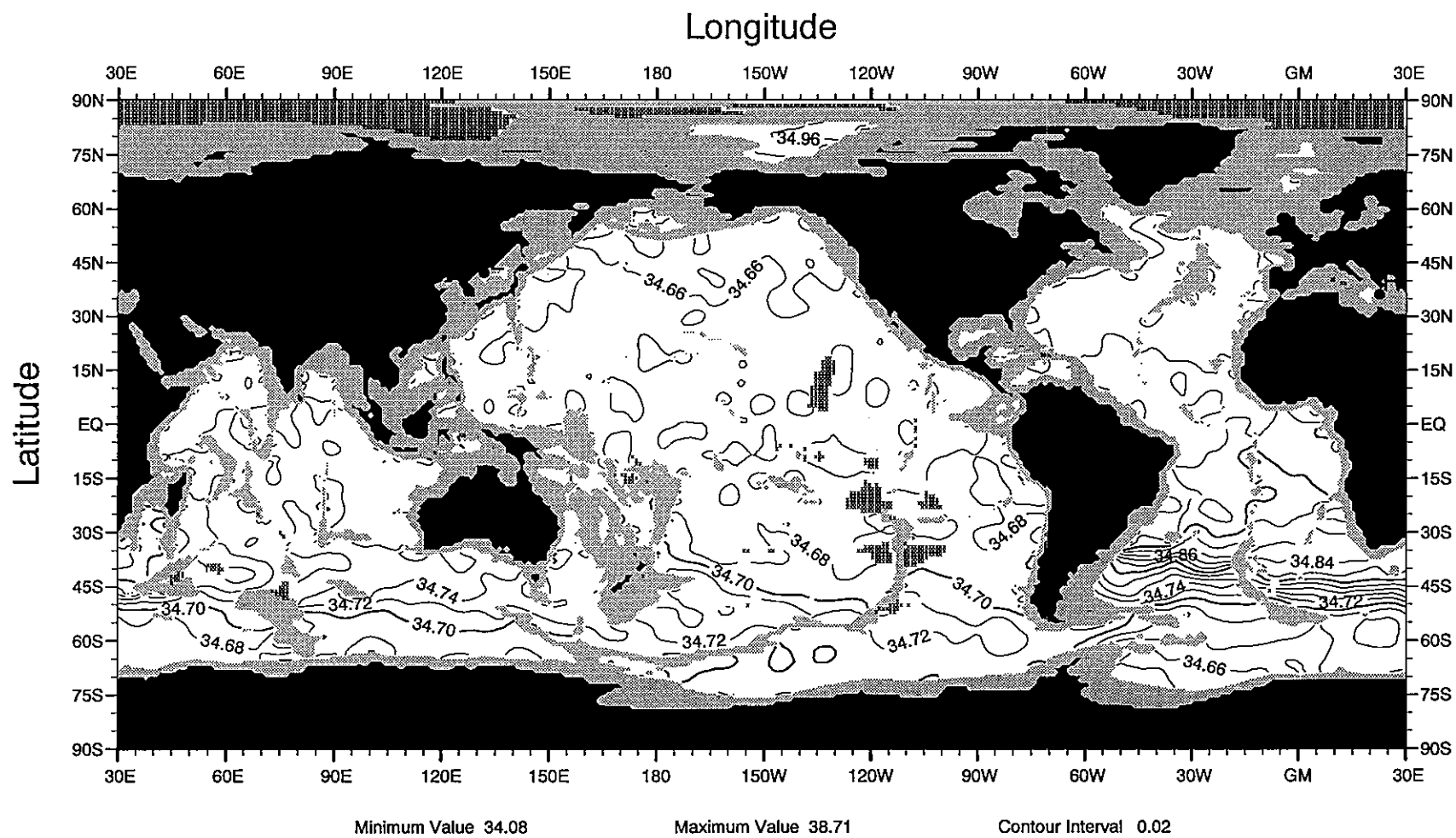


Fig. B20 Annual mean salinity (psu) at 3000 m depth

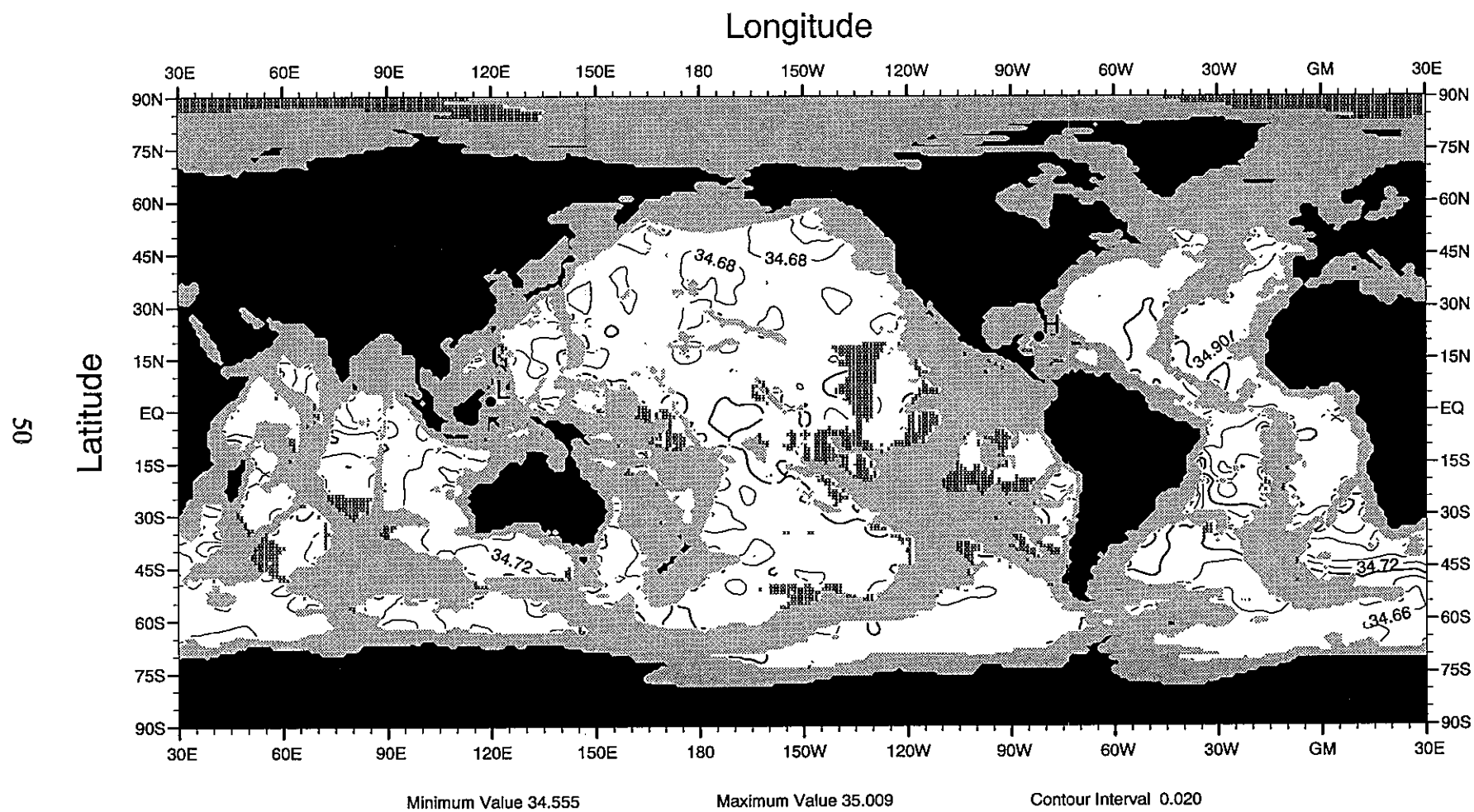


Fig. B21 Annual mean salinity (psu) at 4000 m depth



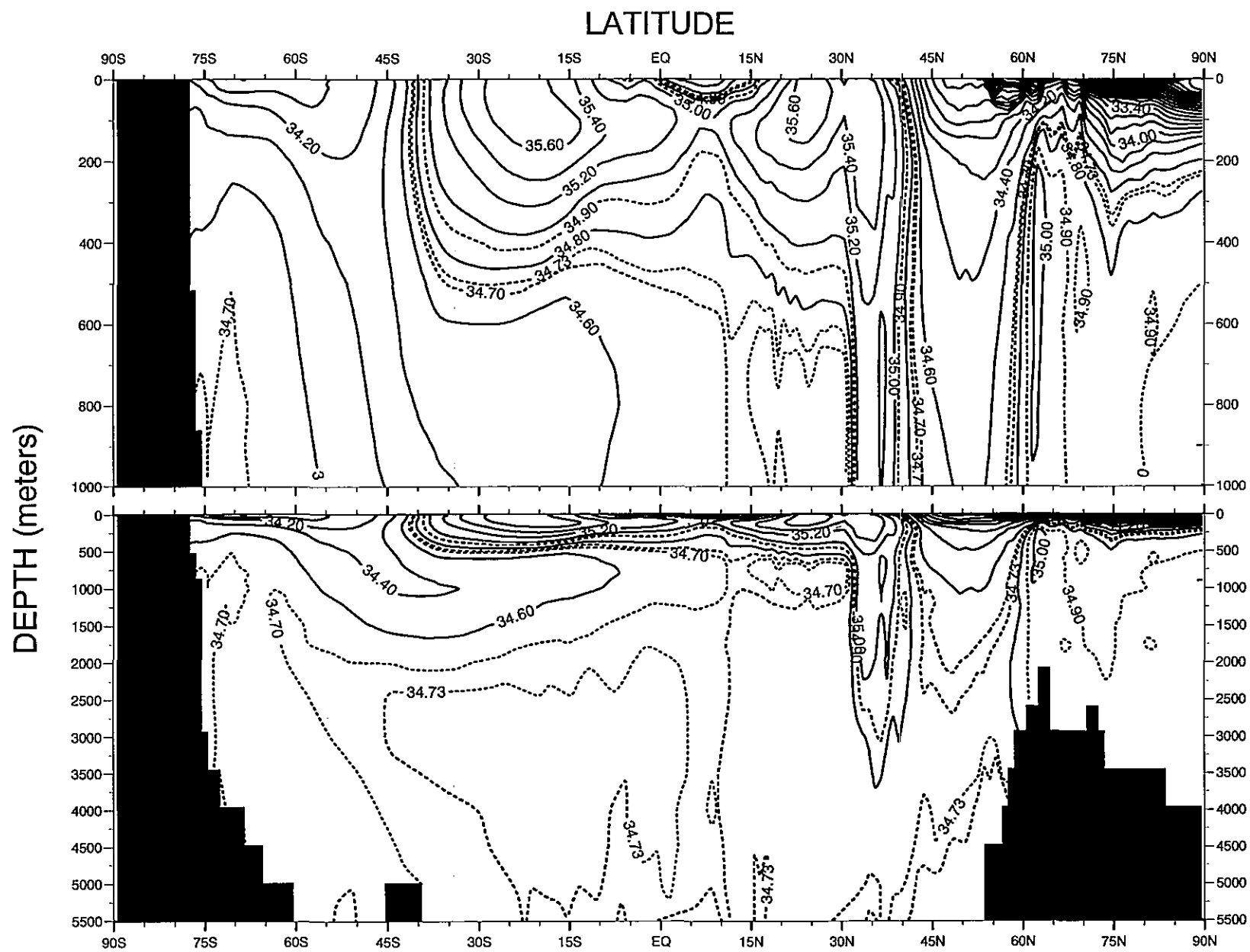


Fig C1. Annual global zonal average (by one-degree squares) of salinity (psu)

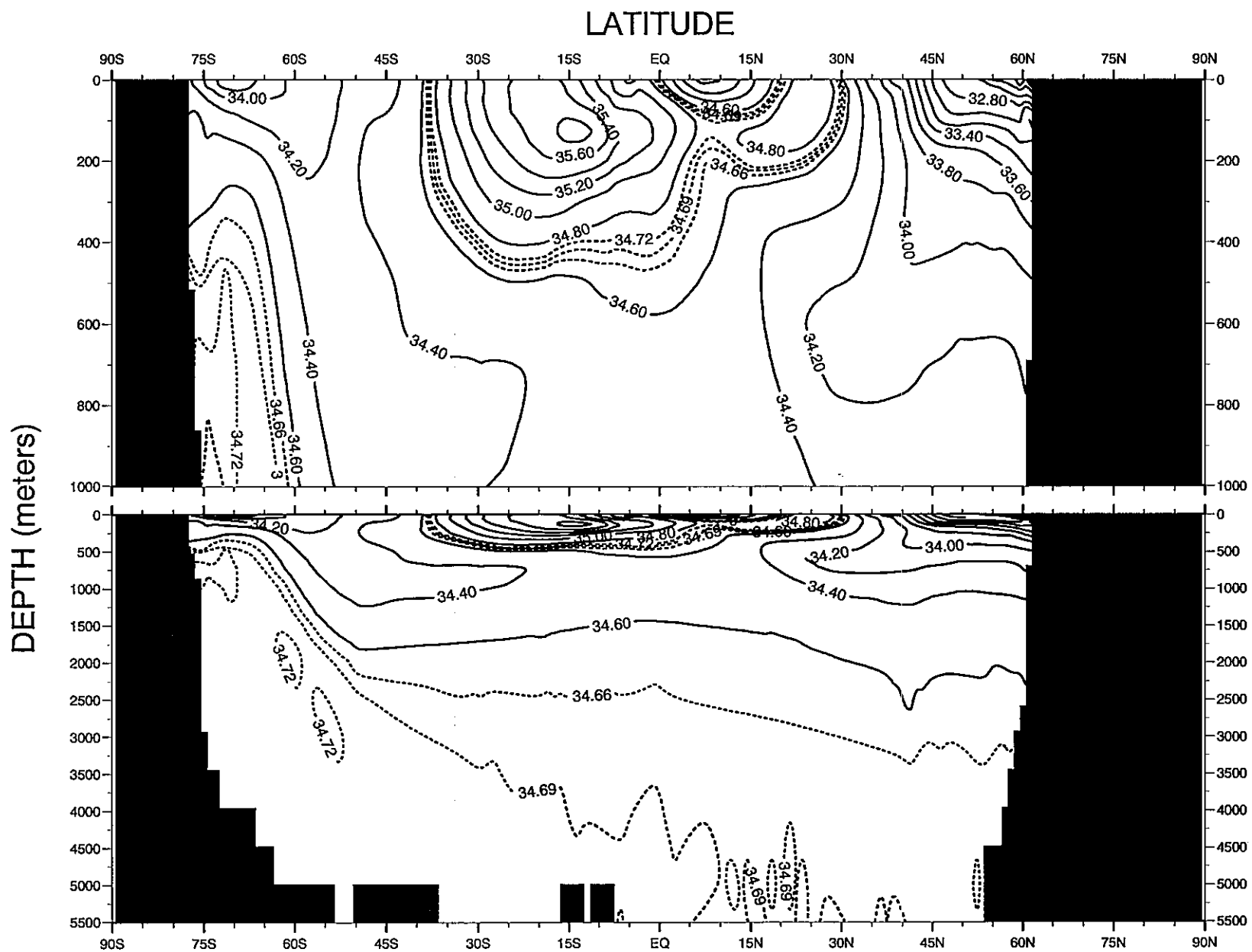


Fig C2. Annual Pacific zonal average (by one-degree squares) of salinity (psu)

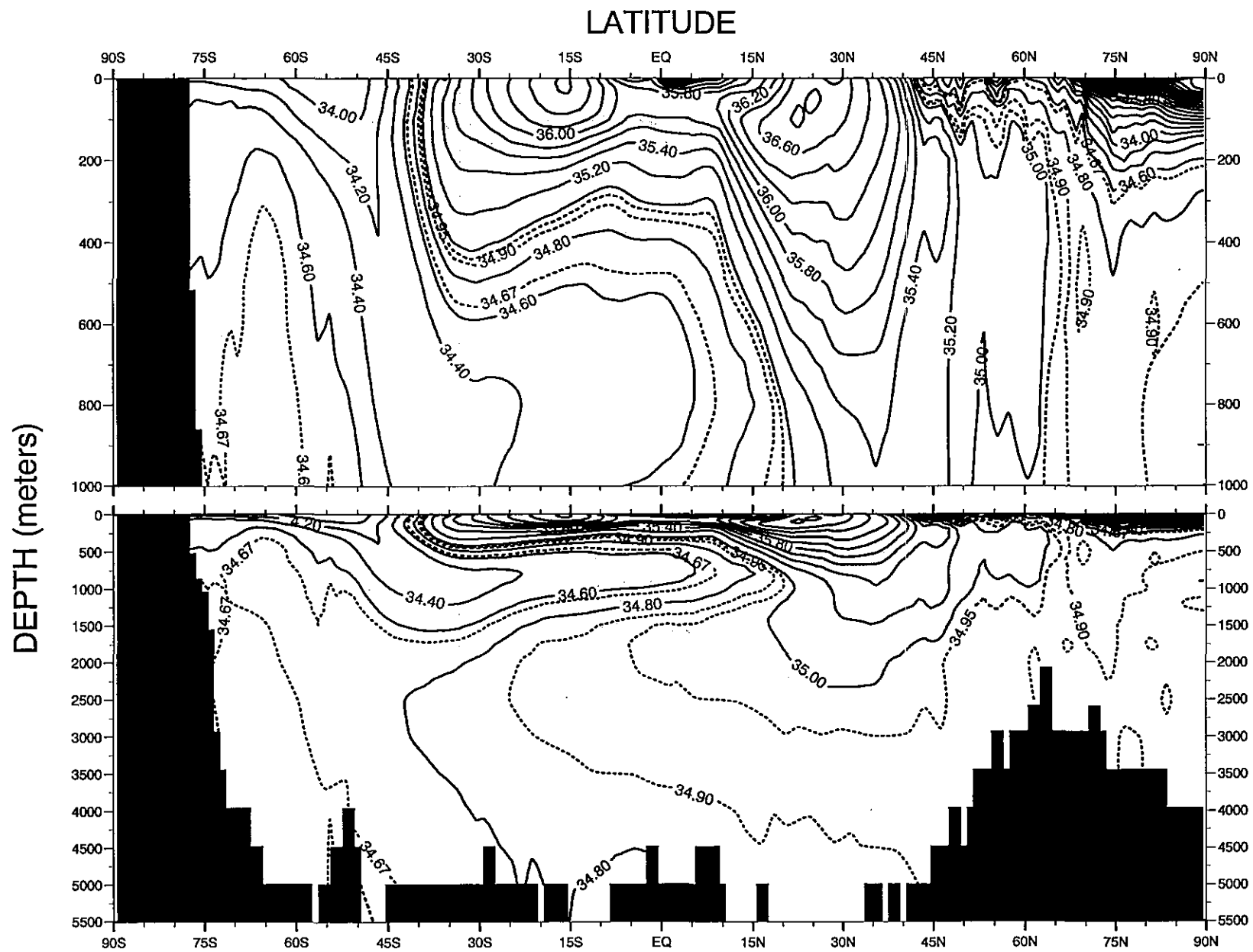


Fig C3. Annual Atlantic zonal average (by one-degree squares) of salinity (psu)

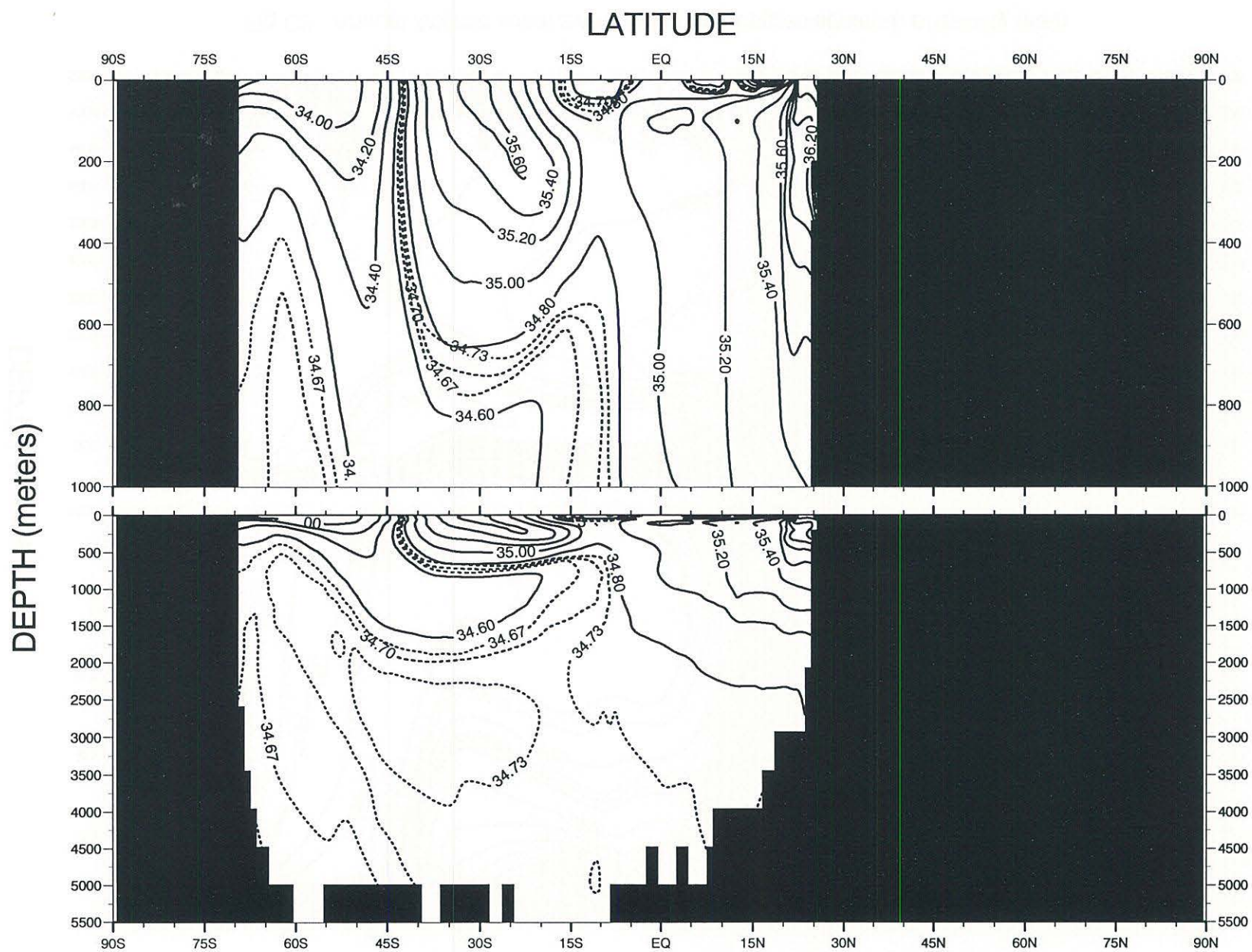


Fig C4. Annual Indian zonal average (by one-degree squares) of salinity (psu)

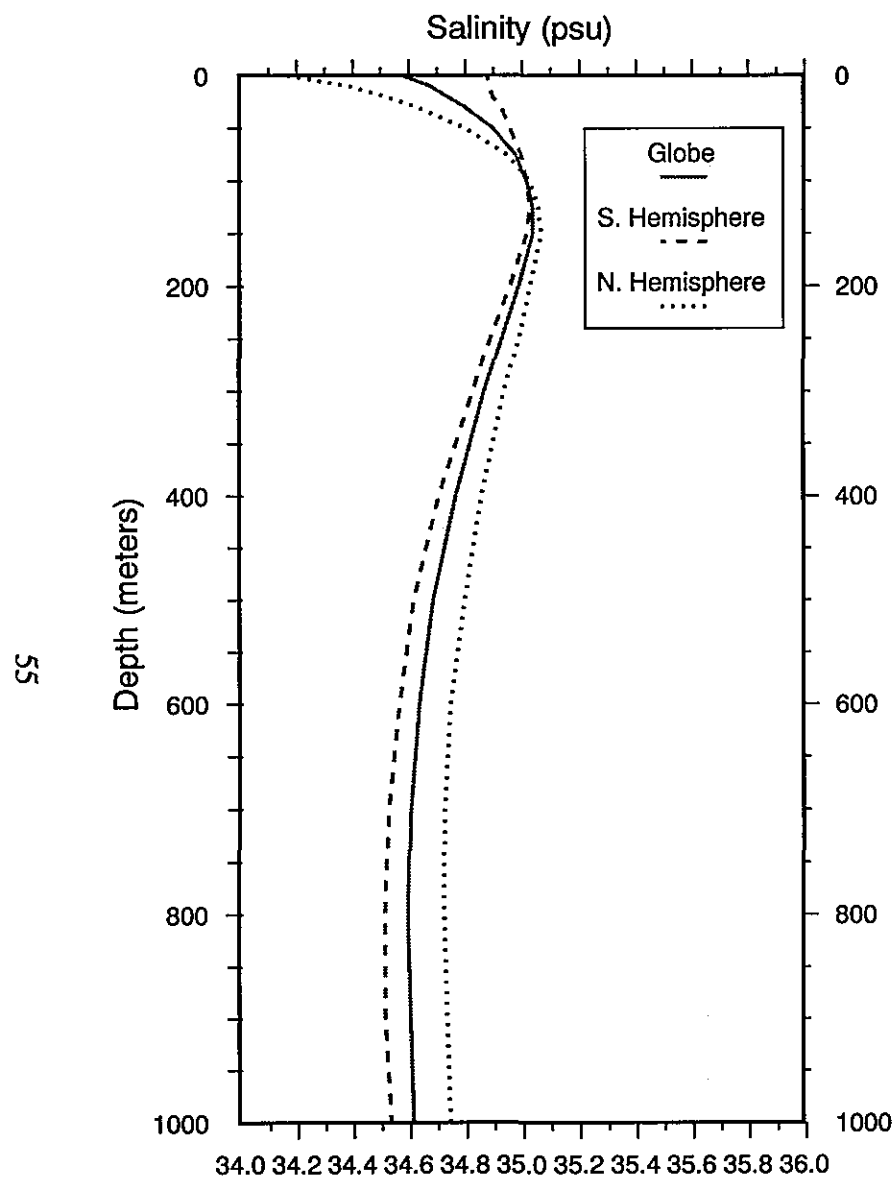


Figure D1a. Global salinity (psu) basin means (0-1000 m)

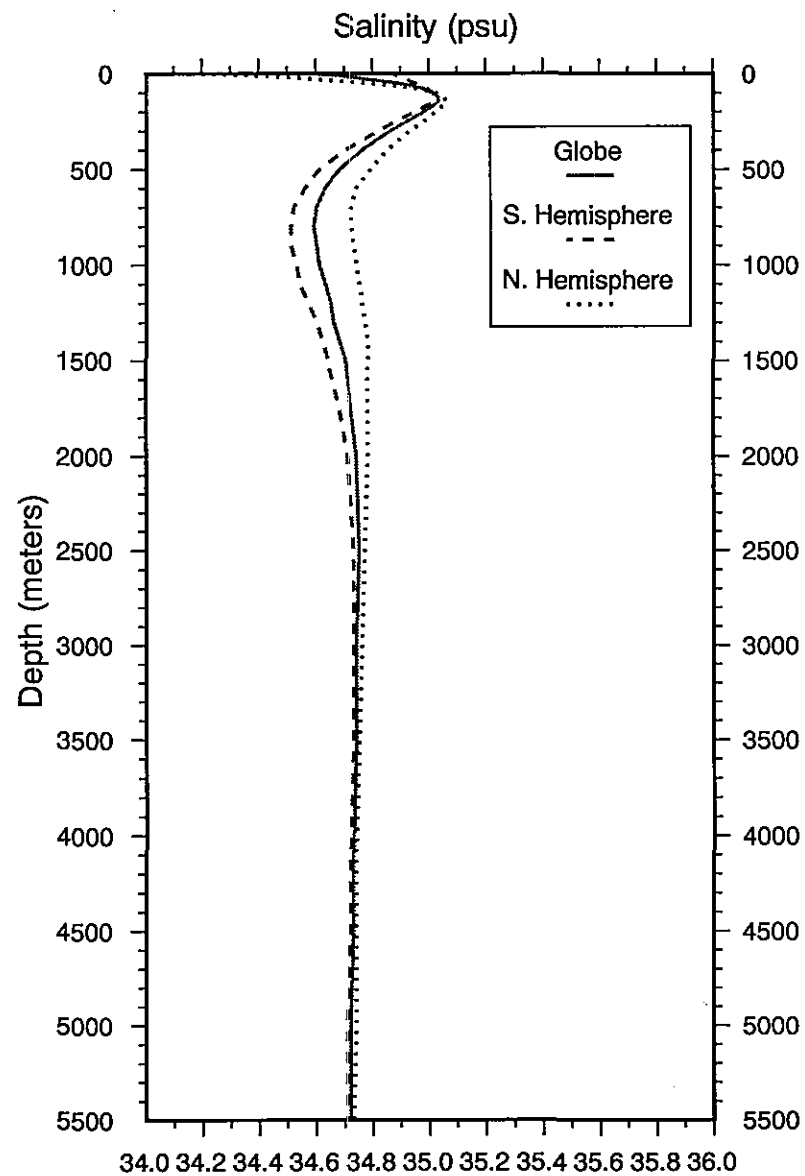


Figure D1b. Global salinity (psu) basin means (0-5500 m)

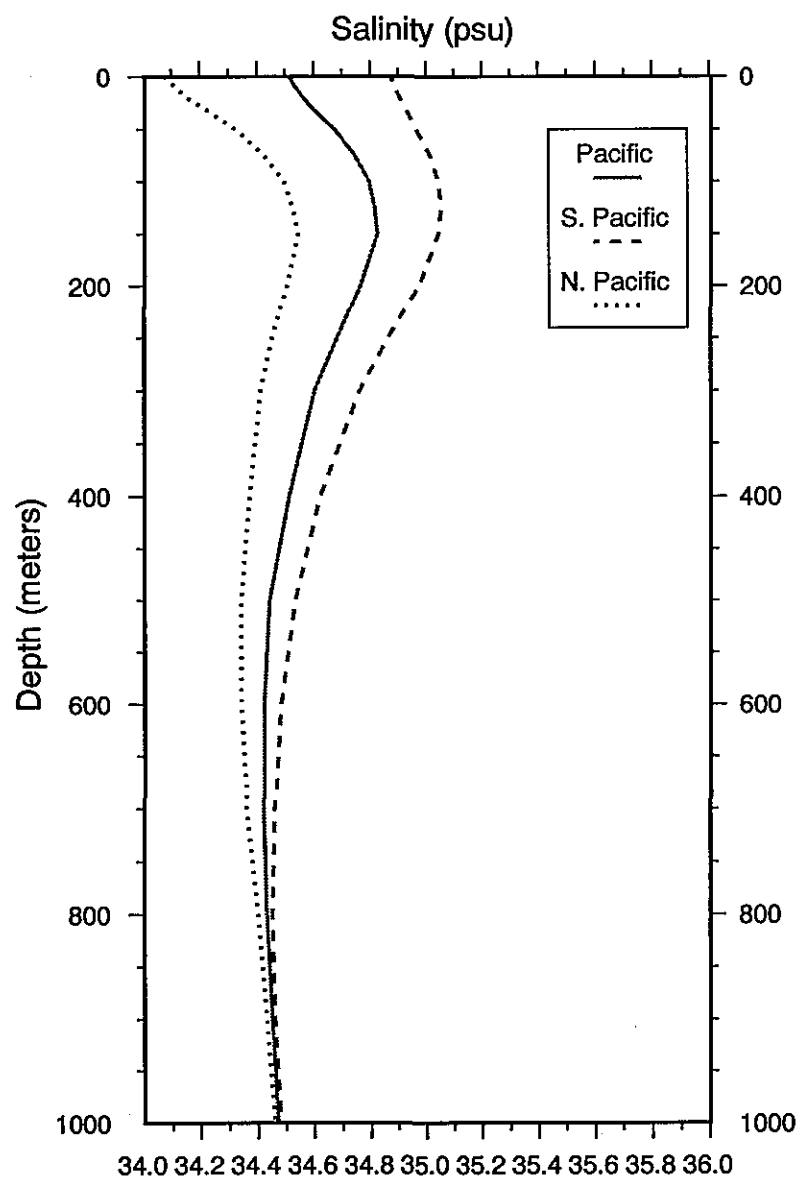


Figure D2a. Pacific salinity (psu) basin means (0-1000 m)

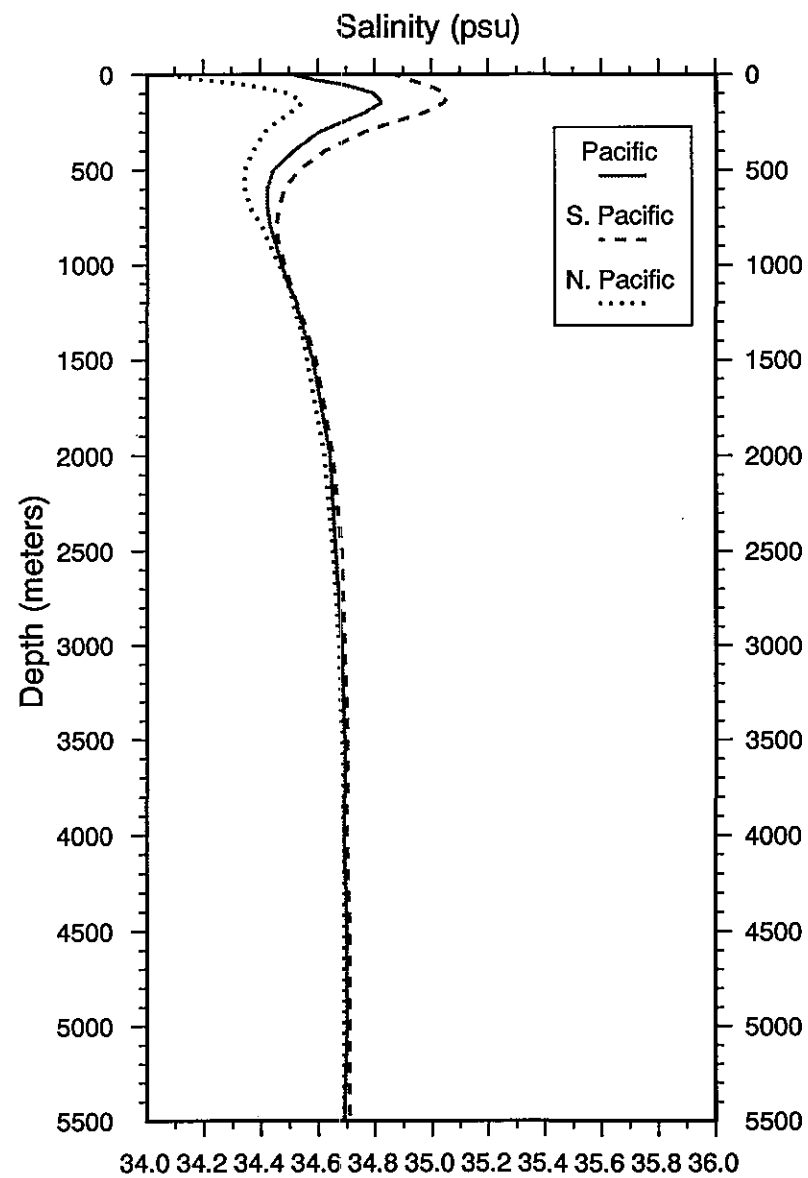


Figure D2b. Pacific salinity (psu) basin means (0-5500 m)

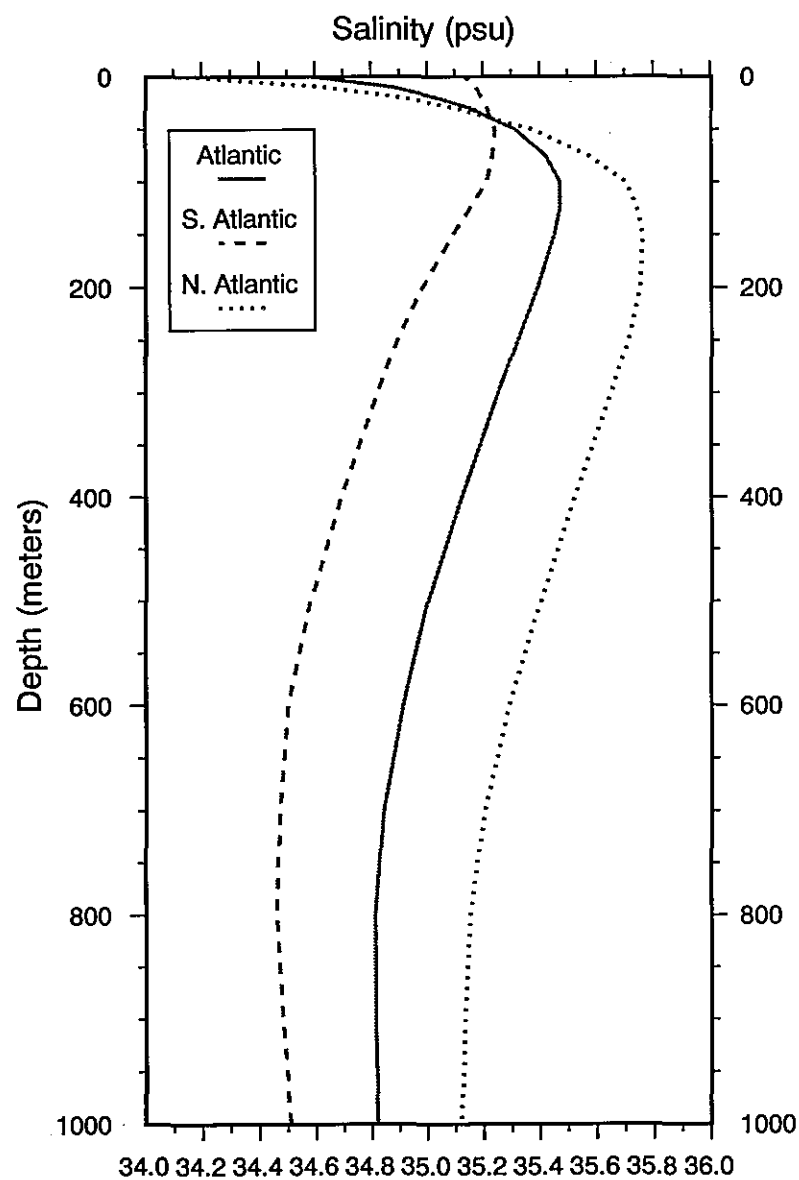


Figure D3a. Atlantic salinity (psu) basin means (0-1000 m)

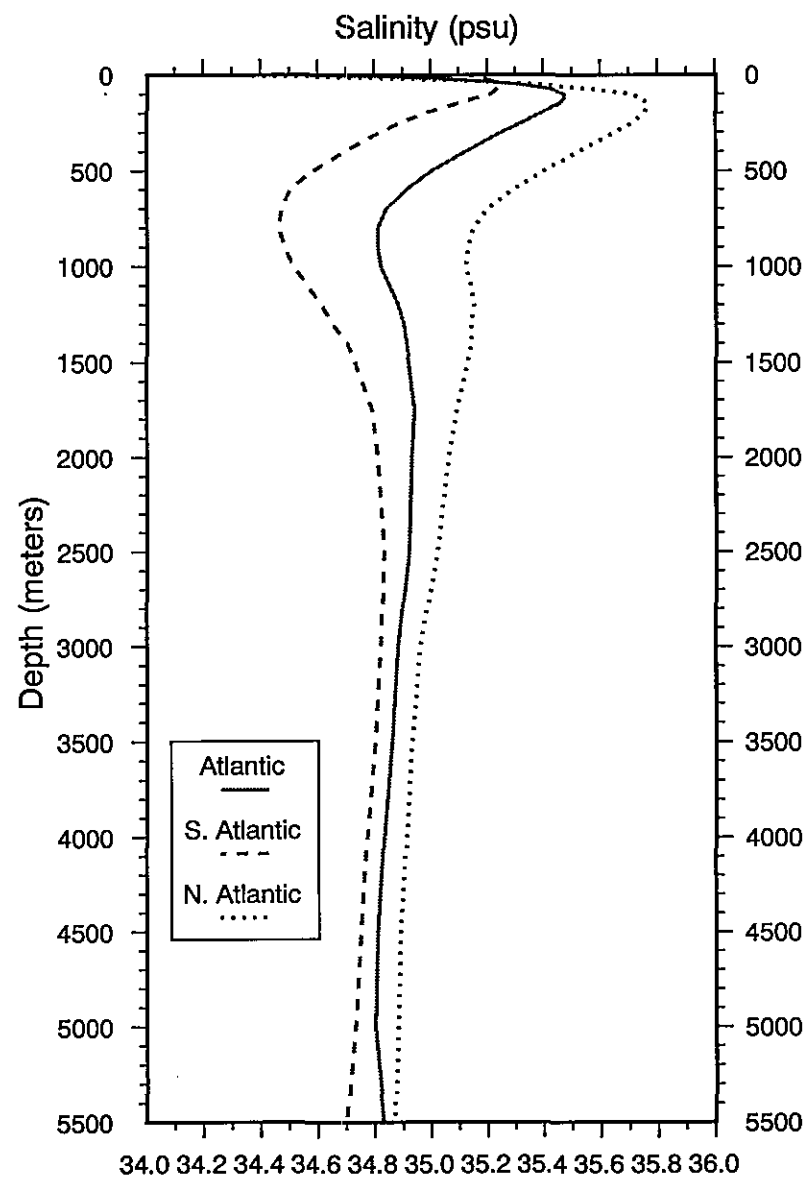


Figure D3b. Atlantic salinity (psu) basin means (0-5500 m)

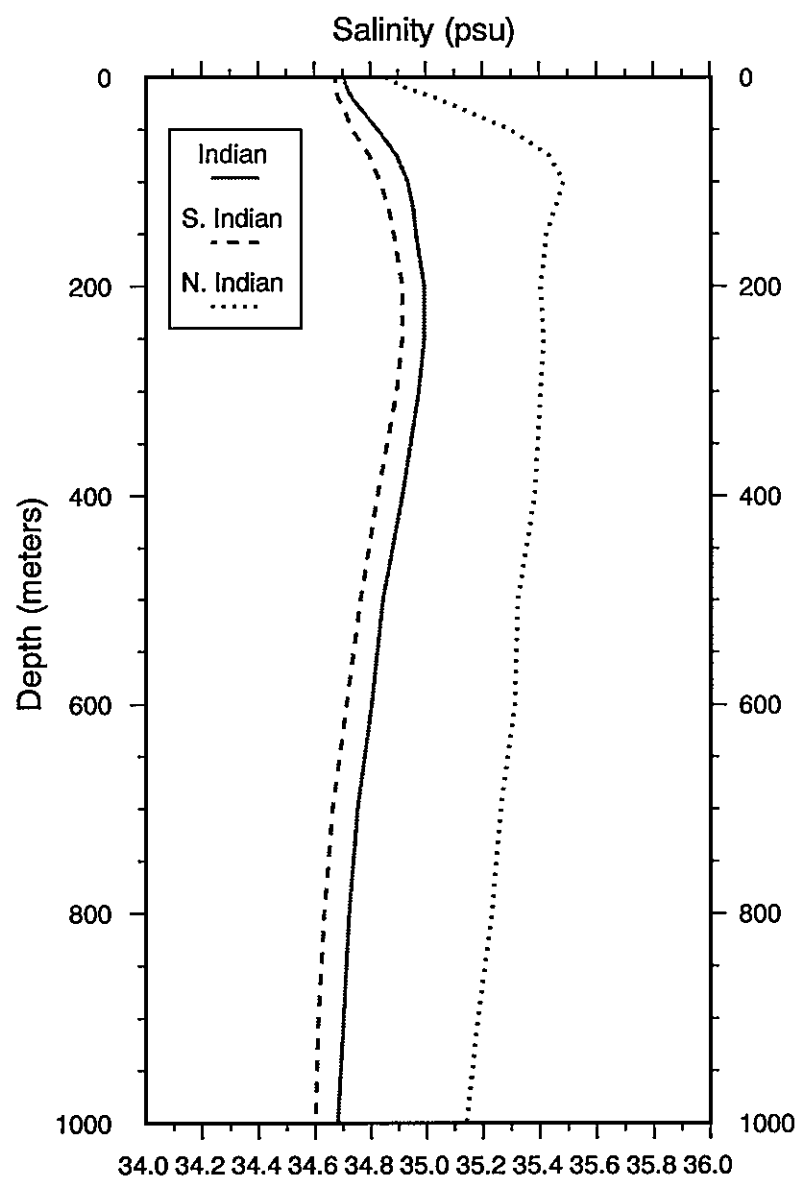


Figure D4a. Indian salinity (psu) basin means (0-1000 m)

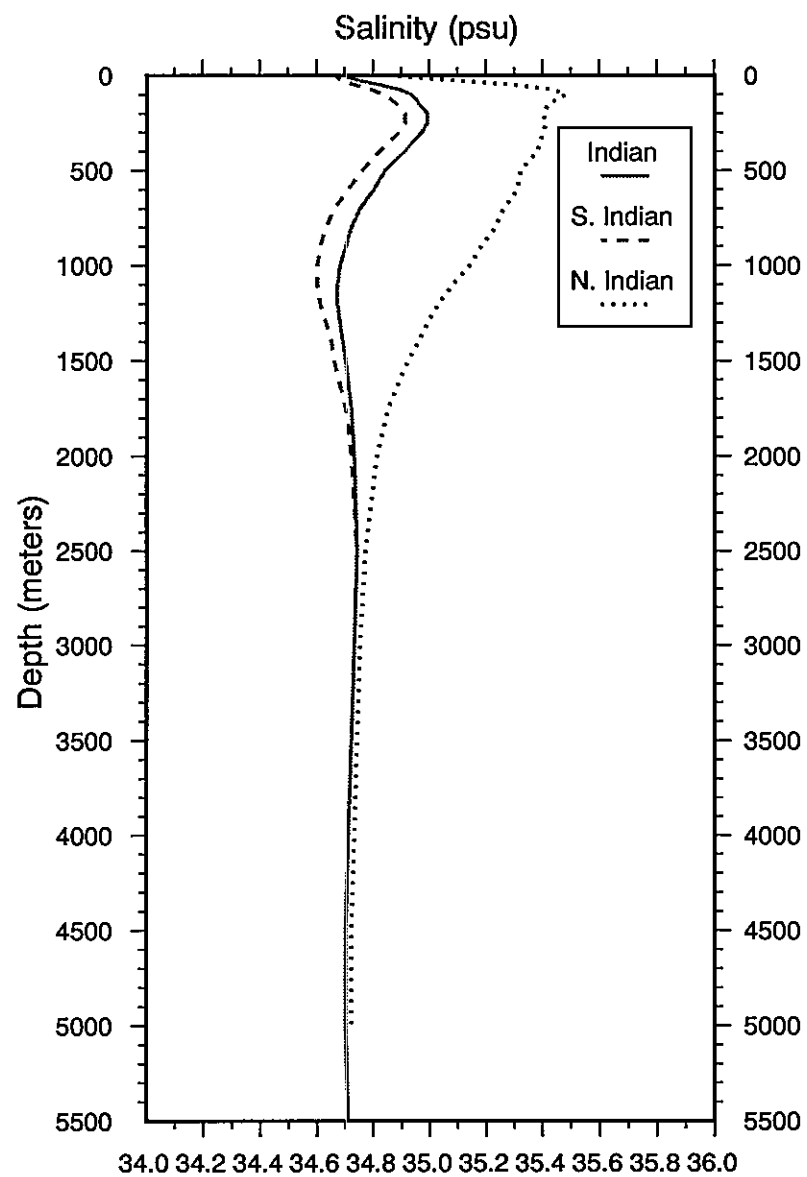


Figure D4b. Indian salinity (psu) basin means (0-5500 m)



Table D1a. Annual salinity (psu) basin means and standard errors for the world ocean and Pacific Ocean as a function of depth

Standard Level	Depth	World Ocean		Southern Hemisphere Ocean		Northern Hemisphere Ocean		Pacific Ocean		South Pacific Ocean		North Pacific Ocean	
		Mean	Standard Error	Mean	Standard Error	Mean	Standard Error	Mean	Standard Error	Mean	Standard Error	Mean	Standard Error
1	0	34.57	0.10	34.87	0.06	34.16	0.22	34.51	0.07	34.87	0.07	34.07	0.10
2	10	34.67	0.08	34.88	0.06	34.38	0.17	34.53	0.06	34.88	0.07	34.11	0.09
3	20	34.73	0.07	34.89	0.06	34.51	0.15	34.56	0.06	34.90	0.07	34.15	0.09
4	30	34.79	0.07	34.92	0.06	34.62	0.14	34.59	0.06	34.92	0.07	34.21	0.08
5	50	34.89	0.06	34.95	0.05	34.79	0.12	34.67	0.06	34.96	0.07	34.32	0.08
6	75	34.97	0.05	34.99	0.05	34.94	0.10	34.74	0.06	35.01	0.07	34.42	0.08
7	100	35.01	0.05	35.01	0.05	35.02	0.10	34.79	0.06	35.04	0.07	34.49	0.08
8	125	35.03	0.05	35.02	0.05	35.05	0.09	34.81	0.05	35.05	0.07	34.52	0.07
9	150	35.03	0.04	35.01	0.05	35.06	0.09	34.82	0.05	35.04	0.07	34.54	0.06
10	200	34.98	0.04	34.95	0.04	35.02	0.08	34.76	0.04	34.97	0.06	34.50	0.05
11	250	34.92	0.04	34.88	0.03	34.98	0.08	34.68	0.04	34.86	0.05	34.45	0.04
12	300	34.86	0.03	34.82	0.03	34.93	0.07	34.60	0.03	34.76	0.04	34.41	0.04
13	400	34.76	0.03	34.70	0.02	34.85	0.07	34.51	0.02	34.62	0.03	34.37	0.03
14	500	34.68	0.03	34.61	0.02	34.79	0.06	34.44	0.02	34.53	0.02	34.34	0.03
15	600	34.63	0.03	34.56	0.01	34.74	0.06	34.42	0.01	34.48	0.01	34.34	0.02
16	700	34.60	0.02	34.52	0.01	34.72	0.06	34.42	0.01	34.46	0.01	34.36	0.02
17	800	34.59	0.02	34.51	0.01	34.72	0.05	34.43	0.01	34.45	0.01	34.40	0.02
18	900	34.60	0.02	34.51	0.01	34.73	0.05	34.45	0.01	34.46	0.01	34.43	0.01
19	1000	34.61	0.02	34.53	0.01	34.74	0.05	34.47	0.01	34.48	0.01	34.46	0.01
20	1100	34.63	0.02	34.54	0.01	34.75	0.05	34.49	0.01	34.50	0.01	34.49	0.01
21	1200	34.65	0.02	34.57	0.01	34.76	0.04	34.52	0.01	34.52	0.01	34.51	0.01
22	1300	34.66	0.02	34.60	0.01	34.77	0.04	34.54	0.01	34.55	0.01	34.53	0.01
23	1400	34.68	0.02	34.62	0.01	34.78	0.04	34.56	0.01	34.57	0.01	34.55	0.01
24	1500	34.70	0.02	34.64	0.01	34.78	0.04	34.58	0.00	34.59	0.01	34.56	0.01
25	1750	34.72	0.02	34.68	0.01	34.78	0.04	34.61	0.00	34.62	0.00	34.59	0.01
26	2000	34.74	0.01	34.71	0.01	34.78	0.03	34.64	0.00	34.65	0.00	34.62	0.01
27	2500	34.75	0.01	34.73	0.01	34.77	0.03	34.66	0.00	34.68	0.00	34.65	0.00
28	3000	34.74	0.01	34.73	0.01	34.76	0.02	34.68	0.00	34.69	0.00	34.67	0.00
29	3500	34.74	0.01	34.73	0.01	34.75	0.01	34.69	0.00	34.70	0.00	34.68	0.00
30	4000	34.73	0.01	34.72	0.01	34.74	0.01	34.69	0.00	34.70	0.00	34.69	0.00
31	4500	34.73	0.01	34.72	0.01	34.74	0.01	34.70	0.00	34.71	0.00	34.69	0.00
32	5000	34.72	0.01	34.71	0.01	34.74	0.01	34.70	0.00	34.71	0.00	34.69	0.00
33	5500	34.72	0.01	34.71	0.01	34.73	0.02	34.69	0.00	34.71	0.01	34.69	0.00

Table D1b. Annual salinity (psu) basin means and standard errors for the Atlantic Ocean and Indian Ocean as a function of depth

Standard Level	Depth	Atlantic Ocean		South Atlantic Ocean		North Atlantic Ocean		Indian Ocean		South Indian Ocean		North Indian Ocean	
		Mean	Standard Error	Mean	Standard Error	Mean	Standard Error	Mean	Standard Error	Mean	Standard Error	Mean	Standard Error
1	0	34.58	0.31	35.13	0.16	34.14	0.53	34.70	0.11	34.67	0.08	34.85	0.51
2	10	34.87	0.24	35.17	0.15	34.63	0.41	34.71	0.10	34.67	0.08	34.92	0.47
3	20	35.03	0.21	35.19	0.15	34.91	0.35	34.73	0.10	34.68	0.08	35.03	0.43
4	30	35.15	0.19	35.21	0.15	35.10	0.32	34.76	0.09	34.70	0.08	35.12	0.39
5	50	35.31	0.17	35.24	0.15	35.37	0.28	34.82	0.09	34.73	0.08	35.29	0.34
6	75	35.42	0.13	35.23	0.14	35.57	0.21	34.89	0.08	34.79	0.07	35.43	0.29
7	100	35.47	0.12	35.21	0.14	35.70	0.18	34.93	0.08	34.83	0.07	35.48	0.27
8	125	35.47	0.11	35.15	0.12	35.74	0.17	34.95	0.08	34.86	0.07	35.45	0.27
9	150	35.45	0.11	35.09	0.11	35.76	0.16	34.96	0.07	34.88	0.07	35.42	0.27
10	200	35.39	0.09	34.98	0.08	35.75	0.14	34.99	0.07	34.91	0.06	35.40	0.26
11	250	35.32	0.09	34.89	0.06	35.71	0.13	34.99	0.07	34.91	0.06	35.41	0.27
12	300	35.25	0.08	34.82	0.05	35.65	0.13	34.97	0.06	34.89	0.05	35.40	0.27
13	400	35.12	0.08	34.69	0.04	35.52	0.12	34.91	0.06	34.82	0.04	35.38	0.27
14	500	35.00	0.07	34.58	0.03	35.40	0.12	34.84	0.05	34.76	0.03	35.32	0.22
15	600	34.91	0.07	34.50	0.02	35.29	0.11	34.80	0.05	34.71	0.02	35.31	0.23
16	700	34.84	0.07	34.47	0.02	35.20	0.11	34.75	0.04	34.66	0.02	35.26	0.20
17	800	34.81	0.07	34.46	0.02	35.15	0.11	34.72	0.04	34.63	0.02	35.23	0.17
18	900	34.81	0.07	34.48	0.02	35.13	0.11	34.70	0.03	34.61	0.02	35.18	0.13
19	1000	34.82	0.06	34.51	0.02	35.12	0.10	34.68	0.03	34.60	0.02	35.14	0.12
20	1100	34.85	0.06	34.56	0.02	35.14	0.10	34.67	0.03	34.60	0.02	35.08	0.08
21	1200	34.88	0.06	34.61	0.02	35.15	0.10	34.67	0.02	34.61	0.02	35.03	0.04
22	1300	34.90	0.06	34.65	0.02	35.14	0.10	34.68	0.02	34.63	0.02	34.99	0.04
23	1400	34.91	0.05	34.70	0.02	35.14	0.10	34.69	0.02	34.65	0.01	34.96	0.03
24	1500	34.92	0.05	34.73	0.02	35.13	0.09	34.70	0.02	34.66	0.01	34.92	0.02
25	1750	34.94	0.05	34.79	0.02	35.09	0.09	34.72	0.01	34.70	0.01	34.85	0.02
26	2000	34.93	0.04	34.81	0.02	35.06	0.09	34.73	0.01	34.72	0.00	34.81	0.01
27	2500	34.92	0.04	34.83	0.02	35.02	0.08	34.74	0.00	34.74	0.00	34.77	0.01
28	3000	34.88	0.03	34.82	0.02	34.96	0.05	34.73	0.00	34.73	0.00	34.75	0.00
29	3500	34.86	0.02	34.80	0.02	34.93	0.03	34.72	0.00	34.72	0.00	34.74	0.01
30	4000	34.83	0.01	34.77	0.02	34.91	0.00	34.71	0.00	34.71	0.00	34.73	0.01
31	4500	34.81	0.02	34.75	0.02	34.89	0.00	34.70	0.00	34.70	0.00	34.72	0.01
32	5000	34.80	0.02	34.73	0.03	34.88	0.01	34.70	0.01	34.70	0.01	34.72	0.01
33	5500	34.83	0.04	34.70	0.05	34.87	0.01	34.71	0.01	34.71	0.01	0.00	0.00

Table E1. Area, volume, and percent volume contribution of each standard level to total basin volume mean, for the world ocean as a function of depth

Standard Level	Depth (m)	World Ocean			Southern Hemisphere Ocean			Northern Hemisphere Ocean		
		Area (10 <sup>4</sup> km <sup>2</sup> )	Volume (10 <sup>4</sup> km <sup>3</sup> )	% Volume	Area (10 <sup>4</sup> km <sup>2</sup> )	Volume (10 <sup>4</sup> km <sup>3</sup> )	% Volume	Area (10 <sup>4</sup> km <sup>2</sup> )	Volume (10 <sup>4</sup> km <sup>3</sup> )	% Volume
1	0	35013	175	0.14	20176	101	0.13	14837	74	0.14
2	10	34934	349	0.27	20149	201	0.26	14786	148	0.28
3	20	34854	349	0.27	20121	201	0.26	14733	147	0.28
4	30	34765	521	0.40	20102	302	0.39	14663	220	0.42
5	50	34354	773	0.60	19967	449	0.58	14386	324	0.62
6	75	34162	854	0.66	19928	498	0.65	14234	356	0.68
7	100	33735	843	0.65	19799	495	0.64	13936	348	0.67
8	125	33665	842	0.65	19790	495	0.64	13875	347	0.67
9	150	33496	1256	0.97	19757	741	0.96	13738	515	0.99
10	200	33182	1659	1.28	19690	985	1.28	13491	675	1.30
11	250	33104	1655	1.28	19677	984	1.28	13427	671	1.29
12	300	32879	2466	1.91	19612	1471	1.91	13267	995	1.91
13	400	32692	3269	2.53	19545	1955	2.53	13147	1315	2.52
14	500	32418	3242	2.51	19409	1941	2.52	13009	1301	2.50
15	600	32267	3227	2.50	19346	1935	2.51	12920	1292	2.48
16	700	32114	3211	2.49	19287	1929	2.50	12826	1283	2.46
17	800	31910	3191	2.47	19197	1920	2.49	12714	1271	2.44
18	900	31803	3180	2.46	19143	1914	2.48	12661	1266	2.43
19	1000	31494	3149	2.44	19008	1901	2.46	12486	1249	2.40
20	1100	31390	3139	2.43	18966	1897	2.46	12424	1242	2.39
21	1200	31203	3120	2.41	18882	1888	2.45	12322	1232	2.37
22	1300	31067	3107	2.40	18824	1882	2.44	12243	1224	2.35
23	1400	30981	3098	2.40	18778	1878	2.43	12203	1220	2.34
24	1500	30721	5376	4.16	18644	3263	4.23	12076	2113	4.06
25	1750	30438	7610	5.89	18498	4624	5.99	11941	2985	5.73
26	2000	29694	11135	8.62	18142	6803	8.82	11552	4332	8.32
27	2500	28546	14273	11.05	17547	8773	11.37	10999	5500	10.56
28	3000	26476	13238	10.24	16290	8145	10.56	10186	5093	9.78
29	3500	23056	11528	8.92	14019	7009	9.09	9037	4518	8.68
30	4000	18419	9209	7.13	10854	5427	7.03	7565	3783	7.26
31	4500	12569	6285	4.86	6850	3425	4.44	5719	2859	5.49
32	5000	6828	3414	2.64	3172	1586	2.06	3657	1828	3.51
33	5500	1911	478	0.37	506	126	0.16	1406	351	0.67

Table E2. Area, volume, and percent volume contribution of each standard level to total basin volume mean, for the Pacific Ocean as a function of depth

Standard Level	Depth (m)	Pacific Ocean			South Pacific Ocean			North Pacific Ocean		
		Area (10 <sup>4</sup> km <sup>2</sup> )	Volume (10 <sup>4</sup> km <sup>3</sup> )	% Volume	Area (10 <sup>4</sup> km <sup>2</sup> )	Volume (10 <sup>4</sup> km <sup>3</sup> )	% Volume	Area (10 <sup>4</sup> km <sup>2</sup> )	Volume (10 <sup>4</sup> km <sup>3</sup> )	% Volume
1	0	17388	87	0.13	9459	47	0.13	7929	40	0.12
2	10	17346	173	0.26	9438	94	0.27	7908	79	0.24
3	20	17306	173	0.25	9417	94	0.27	7889	79	0.24
4	30	17248	259	0.38	9400	141	0.40	7847	118	0.36
5	50	17101	385	0.57	9339	210	0.59	7762	175	0.54
6	75	16994	425	0.62	9309	233	0.66	7685	192	0.59
7	100	16879	422	0.62	9277	232	0.65	7602	190	0.58
8	125	16866	422	0.62	9274	232	0.65	7591	190	0.58
9	150	16861	632	0.93	9273	348	0.98	7588	285	0.88
10	200	16794	840	1.24	9249	462	1.30	7544	377	1.16
11	250	16779	839	1.23	9245	462	1.30	7534	377	1.16
12	300	16718	1254	1.84	9218	691	1.95	7500	562	1.73
13	400	16666	1667	2.45	9193	919	2.59	7473	747	2.30
14	500	16570	1657	2.44	9133	913	2.57	7436	744	2.29
15	600	16518	1652	2.43	9098	910	2.56	7420	742	2.28
16	700	16452	1645	2.42	9060	906	2.55	7392	739	2.27
17	800	16360	1636	2.41	9008	901	2.54	7353	735	2.26
18	900	16309	1631	2.40	8969	897	2.53	7339	734	2.26
19	1000	16182	1618	2.38	8893	889	2.51	7289	729	2.24
20	1100	16125	1613	2.37	8867	887	2.50	7258	726	2.23
21	1200	16054	1605	2.36	8824	882	2.49	7230	723	2.22
22	1300	15996	1600	2.35	8790	879	2.48	7206	721	2.22
23	1400	15955	1596	2.35	8763	876	2.47	7193	719	2.21
24	1500	15858	2775	4.08	8699	1522	4.29	7159	1253	3.85
25	1750	15730	3933	5.78	8612	2153	6.07	7119	1780	5.47
26	2000	15407	5778	8.50	8409	3153	8.89	6998	2624	8.07
27	2500	14976	7488	11.01	8130	4065	11.46	6846	3423	10.53
28	3000	14075	7037	10.35	7534	3767	10.62	6540	3270	10.06
29	3500	12476	6238	9.18	6471	3236	9.12	6005	3002	9.23
30	4000	10069	5034	7.41	4793	2397	6.76	5276	2638	8.11
31	4500	7035	3517	5.17	2813	1406	3.96	4222	2111	6.49
32	5000	4073	2036	3.00	1246	623	1.76	2827	1413	4.35
33	5500	1277	319	0.47	173	43	0.12	1104	276	0.85

Table E3. Area, volume, and percent volume contribution of each standard level to total basin volume mean, for the Atlantic Ocean as a function of depth

Standard Level	Depth (m)	Atlantic Ocean			South Atlantic Ocean			North Atlantic Ocean		
		Area (10 <sup>4</sup> km <sup>2</sup> )	Volume (10 <sup>4</sup> km <sup>3</sup> )	% Volume	Area (10 <sup>4</sup> km <sup>2</sup> )	Volume (10 <sup>4</sup> km <sup>3</sup> )	% Volume	Area (10 <sup>4</sup> km <sup>2</sup> )	Volume (10 <sup>4</sup> km <sup>3</sup> )	% Volume
1	0	10212	51	0.15	4489	22	0.13	5723	29	0.18
2	10	10180	102	0.30	4486	45	0.26	5694	57	0.35
3	20	10152	102	0.30	4486	45	0.26	5667	57	0.35
4	30	10125	152	0.45	4484	67	0.38	5642	85	0.52
5	50	9934	224	0.66	4447	100	0.57	5487	123	0.76
6	75	9858	246	0.73	4443	111	0.63	5415	135	0.84
7	100	9624	241	0.71	4394	110	0.63	5230	131	0.81
8	125	9569	239	0.71	4389	110	0.62	5180	130	0.80
9	150	9415	353	1.05	4361	164	0.93	5054	190	1.17
10	200	9206	460	1.36	4342	217	1.24	4864	243	1.50
11	250	9145	457	1.35	4335	217	1.23	4811	241	1.49
12	300	9012	676	2.00	4319	324	1.84	4693	352	2.17
13	400	8895	890	2.64	4293	429	2.44	4602	460	2.84
14	500	8802	880	2.61	4266	427	2.43	4536	454	2.80
15	600	8724	872	2.58	4253	425	2.42	4470	447	2.76
16	700	8655	866	2.56	4240	424	2.41	4415	441	2.73
17	800	8563	856	2.54	4213	421	2.40	4350	435	2.69
18	900	8521	852	2.52	4206	421	2.39	4315	431	2.67
19	1000	8414	841	2.49	4193	419	2.39	4221	422	2.61
20	1100	8378	838	2.48	4184	418	2.38	4194	419	2.59
21	1200	8297	830	2.46	4160	416	2.37	4136	414	2.56
22	1300	8237	824	2.44	4151	415	2.36	4085	409	2.52
23	1400	8207	821	2.43	4148	415	2.36	4059	406	2.51
24	1500	8127	1422	4.21	4131	723	4.11	3996	699	4.32
25	1750	8020	2005	5.94	4109	1027	5.85	3911	978	6.04
26	2000	7766	2912	8.63	4064	1524	8.67	3702	1388	8.58
27	2500	7348	3674	10.88	3961	1981	11.27	3386	1693	10.46
28	3000	6693	3347	9.91	3707	1853	10.55	2986	1493	9.22
29	3500	5793	2897	8.58	3263	1632	9.29	2530	1265	7.81
30	4000	4592	2296	6.80	2627	1314	7.48	1965	983	6.07
31	4500	3182	1591	4.71	1787	894	5.09	1395	697	4.31
32	5000	1688	844	2.50	877	438	2.50	812	406	2.51
33	5500	386	96	0.29	84	21	0.12	301	75	0.47

Table E4. Area, volume, and percent volume contribution of each standard level to total basin volume mean, for the Indian Ocean as a function of depth

Standard Level	Depth (m)	Indian Ocean			South Indian Ocean			North Indian Ocean		
		Area (10 <sup>4</sup> km <sup>2</sup> )	Volume (10 <sup>4</sup> km <sup>3</sup> )	% Volume	Area (10 <sup>4</sup> km <sup>2</sup> )	Volume (10 <sup>4</sup> km <sup>3</sup> )	% Volume	Area (10 <sup>4</sup> km <sup>2</sup> )	Volume (10 <sup>4</sup> km <sup>3</sup> )	% Volume
1	0	7411	37	0.13	6240	31	0.13	1171	6	0.17
2	10	7409	74	0.27	6240	62	0.26	1169	12	0.35
3	20	7402	74	0.27	6235	62	0.26	1167	12	0.35
4	30	7398	111	0.40	6235	94	0.39	1164	17	0.52
5	50	7332	165	0.60	6198	139	0.58	1134	26	0.75
6	75	7325	183	0.67	6193	155	0.64	1131	28	0.84
7	100	7249	181	0.66	6145	154	0.64	1104	28	0.82
8	125	7247	181	0.66	6143	154	0.64	1104	28	0.82
9	150	7236	271	0.99	6140	230	0.95	1097	41	1.22
10	200	7198	360	1.31	6115	306	1.27	1083	54	1.60
11	250	7197	360	1.31	6114	306	1.27	1083	54	1.60
12	300	7166	537	1.95	6092	457	1.89	1074	81	2.38
13	400	7147	715	2.60	6075	608	2.52	1072	107	3.17
14	500	7063	706	2.57	6025	603	2.50	1037	104	3.07
15	600	7041	704	2.56	6011	601	2.49	1030	103	3.05
16	700	7022	702	2.55	6002	600	2.49	1020	102	3.02
17	800	7002	700	2.54	5991	599	2.48	1011	101	2.99
18	900	6989	699	2.54	5983	598	2.48	1006	101	2.98
19	1000	6912	691	2.51	5935	593	2.46	977	98	2.89
20	1100	6900	690	2.51	5928	593	2.46	972	97	2.88
21	1200	6865	686	2.49	5909	591	2.45	956	96	2.83
22	1300	6846	685	2.49	5894	589	2.44	952	95	2.82
23	1400	6831	683	2.48	5880	588	2.44	951	95	2.81
24	1500	6748	1181	4.29	5827	1020	4.22	922	161	4.77
25	1750	6700	1675	6.08	5789	1447	5.99	911	228	6.74
26	2000	6533	2450	8.90	5680	2130	8.82	853	320	9.46
27	2500	6234	3117	11.32	5467	2733	11.32	767	384	11.35
28	3000	5716	2858	10.38	5058	2529	10.47	659	329	9.75
29	3500	4792	2396	8.71	4290	2145	8.88	502	251	7.43
30	4000	3760	1880	6.83	3436	1718	7.11	324	162	4.80
31	4500	2353	1176	4.27	2250	1125	4.66	103	51	1.52
32	5000	1067	534	1.94	1049	525	2.17	18	9	0.27
33	5500	249	62	0.23	249	62	0.26	0	0	0.00

Table E5a. Number of independent points ( $N_I$ ) used in the standard error computation for the world ocean and Pacific Ocean.

Standard Level	Depth (m)	World Ocean	Southern Hemisphere	Northern Hemisphere	Pacific Ocean	South Pacific Ocean	North Pacific Ocean
		$N_I$	$N_I$	$N_I$	$N_I$	$N_I$	$N_I$
1	0	361.8	208.5	153.3	179.7	97.8	81.9
2	10	361.0	208.2	152.8	179.3	97.5	81.7
3	20	360.2	207.9	152.3	178.8	97.3	81.5
4	30	359.3	207.7	151.5	178.2	97.1	81.1
5	50	355.0	206.3	148.7	176.7	96.5	80.2
6	75	353.0	205.9	147.1	175.6	96.2	79.4
7	100	348.6	204.6	144.0	174.4	95.9	78.6
8	125	347.9	204.5	143.4	174.3	95.8	78.5
9	150	346.1	204.2	142.0	174.2	95.8	78.4
10	200	342.9	203.5	139.4	173.6	95.6	78.0
11	250	342.1	203.3	138.8	173.4	95.5	77.9
12	300	339.8	202.7	137.1	172.8	95.3	77.5
13	400	337.8	202.0	135.9	172.2	95.0	77.2
14	500	335.0	200.6	134.4	171.2	94.4	76.8
15	600	333.5	199.9	133.5	170.7	94.0	76.7
16	700	331.9	199.3	132.6	170.0	93.6	76.4
17	800	329.8	198.4	131.4	169.1	93.1	76.0
18	900	328.7	197.8	130.8	168.5	92.7	75.8
19	1000	325.5	196.4	129.0	167.2	91.9	75.3
20	1100	324.4	196.0	128.4	166.6	91.6	75.0
21	1200	322.5	195.1	127.3	165.9	91.2	74.7
22	1300	321.1	194.5	126.5	165.3	90.8	74.5
23	1400	320.2	194.1	126.1	164.9	90.6	74.3
24	1500	317.5	192.7	124.8	163.9	89.9	74.0
25	1750	314.6	191.2	123.4	162.6	89.0	73.6
26	2000	306.9	187.5	119.4	159.2	86.9	72.3
27	2500	295.0	181.3	113.7	154.8	84.0	70.7
28	3000	273.6	168.3	105.3	145.5	77.9	67.6
29	3500	238.3	144.9	93.4	128.9	66.9	62.1
30	4000	190.3	112.2	78.2	104.1	49.5	54.5
31	4500	129.9	70.8	59.1	72.7	29.1	43.6
32	5000	70.6	32.8	37.8	42.1	12.9	29.2
33	5500	19.8	5.2	14.5	13.2	1.8	11.4

Table E5b. Number of independent points ( $N_I$ ) used in the standard error computation for the Atlantic Ocean and Indian Ocean.

		Atlantic Ocean	South Atlantic Ocean	North Atlantic Ocean	Indian Ocean	South Indian Ocean	North Indian Ocean
Standard Level	Depth (m)	$N_I$	$N_I$	$N_I$	$N_I$	$N_I$	$N_I$
1	0	105.5	46.4	59.1	76.6	64.5	12.1
2	10	105.2	46.4	58.8	76.6	64.5	12.1
3	20	104.9	46.4	58.6	76.5	64.4	12.1
4	30	104.6	46.3	58.3	76.5	64.4	12.0
5	50	102.7	46.0	56.7	75.8	64.1	11.7
6	75	101.9	45.9	56.0	75.7	64.0	11.7
7	100	99.5	45.4	54.1	74.9	63.5	11.4
8	125	98.9	45.4	53.5	74.9	63.5	11.4
9	150	97.3	45.1	52.2	74.8	63.4	11.3
10	200	95.1	44.9	50.3	74.4	63.2	11.2
11	250	94.5	44.8	49.7	74.4	63.2	11.2
12	300	93.1	44.6	48.5	74.1	63.0	11.1
13	400	91.9	44.4	47.6	73.9	62.8	11.1
14	500	91.0	44.1	46.9	73.0	62.3	10.7
15	600	90.2	44.0	46.2	72.8	62.1	10.6
16	700	89.4	43.8	45.6	72.6	62.0	10.5
17	800	88.5	43.5	45.0	72.4	61.9	10.4
18	900	88.1	43.5	44.6	72.2	61.8	10.4
19	1000	86.9	43.3	43.6	71.4	61.3	10.1
20	1100	86.6	43.2	43.3	71.3	61.3	10.0
21	1200	85.7	43.0	42.7	70.9	61.1	9.9
22	1300	85.1	42.9	42.2	70.8	60.9	9.8
23	1400	84.8	42.9	41.9	70.6	60.8	9.8
24	1500	84.0	42.7	41.3	69.7	60.2	9.5
25	1750	82.9	42.5	40.4	69.2	59.8	9.4
26	2000	80.3	42.0	38.3	67.5	58.7	8.8
27	2500	75.9	40.9	35.0	64.4	56.5	7.9
28	3000	69.2	38.3	30.9	59.1	52.3	6.8
29	3500	59.9	33.7	26.1	49.5	44.3	5.2
30	4000	47.5	27.2	20.3	38.9	35.5	3.4
31	4500	32.9	18.5	14.4	24.3	23.3	1.1
32	5000	17.4	9.1	8.4	11.0	10.8	0.0
33	5500	4.0	0.9	3.1	2.6	2.6	0.0



Table E6. Volume means of salinity for the major ocean basins and the volume of each basin

Basin	Volume ( $10^4 \text{km}^3$ )	Salinity (psu)
Globe	129223	34.73
Southern Hemisphere	77144	34.69
Northern Hemisphere	52079	34.77
Pacific	67985	34.62
South Pacific	35473	34.65
North Pacific	32512	34.58
Atlantic	33756	34.93
South Atlantic	17569	34.75
North Atlantic	16187	35.12
Indian	27526	34.75
South Indian	24147	34.71
North Indian	3379	34.98

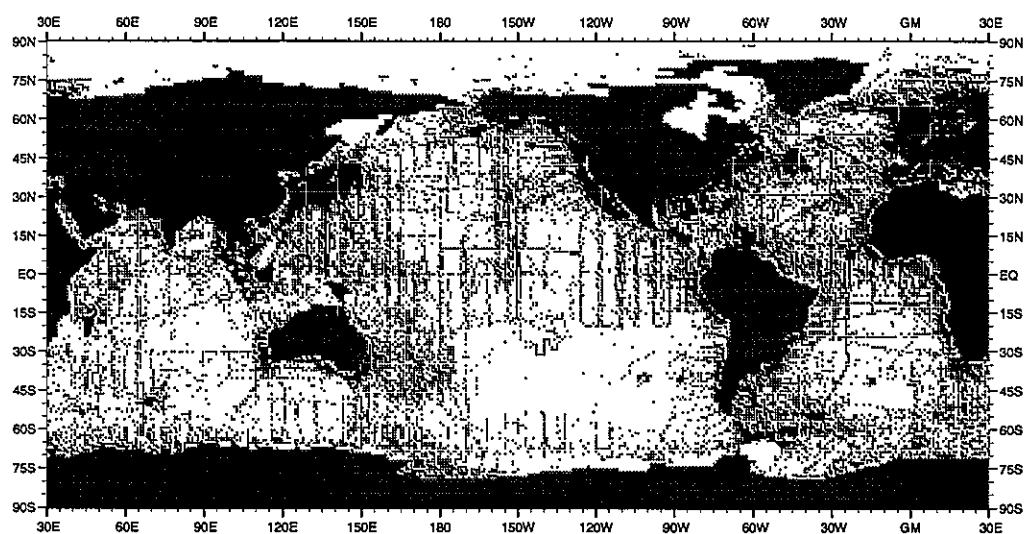


Fig. F1 Winter (Jan.-Mar.) distribution of salinity observations at the surface

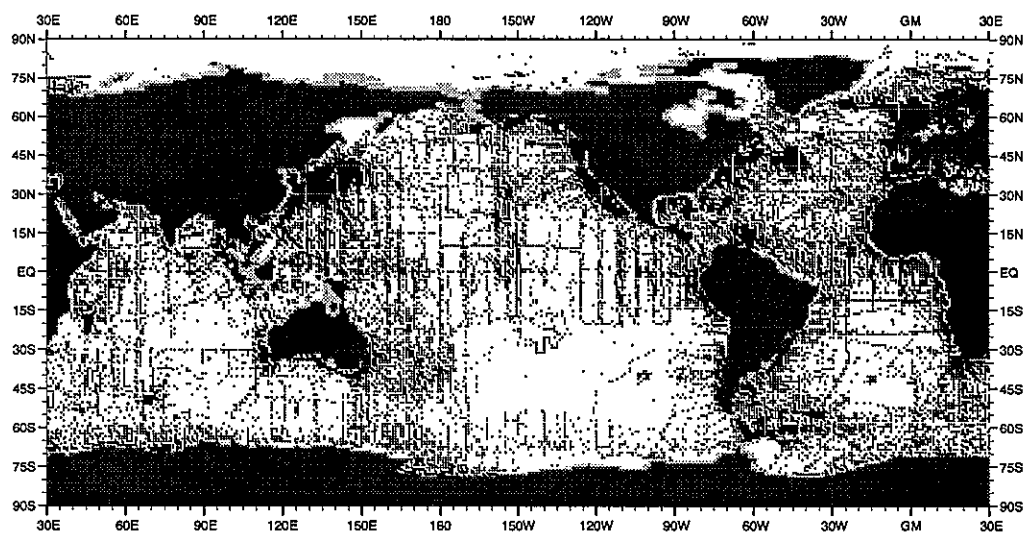


Fig. F2 Winter (Jan.-Mar.) distribution of salinity observations at 50 m depth

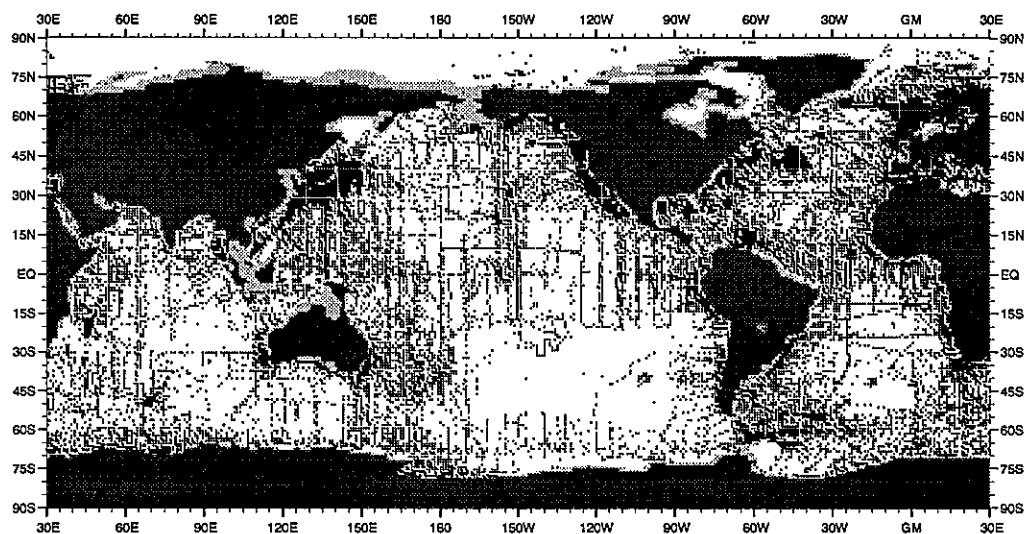


Fig. F3 Winter (Jan.-Mar.) distribution of salinity observations at 75 m depth

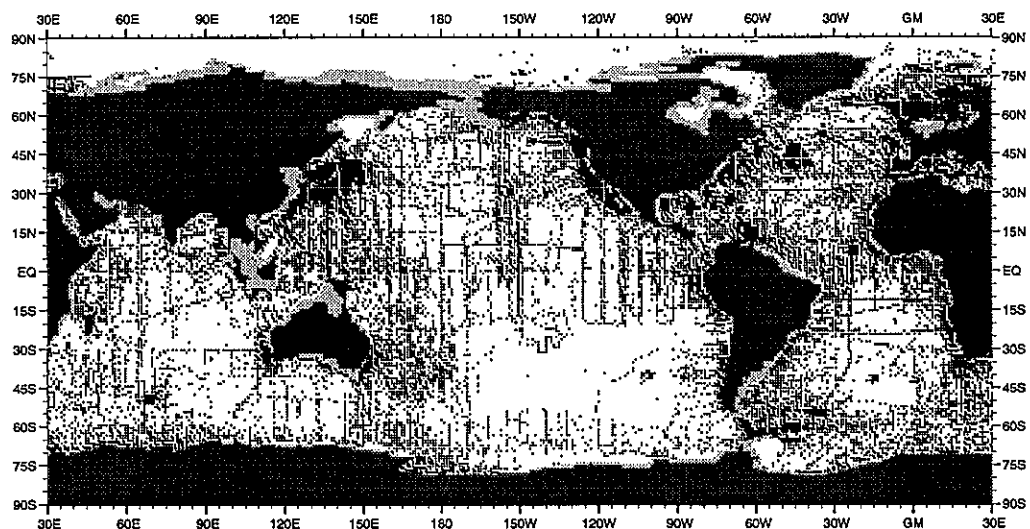


Fig. F4 Winter (Jan.-Mar.) distribution of salinity observations at 100 m depth

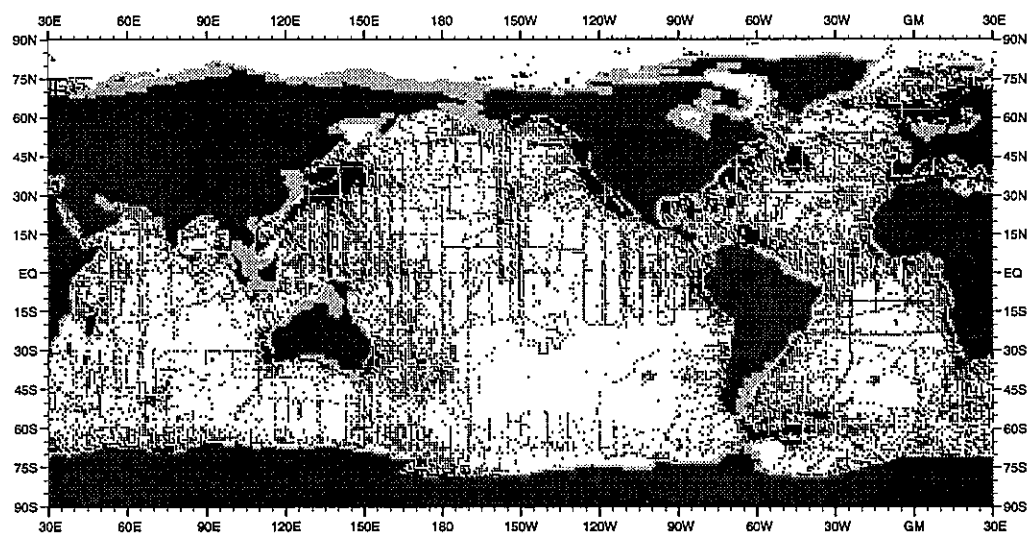


Fig. F5 Winter (Jan.-Mar.) distribution of salinity observations at 125 m depth

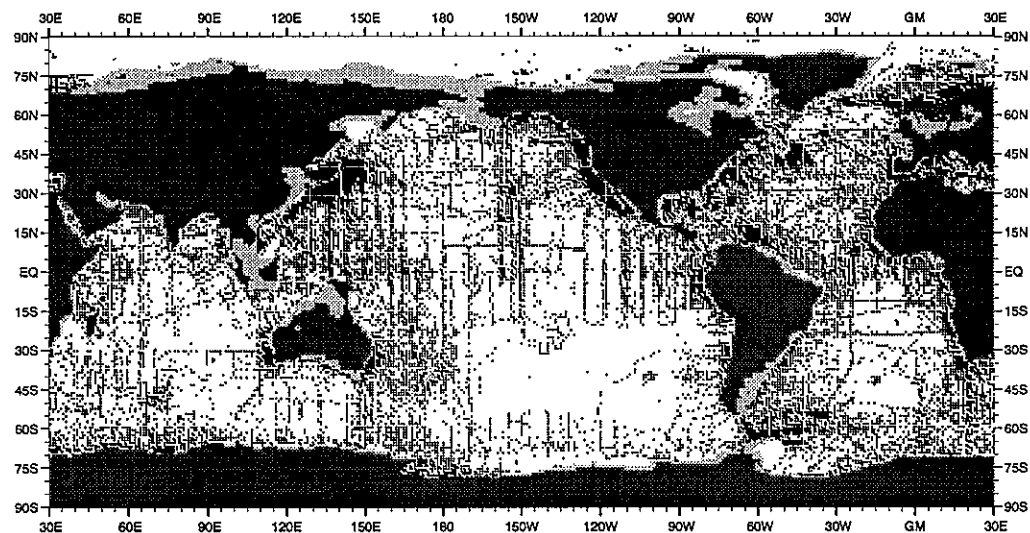


Fig. F6 Winter (Jan.-Mar.) distribution of salinity observations at 150 m depth

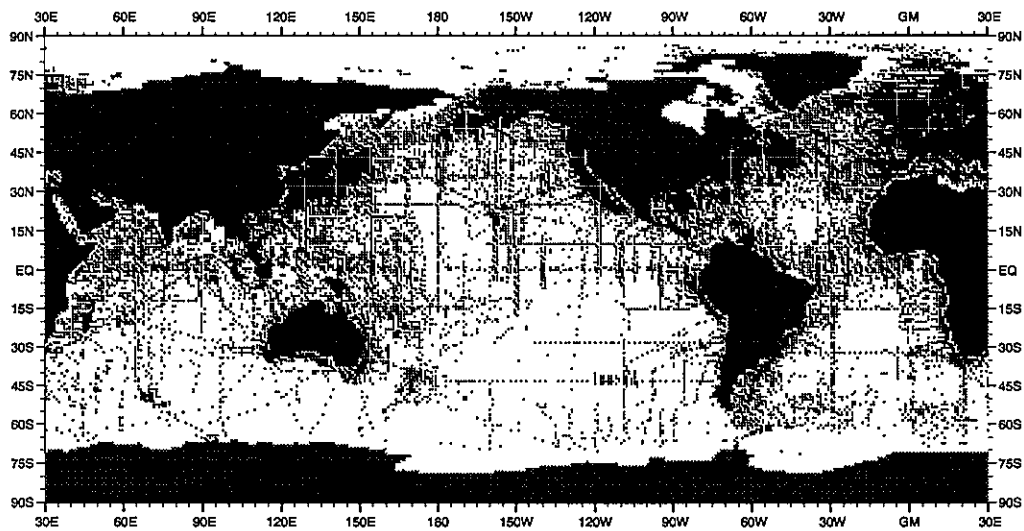


Fig. F7 Spring (Apr.-Jun.) distribution of salinity observations at the surface

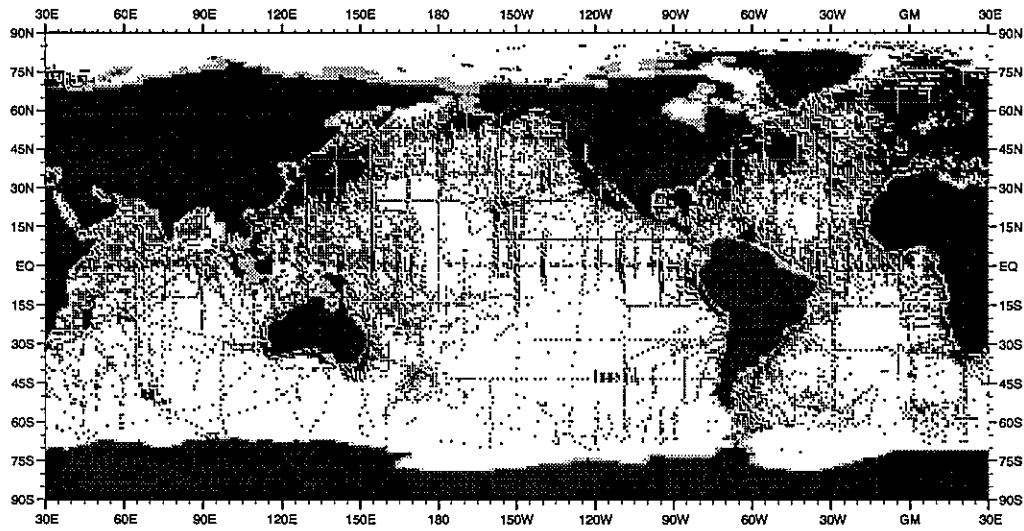


Fig. F8 Spring (Apr.-Jun.) distribution of salinity observations at 50 m depth

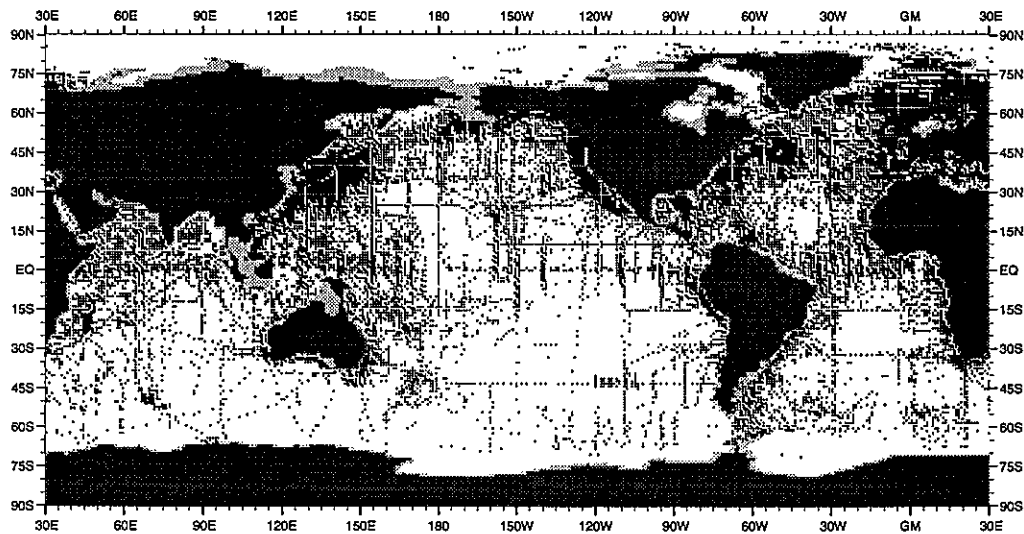


Fig. F9 Spring (Apr.-Jun.) distribution of salinity observations at 75 m depth

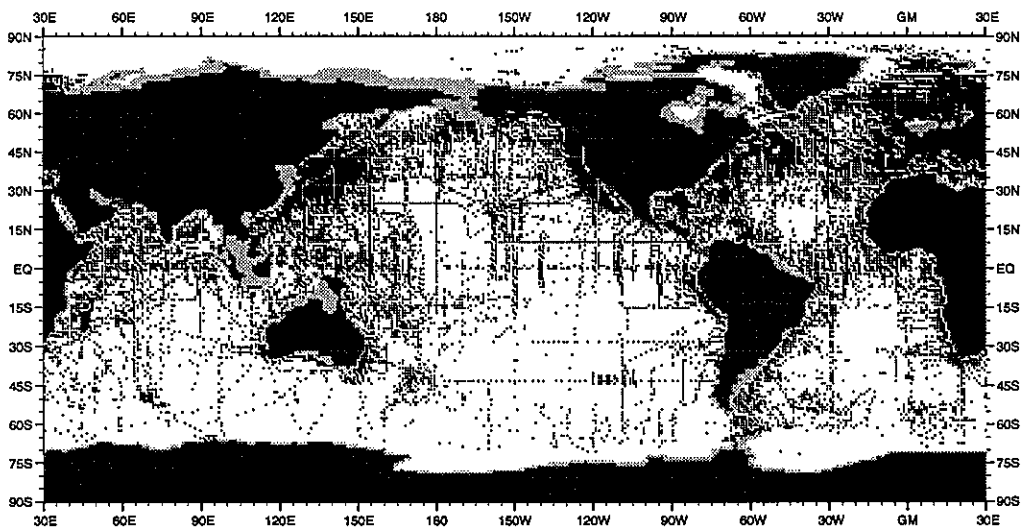


Fig. F10 Spring (Apr.-Jun.) distribution of salinity observations at 100 m depth

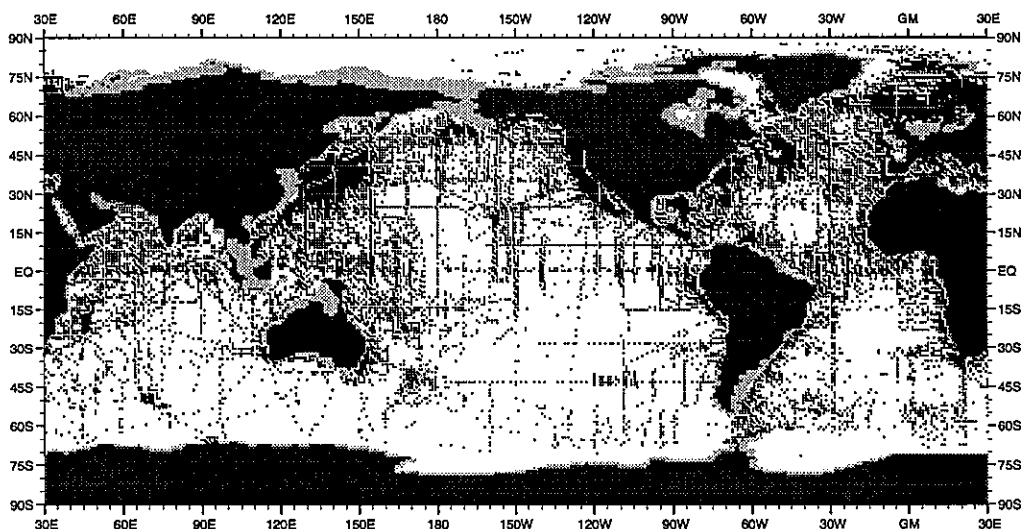


Fig. F11 Spring (Apr.-Jun.) distribution of salinity observations at 125 m depth

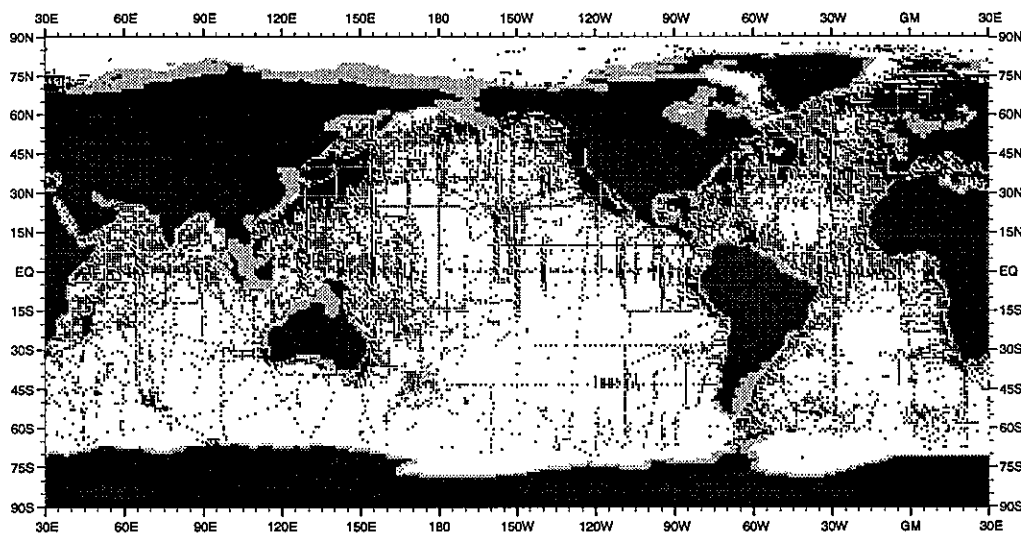


Fig. F12 Spring (Apr.-Jun.) distribution of salinity observations at 150 m depth

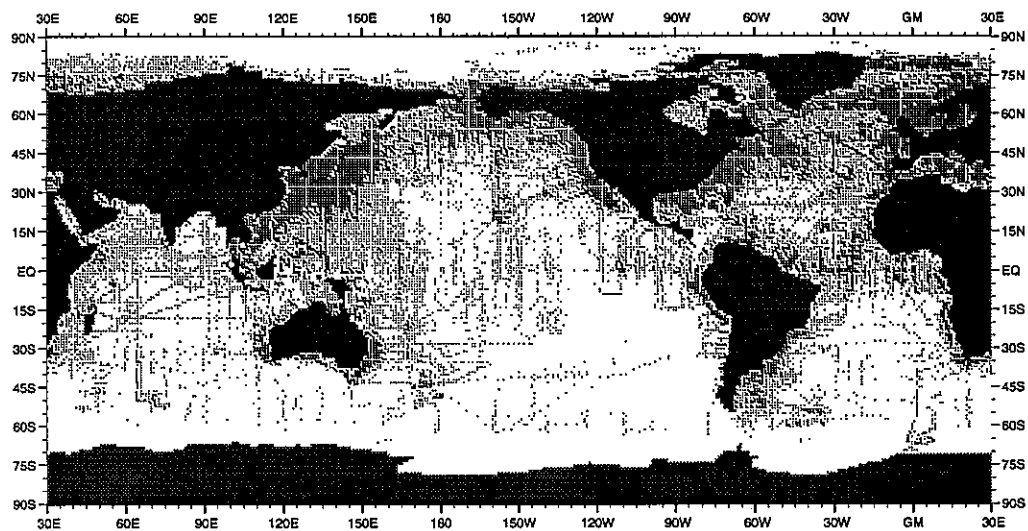


Fig. F13 Summer (Jul.-Sep.) distribution of salinity observations at the surface

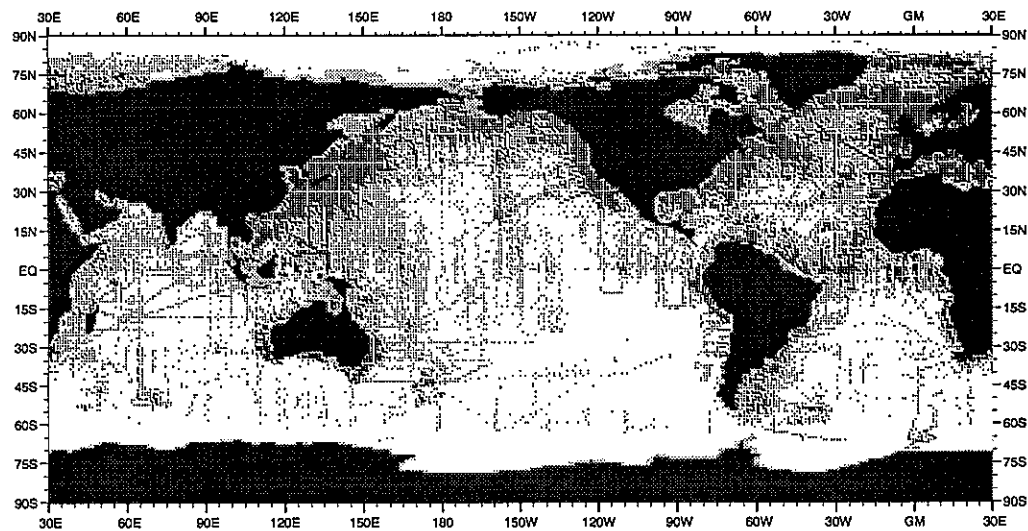


Fig. F14 Summer (Jul.-Sep.) distribution of salinity observations at 50 m depth

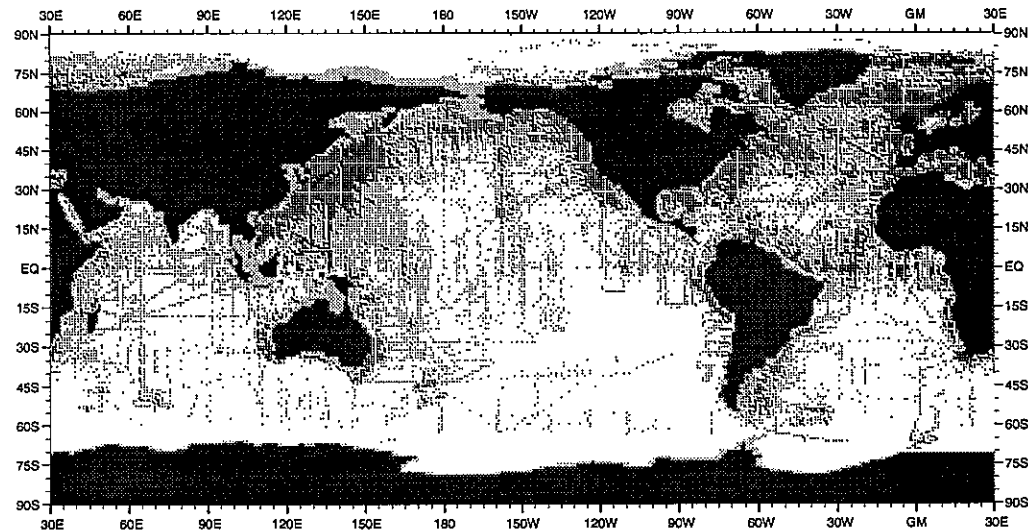


Fig. F15 Summer (Jul.-Sep.) distribution of salinity observations at 75 m depth

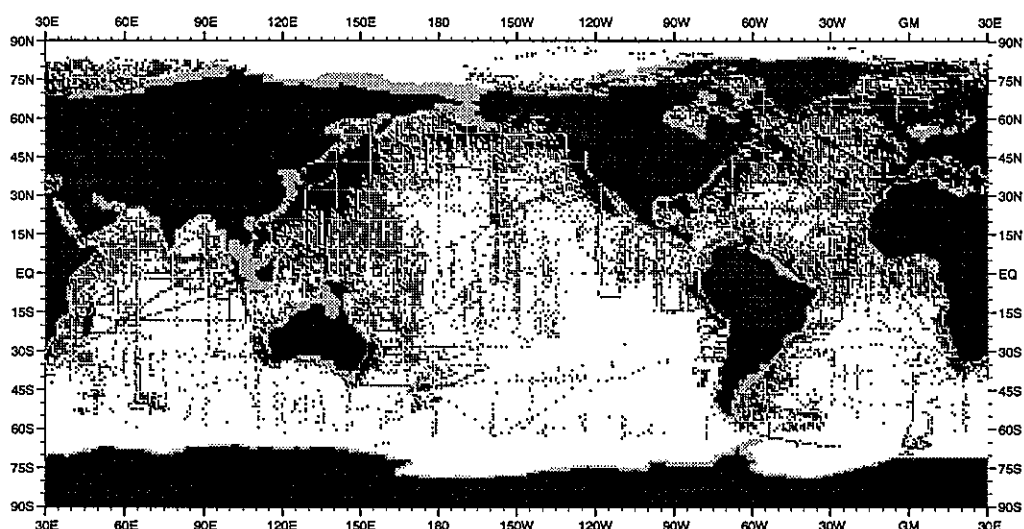


Fig. F16 Summer (Jul-Sep.) distribution of salinity observations at 100 m depth

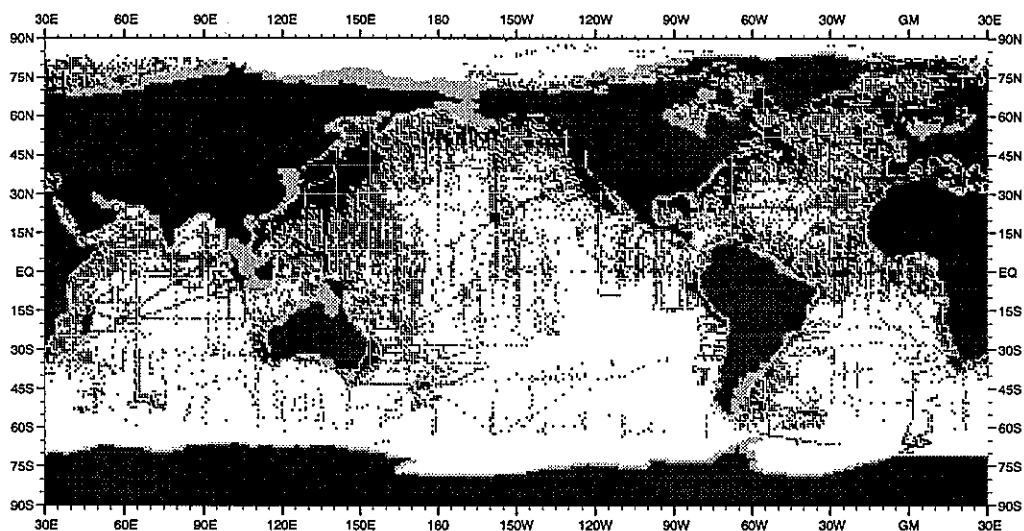


Fig. F17 Summer (Jul-Sep.) distribution of salinity observations at 125 m depth

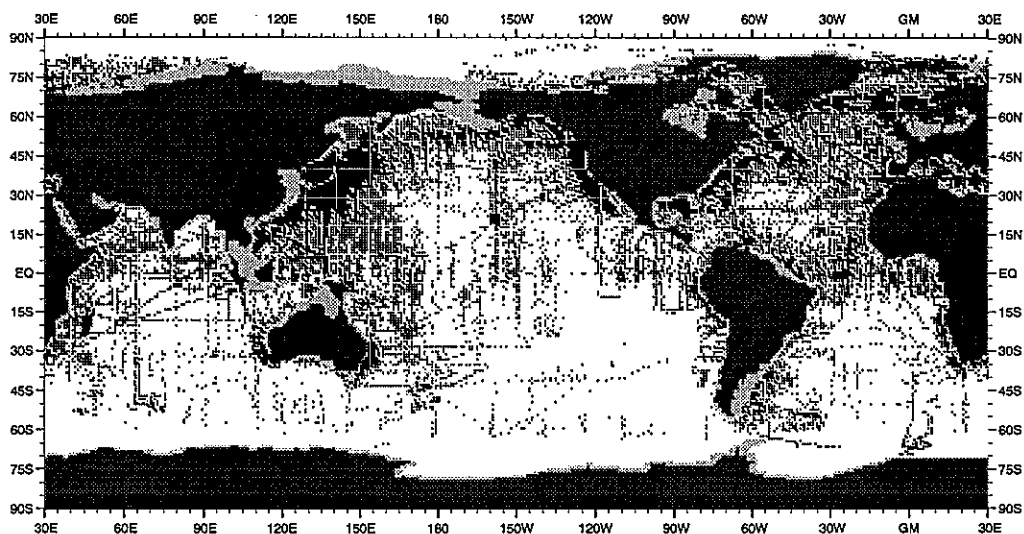


Fig. F18 Summer (Jul-Sep.) distribution of salinity observations at 150 m depth

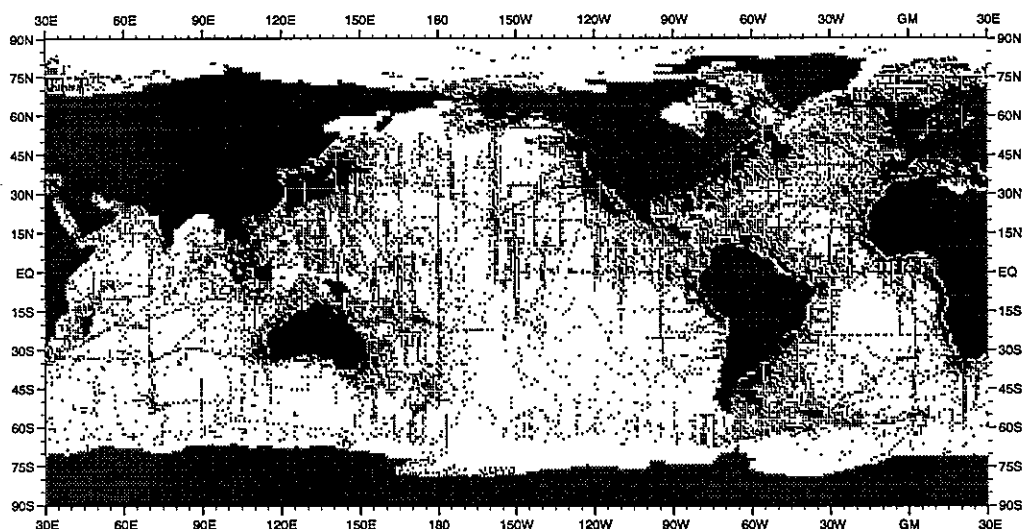


Fig. F19 Fall (Oct.-Dec.) distribution of salinity observations at the surface

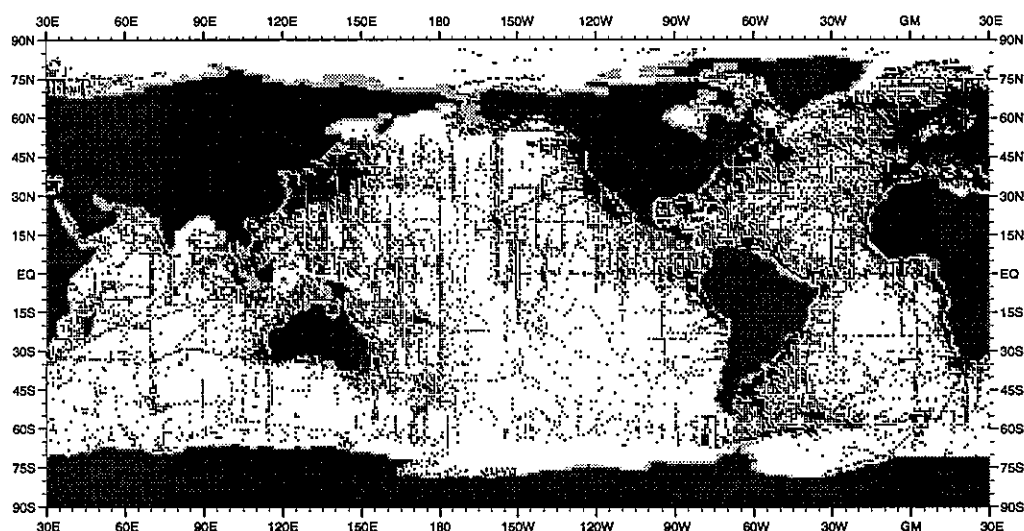


Fig. F20 Fall (Oct.-Dec.) distribution of salinity observations at 50 m depth

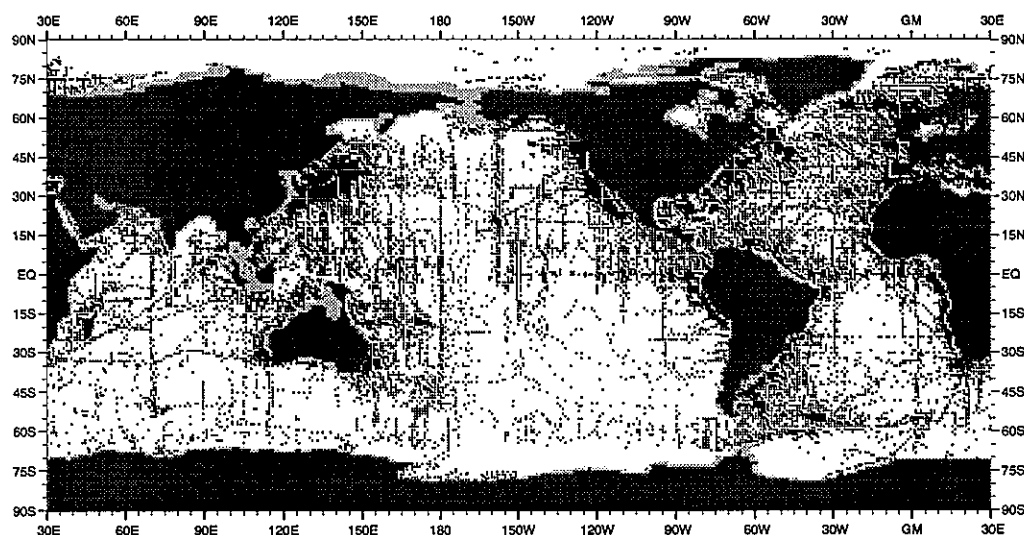


Fig. F21 Fall (Oct.-Dec.) distribution of salinity observations at 75 m depth



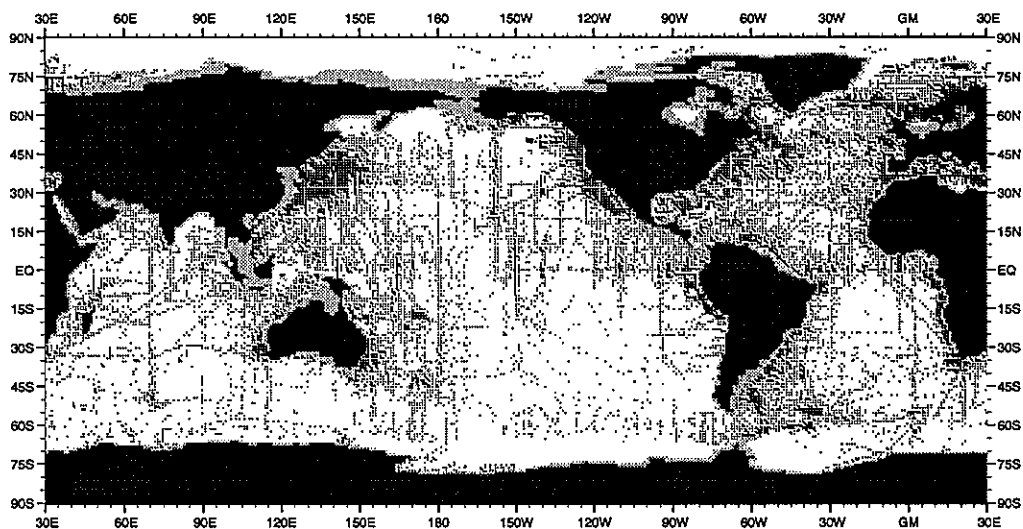


Fig. F22 Fall (Oct.-Dec.) distribution of salinity observations at 100 m depth

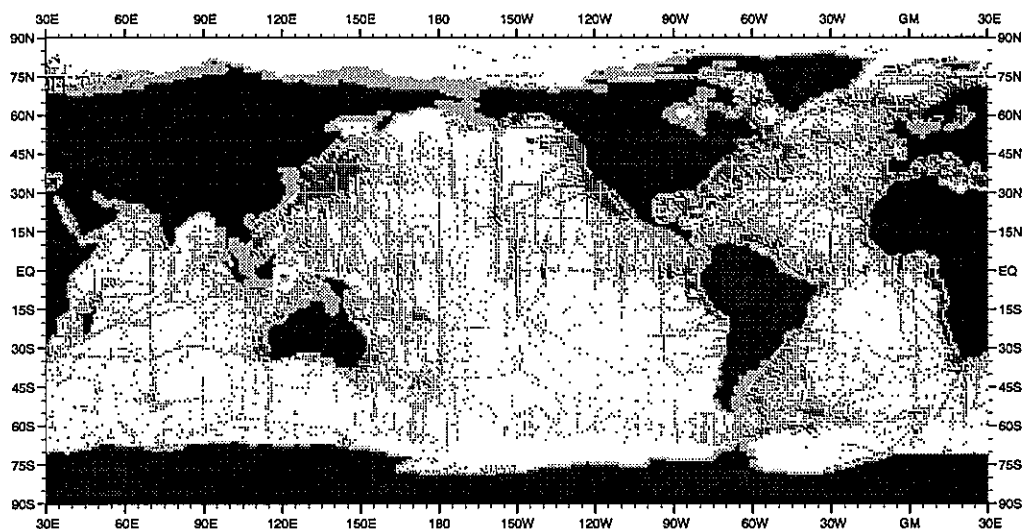


Fig. F23 Fall (Oct.-Dec.) distribution of salinity observations at 125 m depth

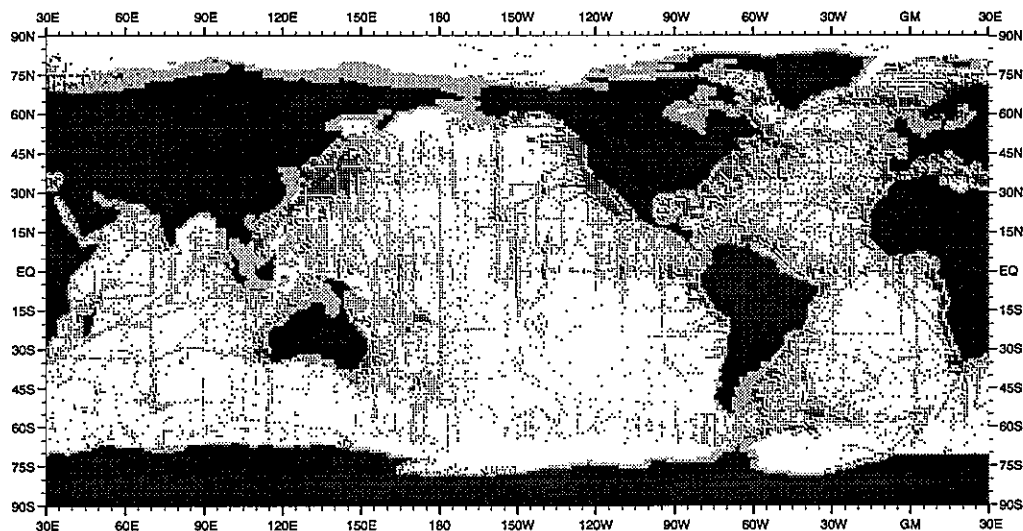


Fig. F24 Fall (Oct.-Dec.) distribution of salinity observations at 150 m depth

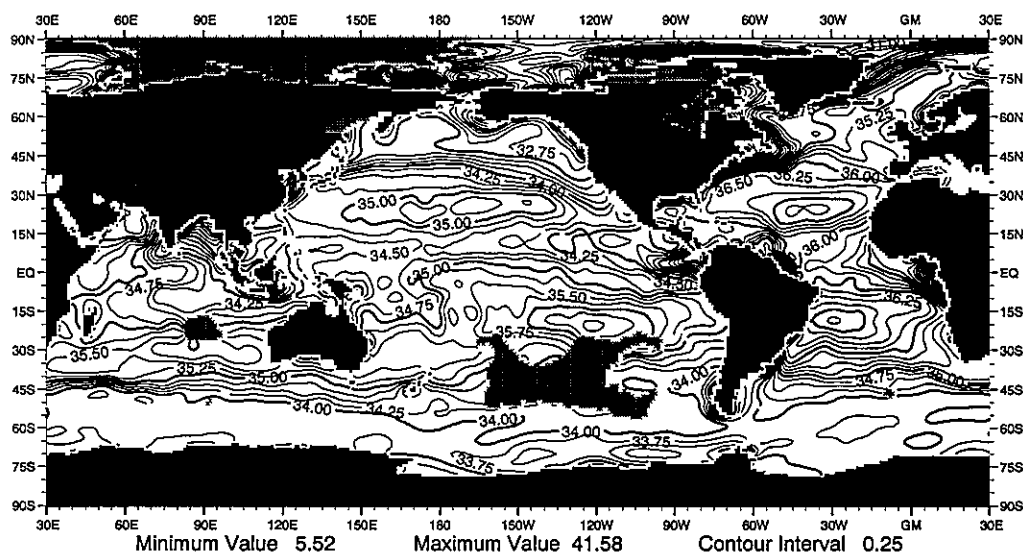


Fig. G1 Winter (Jan.-Mar.) mean salinity (psu) at the surface

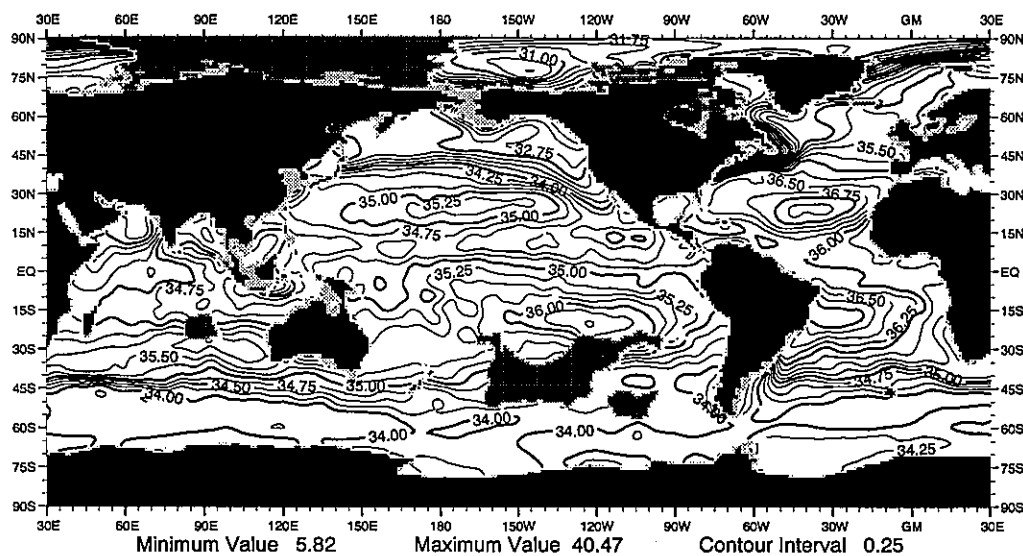


Fig. G2 Winter (Jan.-Mar.) mean salinity (psu) at 50 m depth

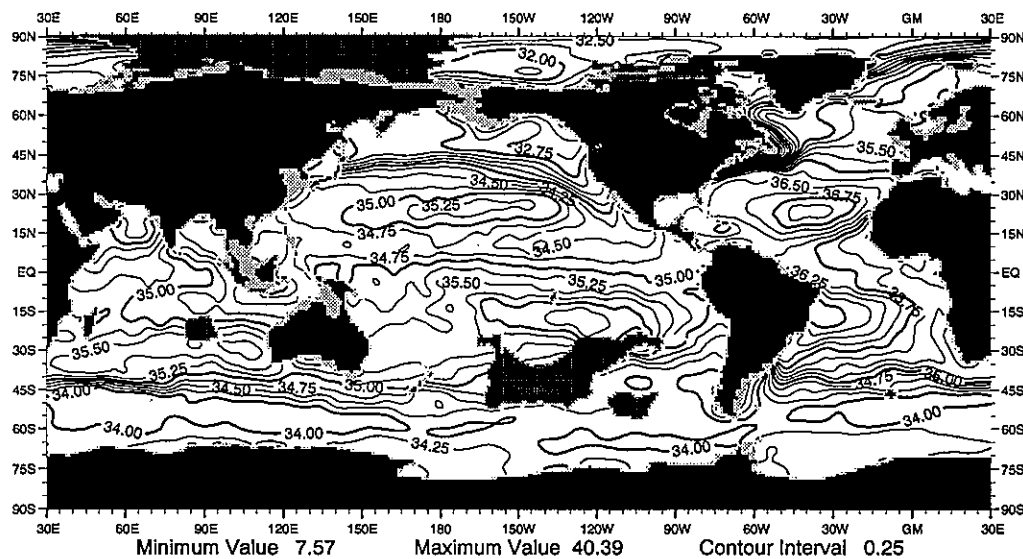


Fig. G3 Winter (Jan.-Mar.) mean salinity (psu) at 75 m depth

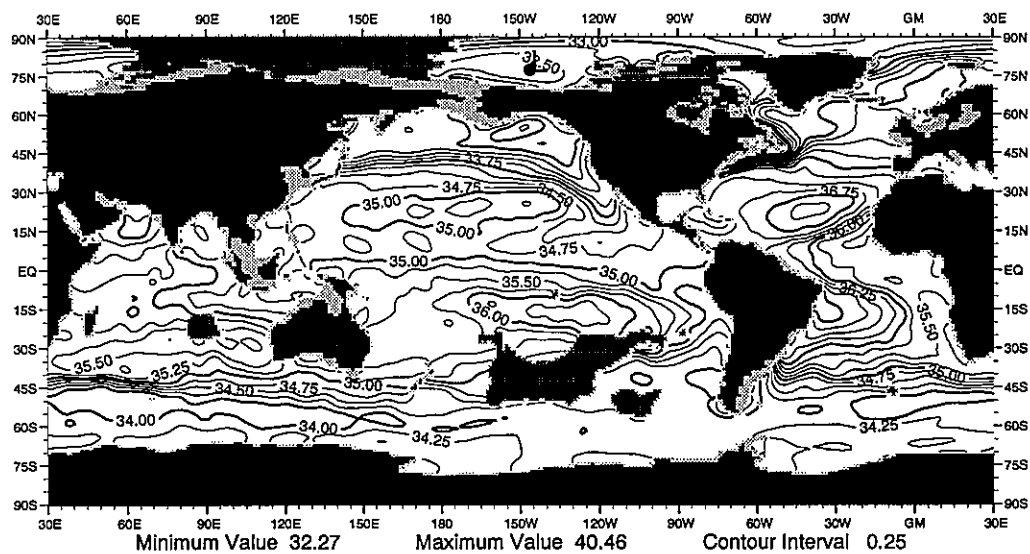


Fig. G4 Winter (Jan.-Mar.) mean salinity (psu) at 100 m depth

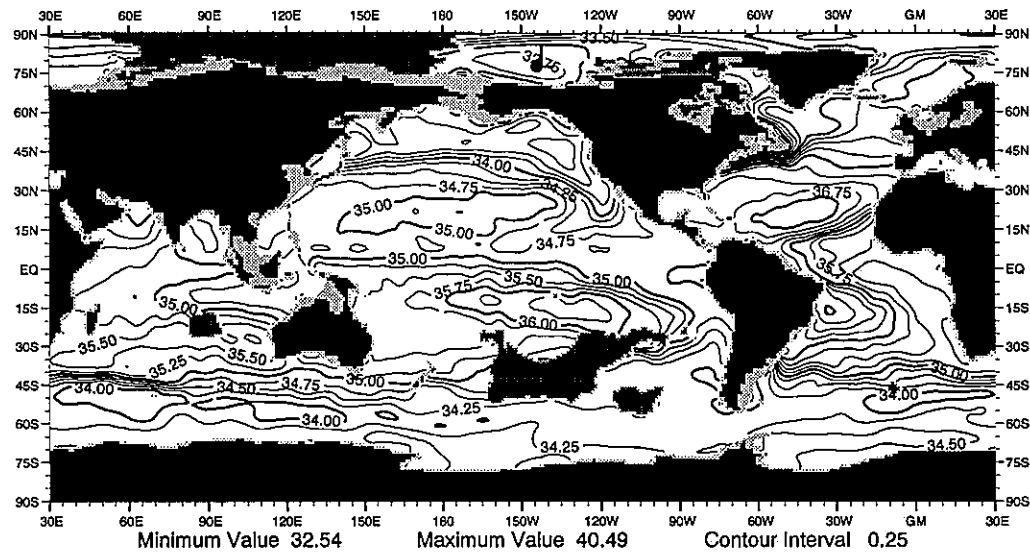


Fig. G5 Winter (Jan.-Mar.) mean salinity (psu) at 125 m depth

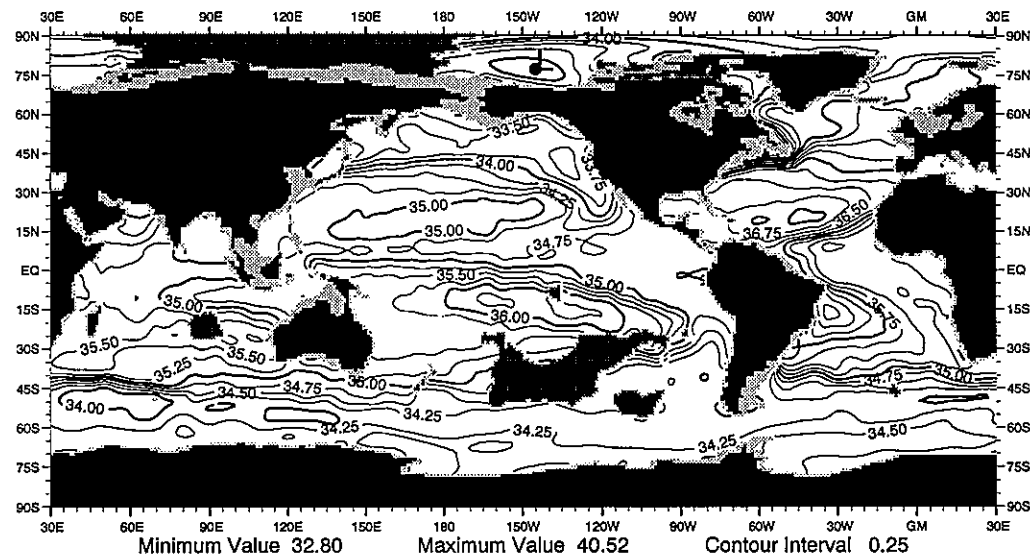


Fig. G6 Winter (Jan.-Mar.) mean salinity (psu) at 150 m depth

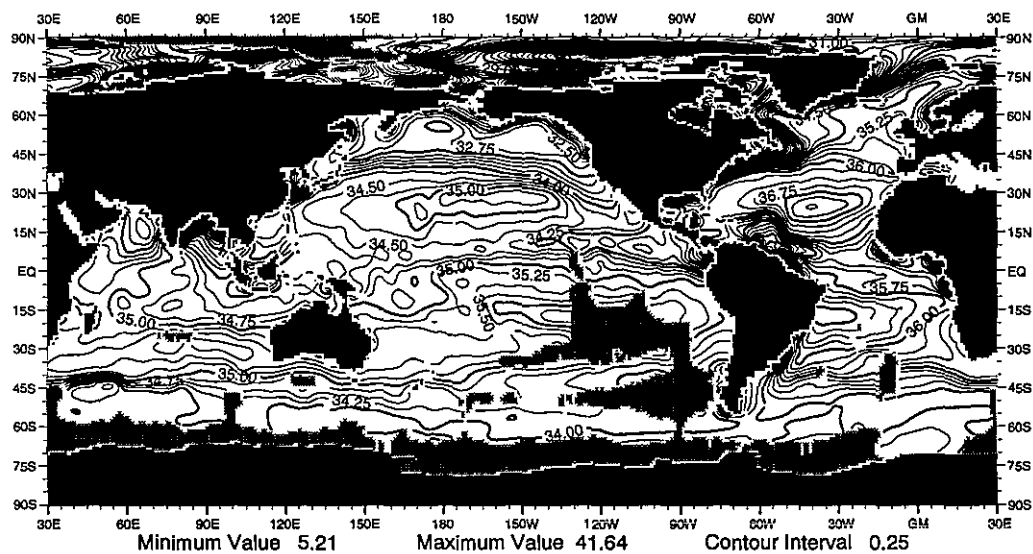


Fig. G13 Summer (Jul.-Sep.) mean salinity (psu) at the surface

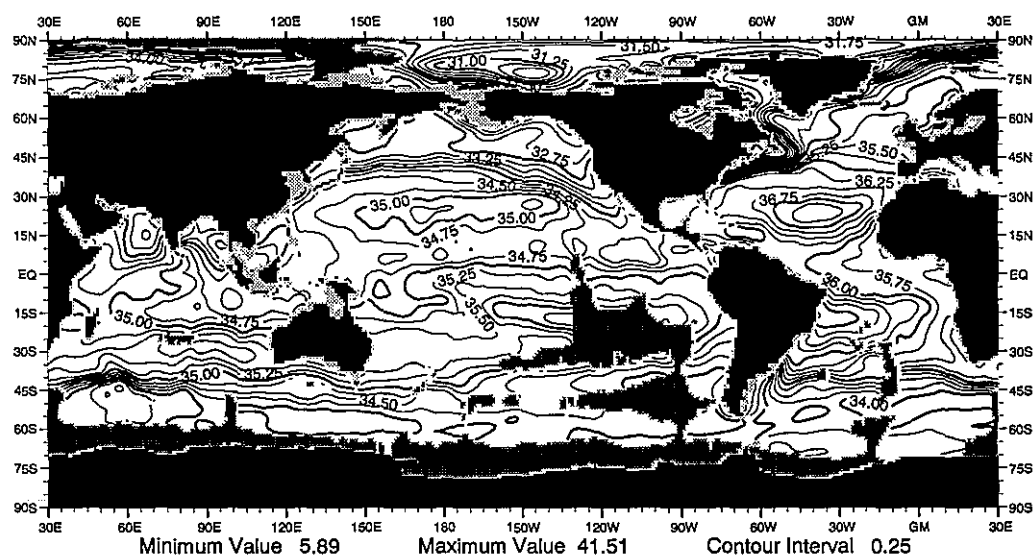


Fig. G14 Summer (Jul.-Sep.) mean salinity (psu) at 50 m depth

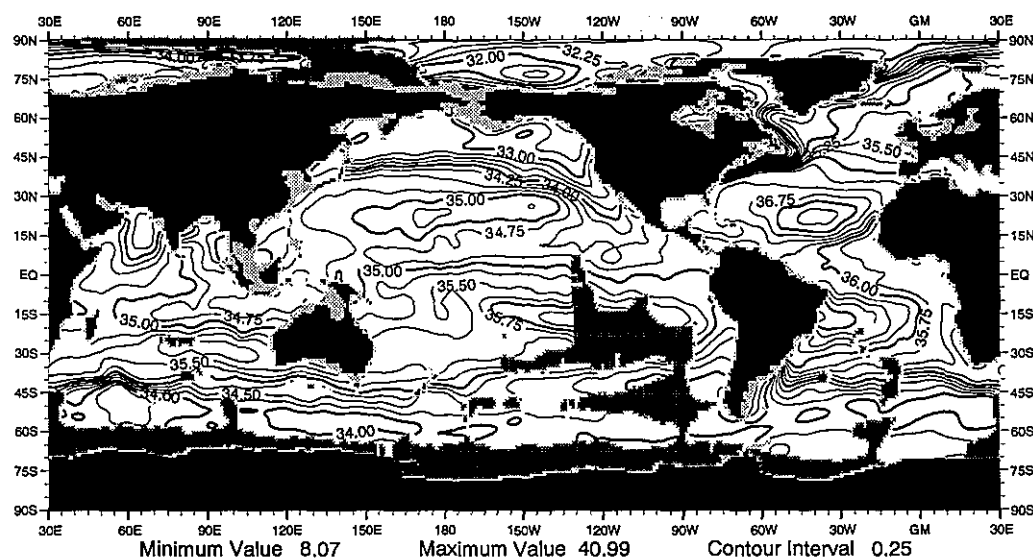


Fig. G15 Summer (Jul.-Sep.) mean salinity (psu) at 75 m depth

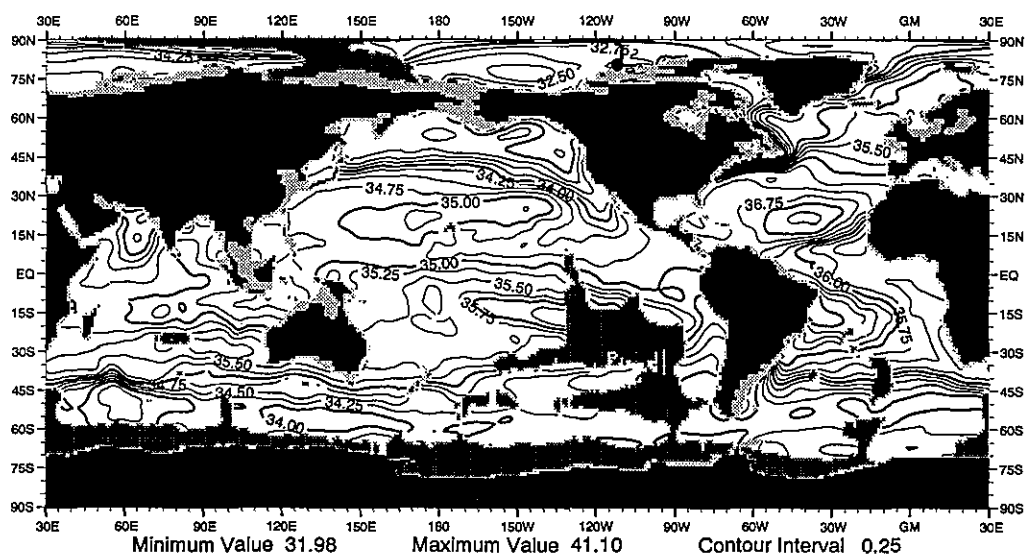


Fig. G16 Summer (Jul.-Sep.) mean salinity (psu) at 100 m depth

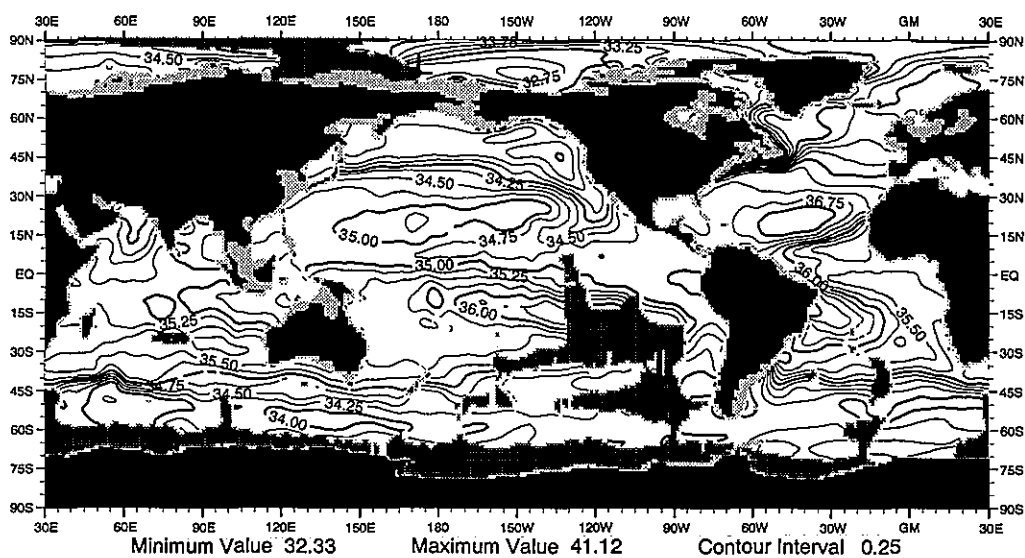


Fig. G17 Summer (Jul.-Sep.) mean salinity (psu) at 125 m depth

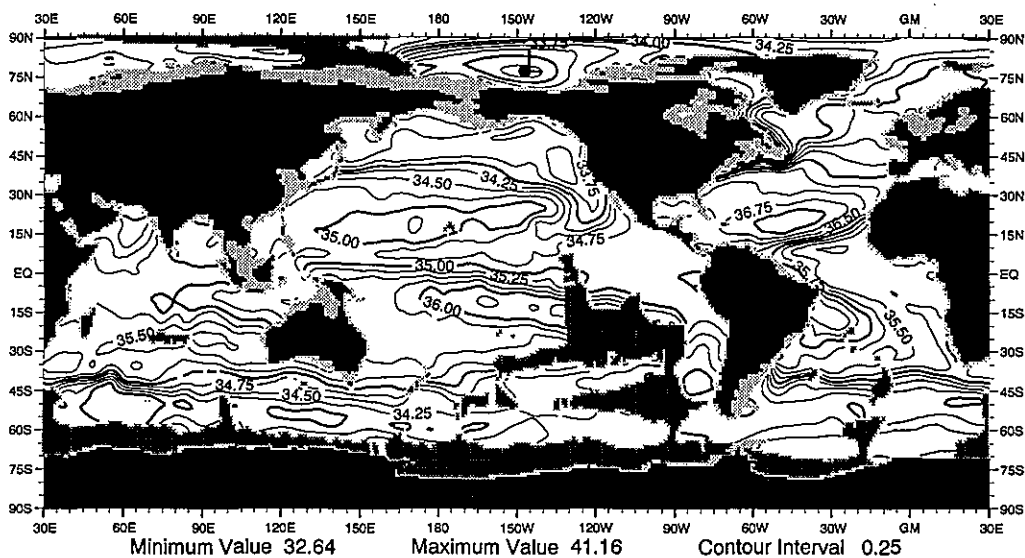


Fig. G18 Summer (Jul.-Sep.) mean salinity (psu) at 150 m depth

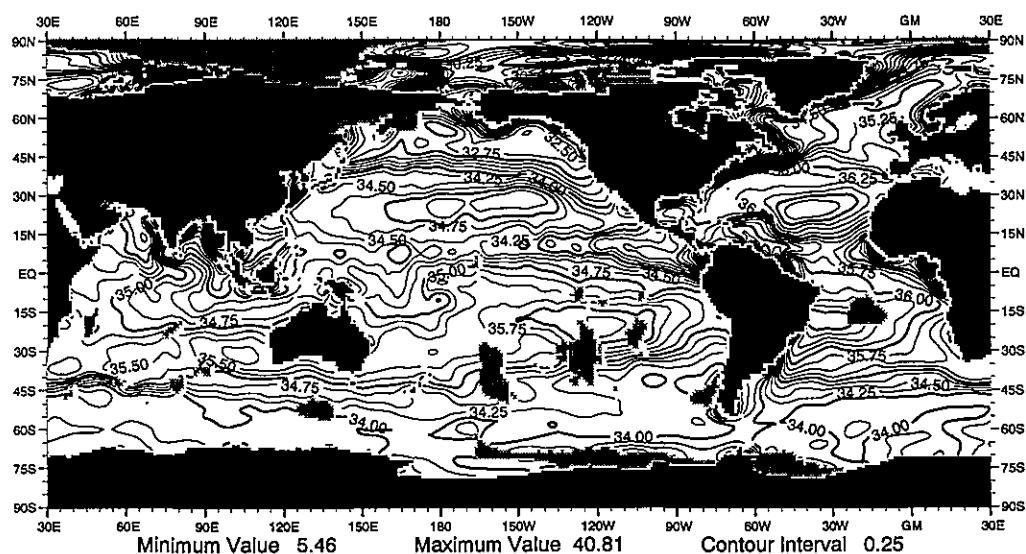


Fig. G19 Fall (Oct.-Dec.) mean salinity (psu) at the surface

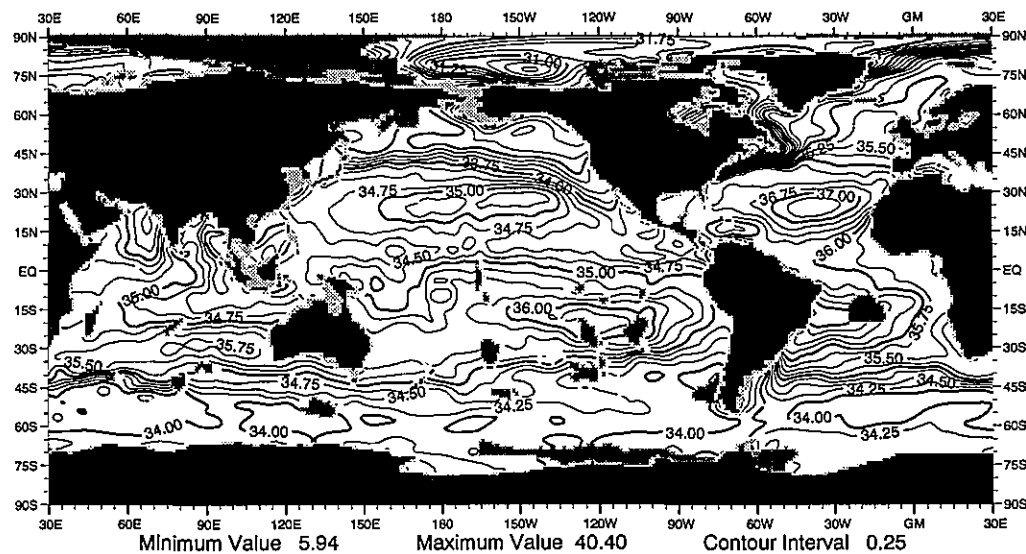


Fig. G20 Fall (Oct.-Dec.) mean salinity (psu) at 50 m depth

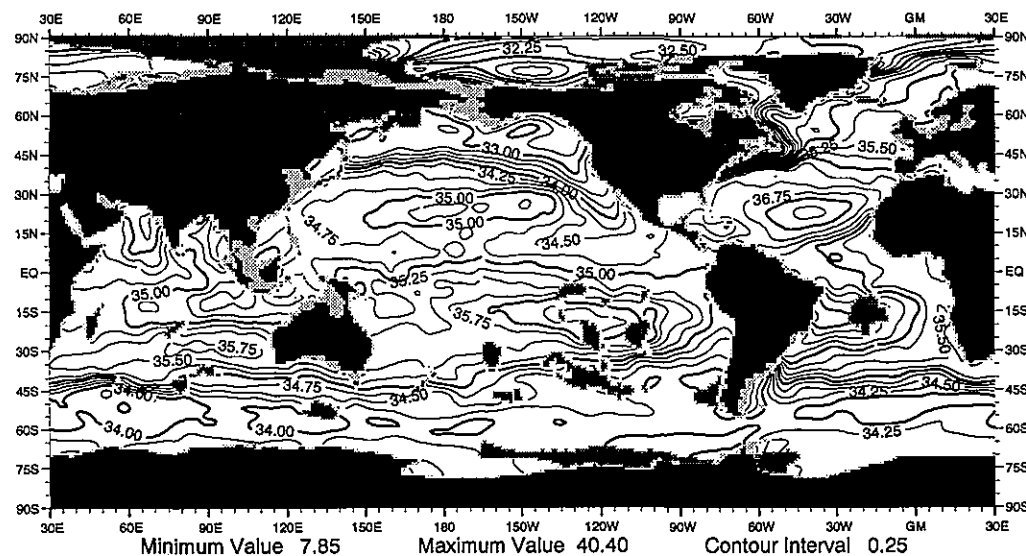


Fig. G21 Fall (Oct.-Dec.) mean salinity (psu) at 75 m depth

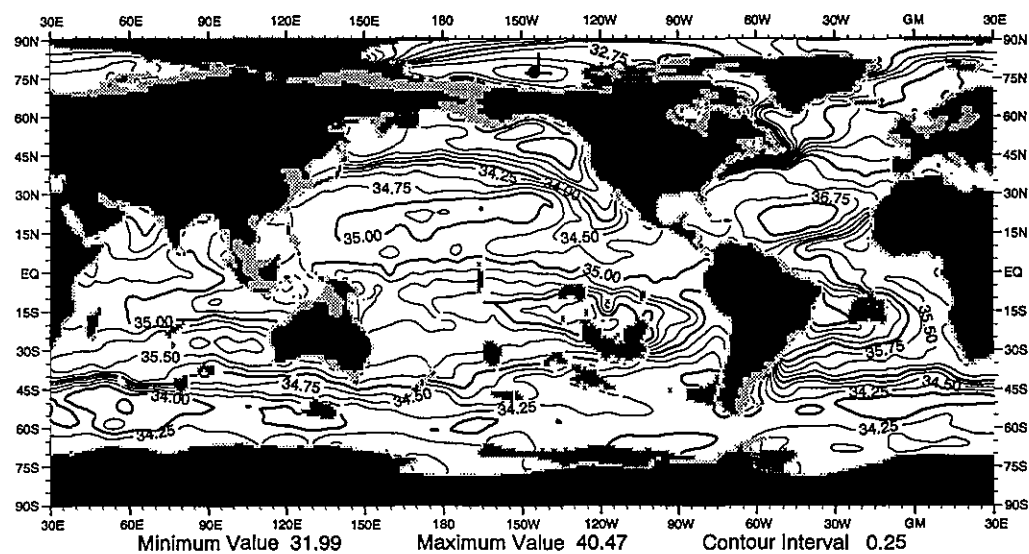


Fig. G22 Fall (Oct.-Dec.) mean salinity (psu) at 100 m depth

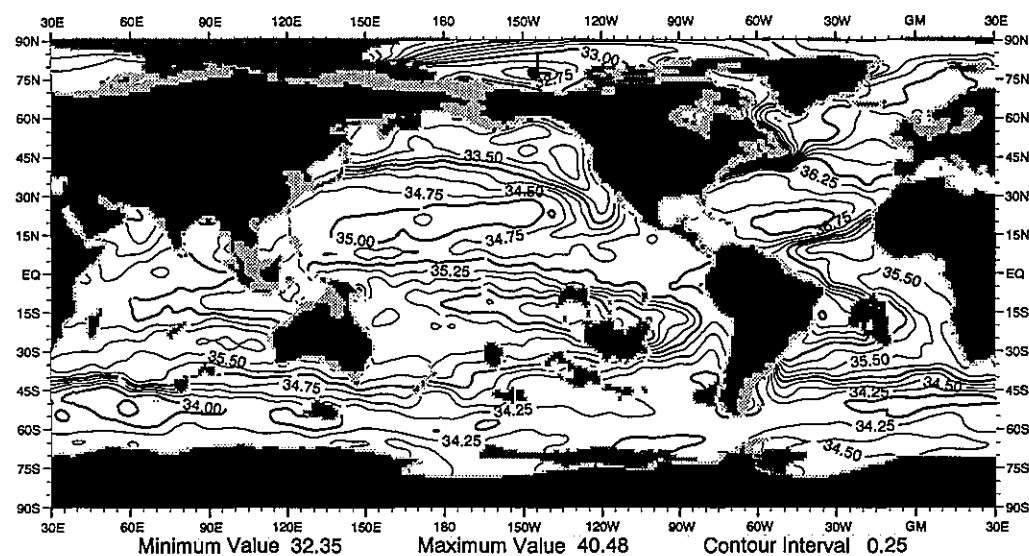


Fig. G23 Fall (Oct.-Dec.) mean salinity (psu) at 125 m depth

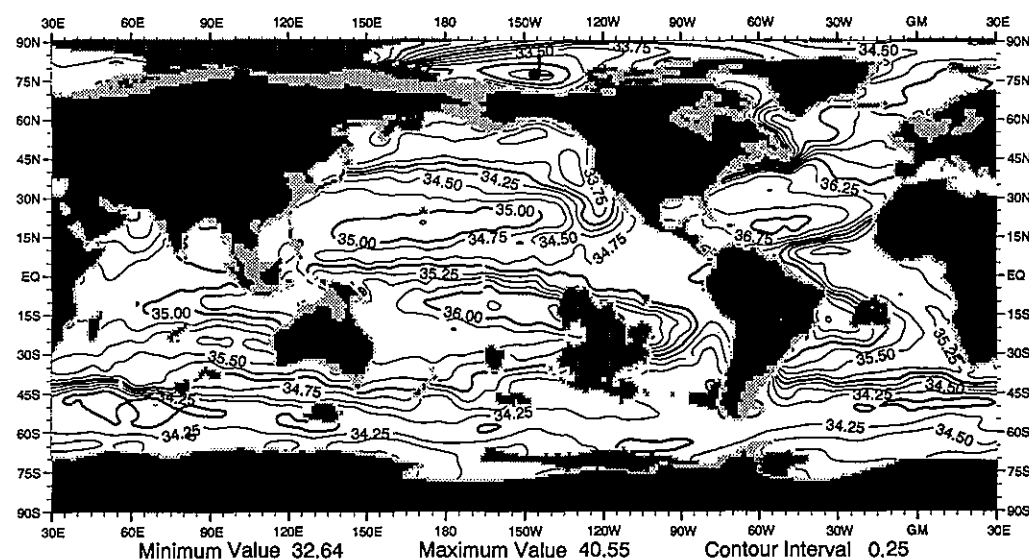


Fig. G24 Fall (Oct.-Dec.) mean salinity (psu) at 150 m depth

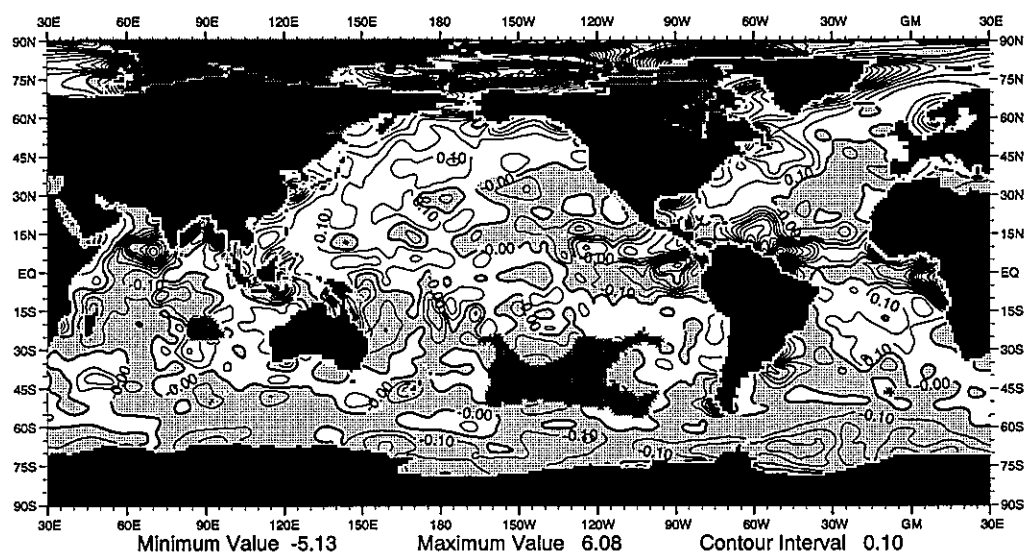


Fig. H1 Winter (Jan.-Mar.) minus annual mean salinity (psu) at the surface

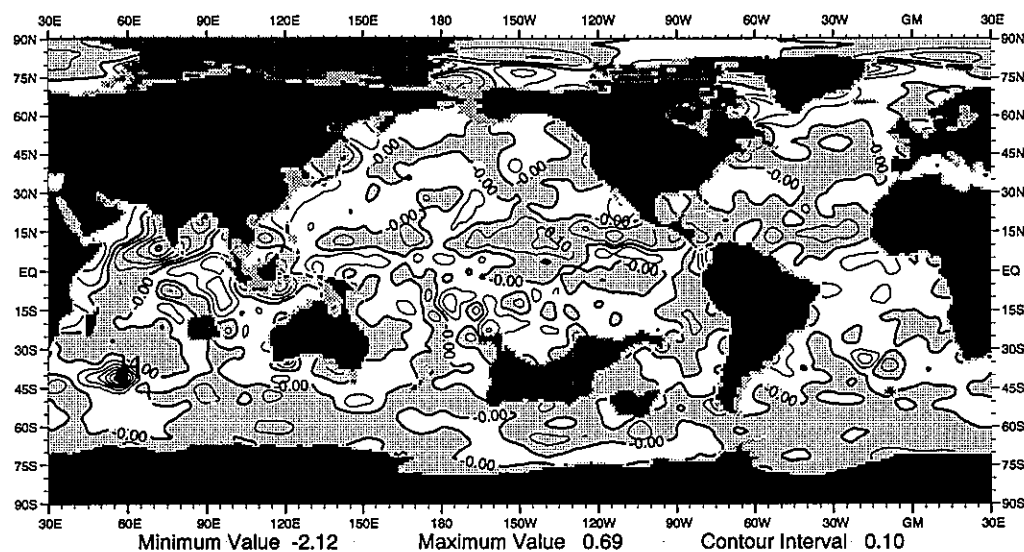


Fig. H2 Winter (Jan.-Mar.) minus annual mean salinity (psu) at 50 m depth

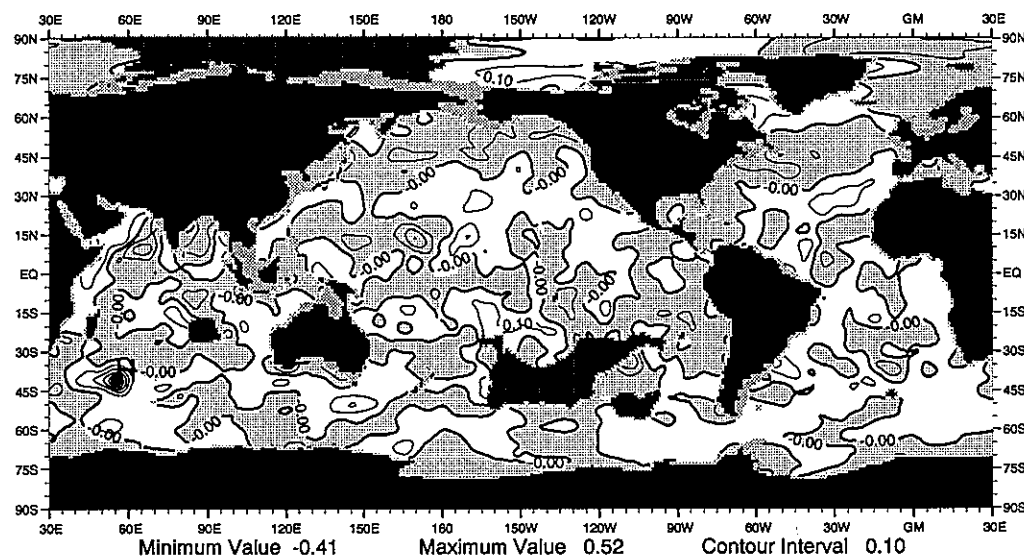


Fig. H3 Winter (Jan.-Mar.) minus annual mean salinity (psu) at 100 m depth



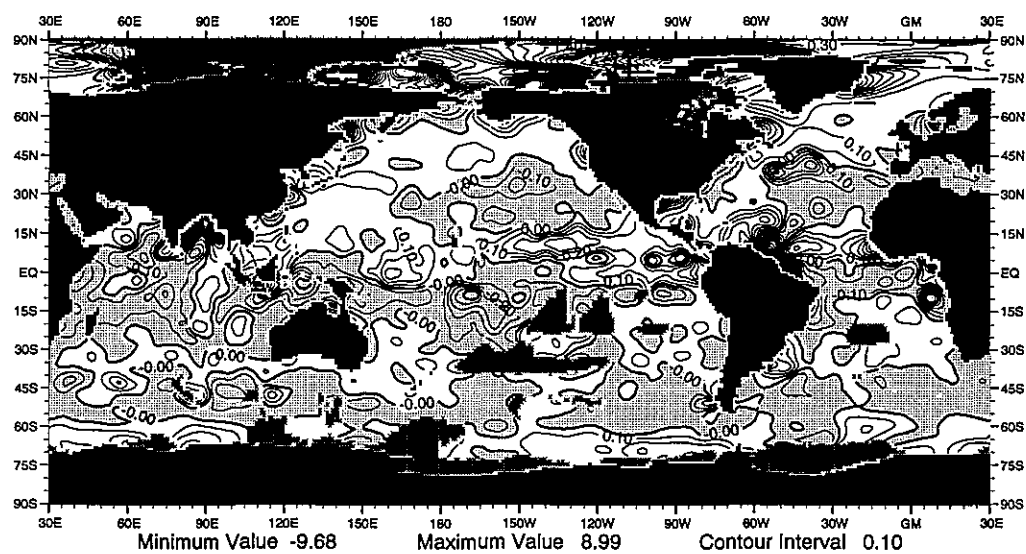


Fig. H4 Spring (Apr.-Jun.) minus annual mean salinity (psu) at the surface

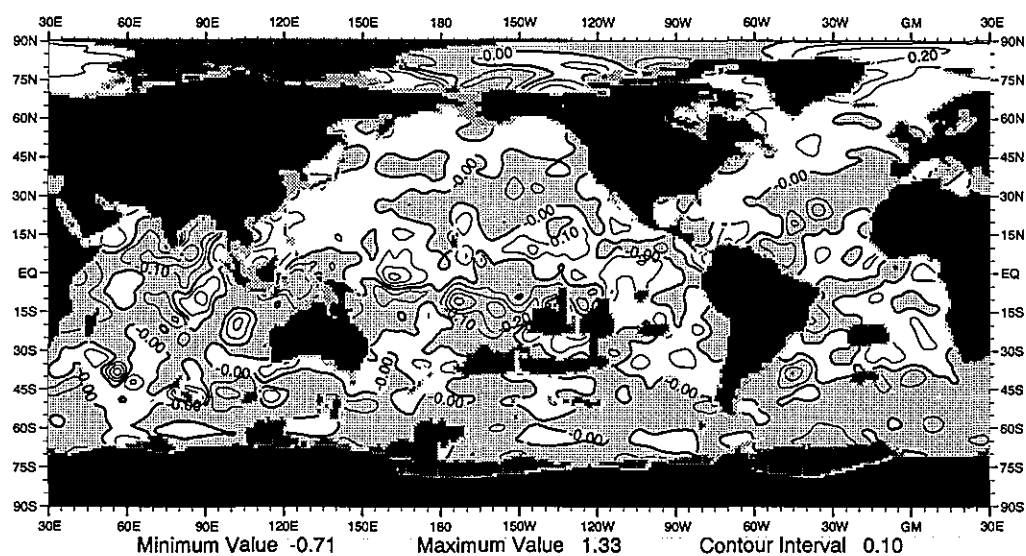


Fig. H5 Spring (Apr.-Jun.) minus annual mean salinity (psu) at 50 m depth

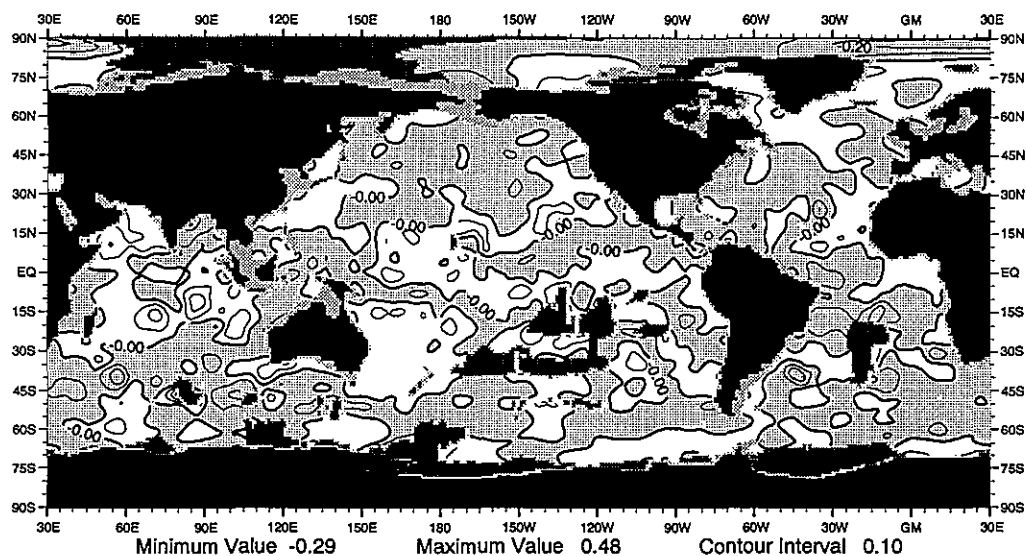


Fig. H6 Spring (Apr.-Jun.) minus annual mean salinity (psu) at 100 m depth

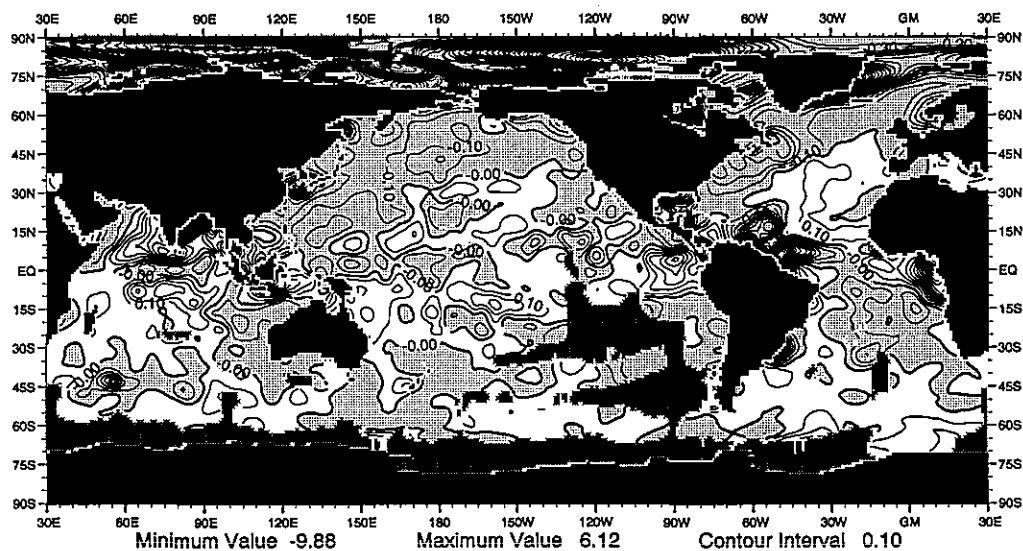


Fig. H7 Summer (Jul.-Sep.) minus annual mean salinity (psu) at the surface

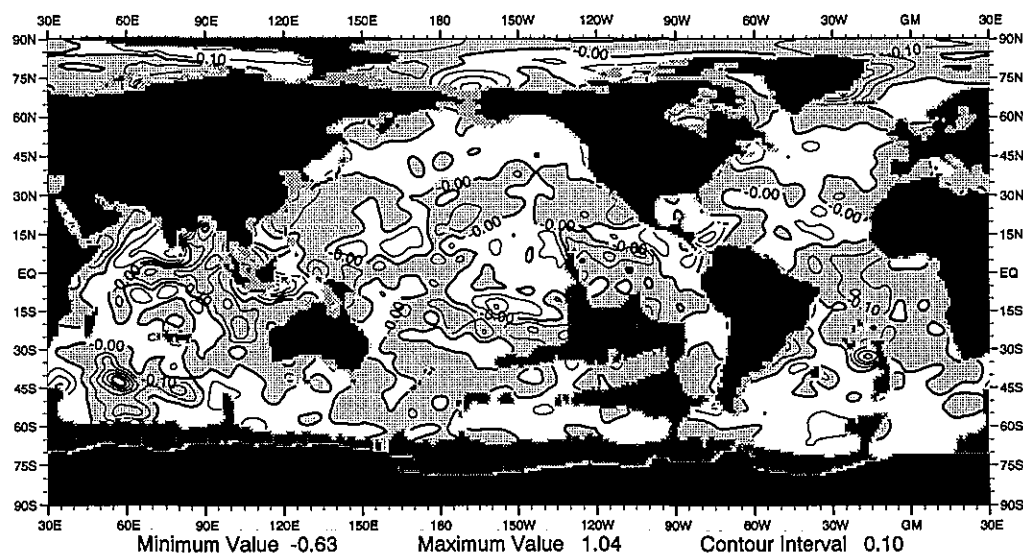


Fig. H8 Summer (Jul.-Sep.) minus annual mean salinity (psu) at 50 m depth

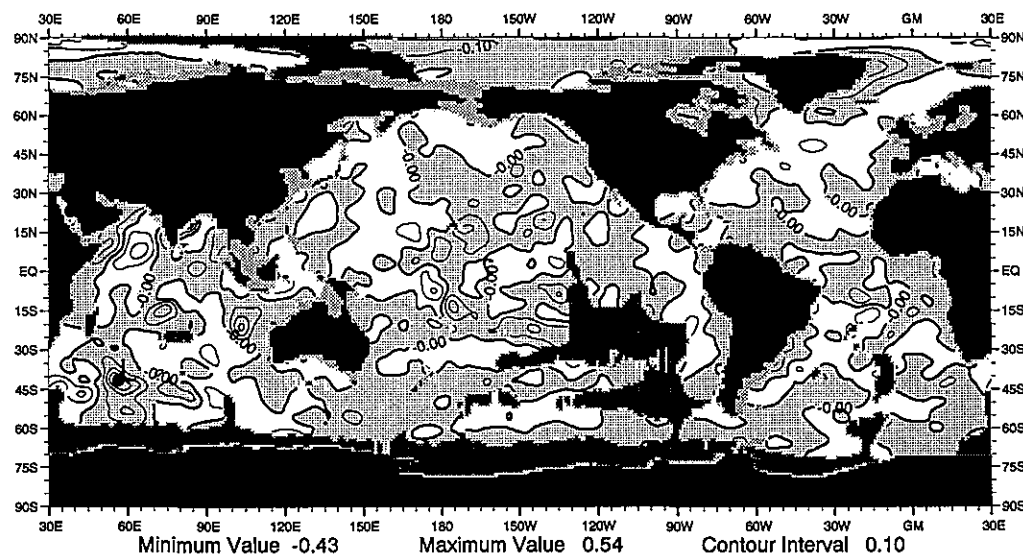


Fig. H9 Summer (Jul.-Sep.) minus annual mean salinity (psu) at 100 m depth

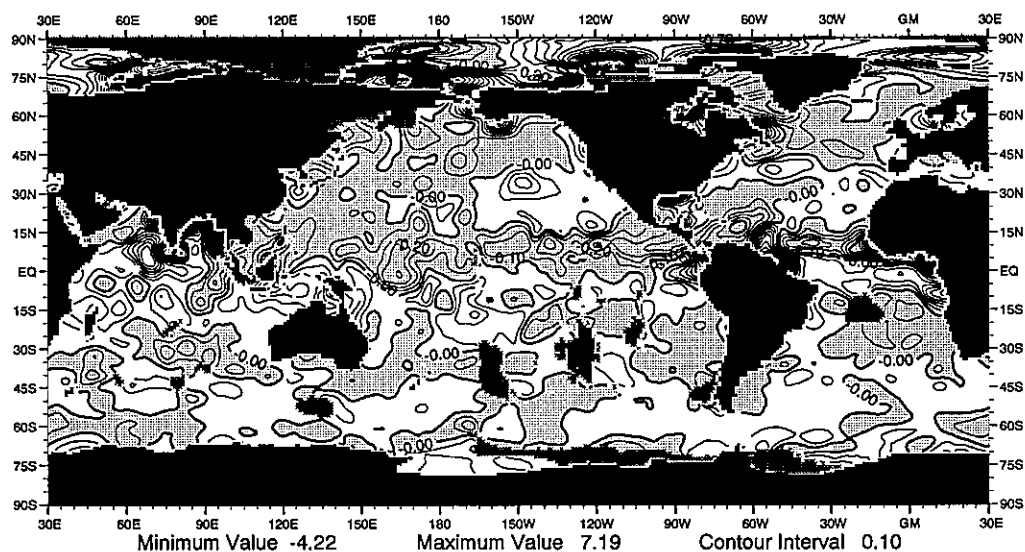


Fig. H10 Fall (Oct.-Dec.) minus annual mean salinity (psu) at the surface

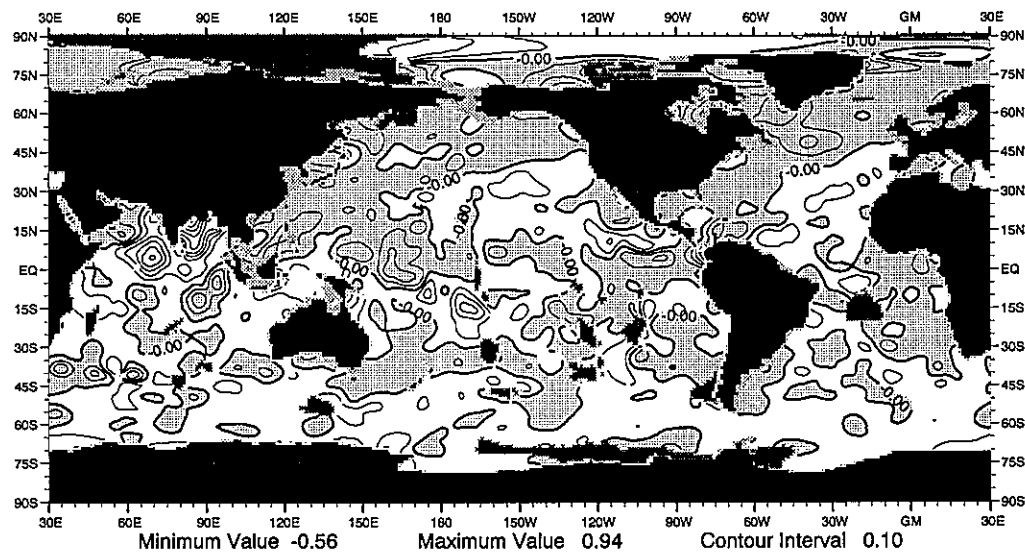


Fig. H11 Fall (Oct.-Dec.) minus annual mean salinity (psu) at 50 m depth

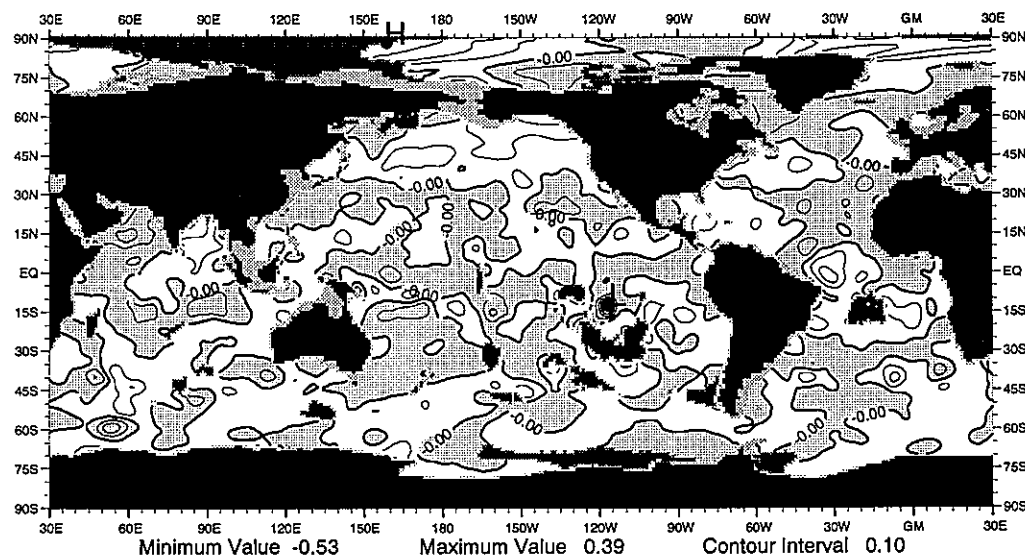


Fig. H12 Fall (Oct.-Dec.) minus annual mean salinity (psu) at 100 m depth

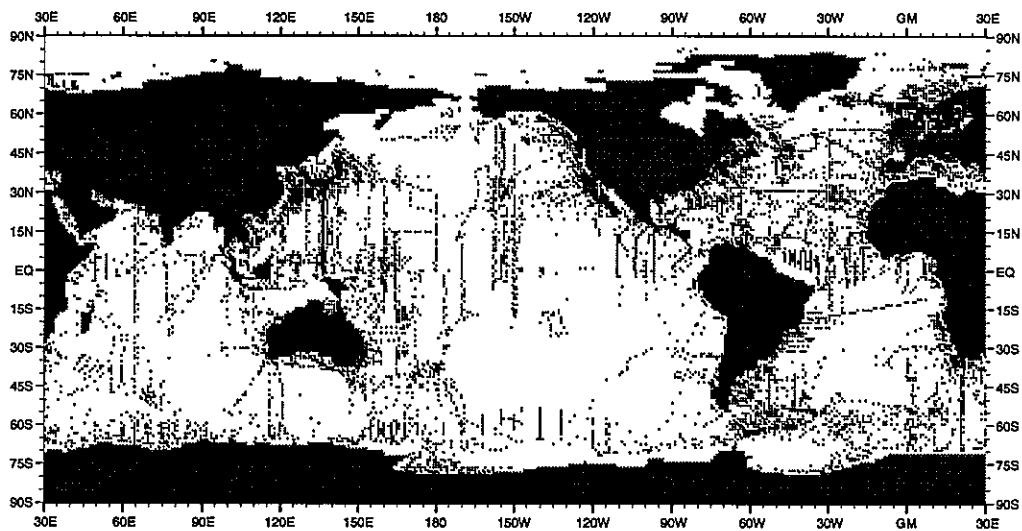


Fig. I1 January distribution of salinity observations at the surface

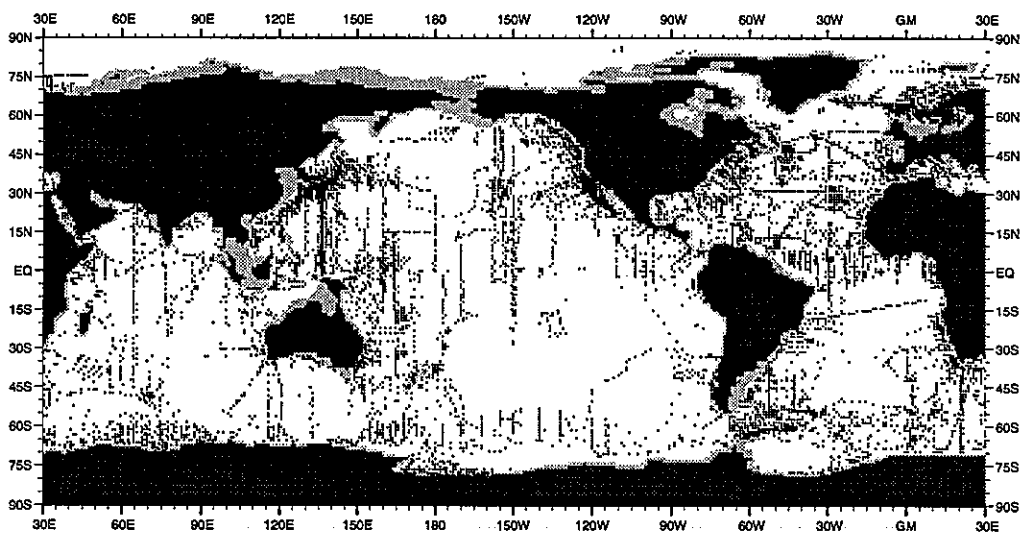


Fig. I2 January distribution of salinity observations at 125 m depth

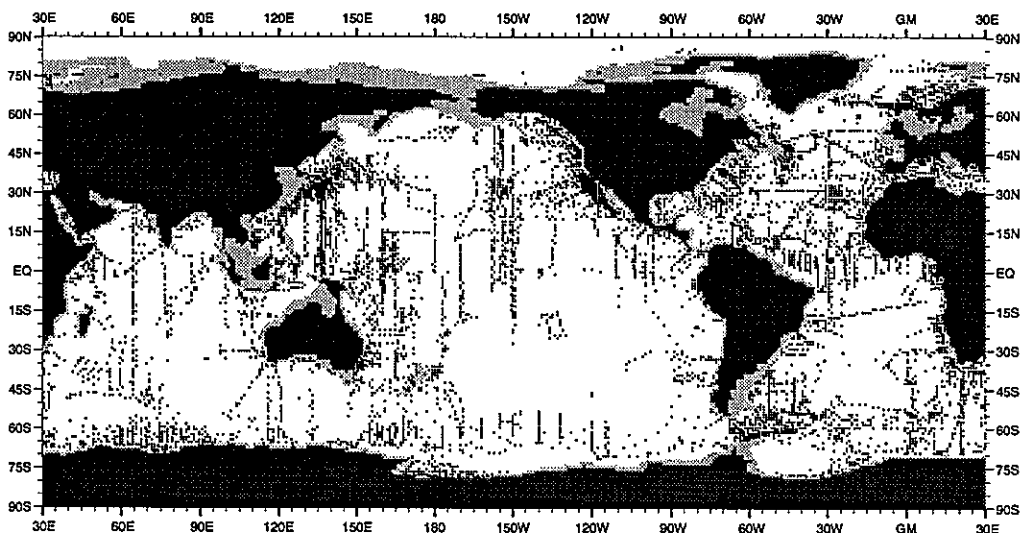


Fig. I3 January distribution of salinity observations at 250 m depth

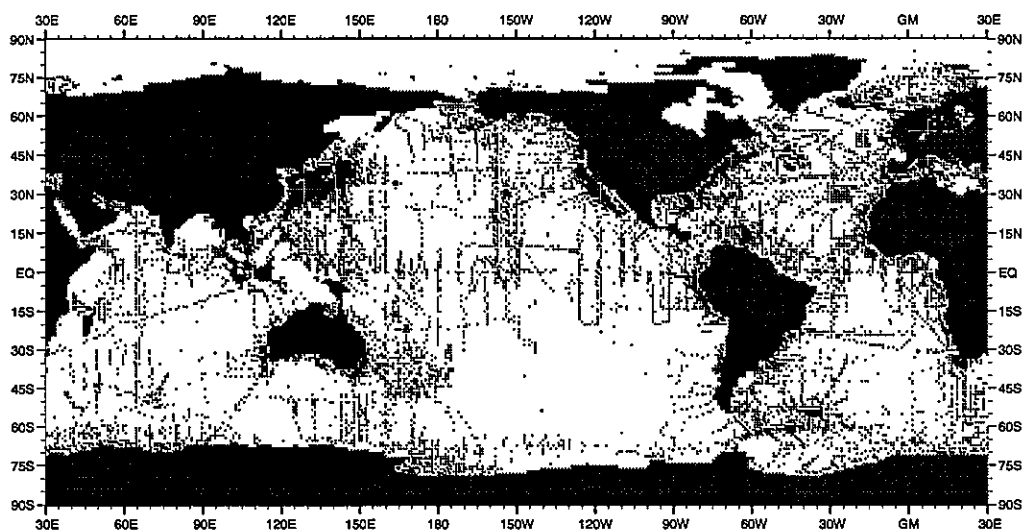


Fig. 14 February distribution of salinity observations at the surface

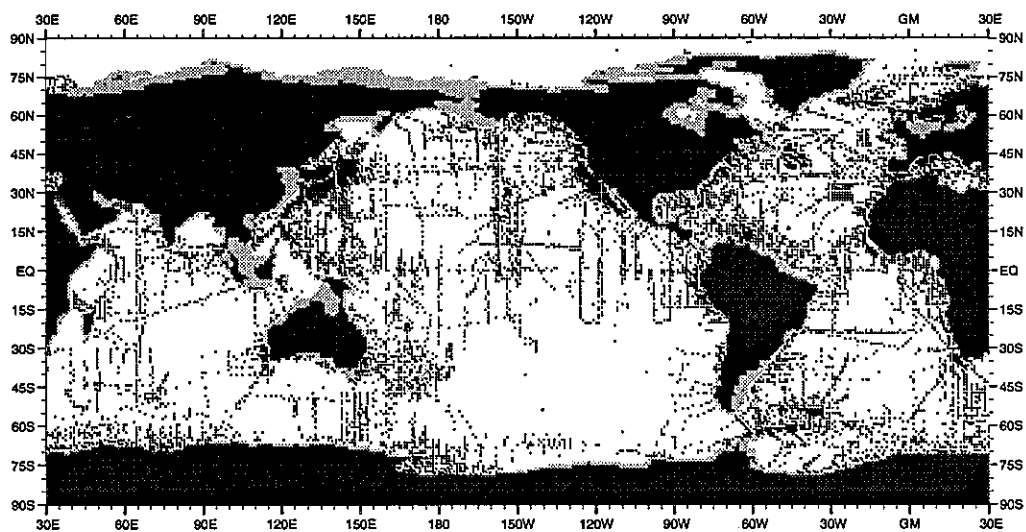


Fig. 15 February distribution of salinity observations at 125 m depth

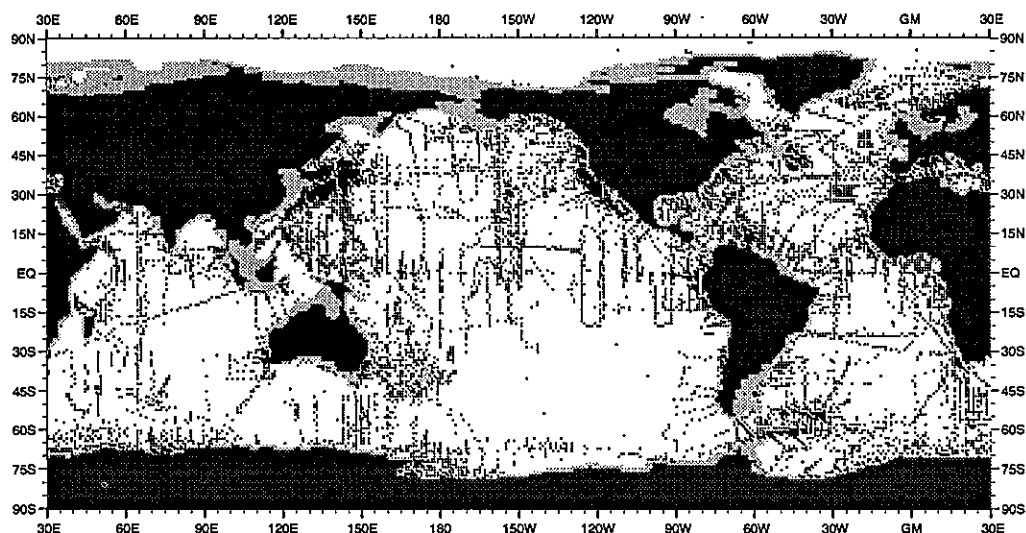


Fig. 16 February distribution of salinity observations at 250 m depth

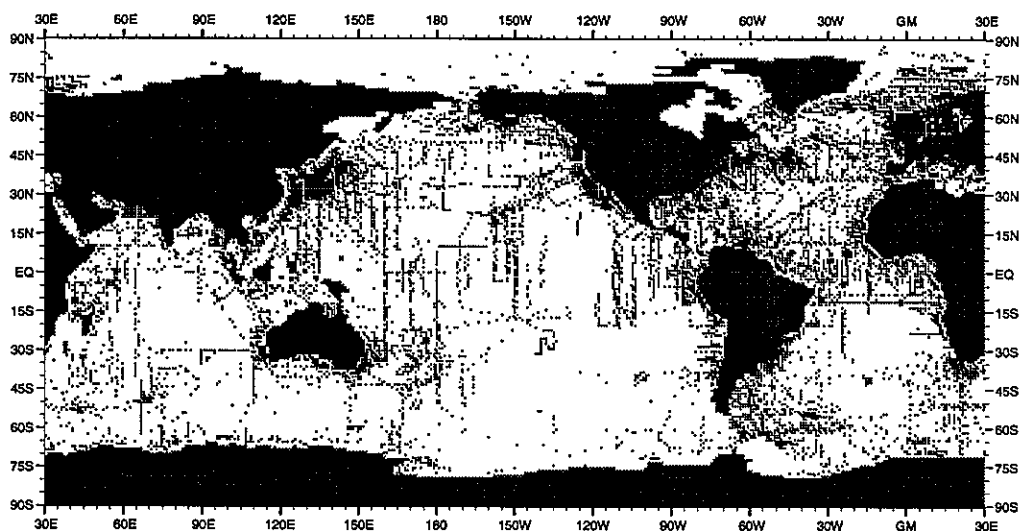


Fig. 17 March distribution of salinity observations at the surface

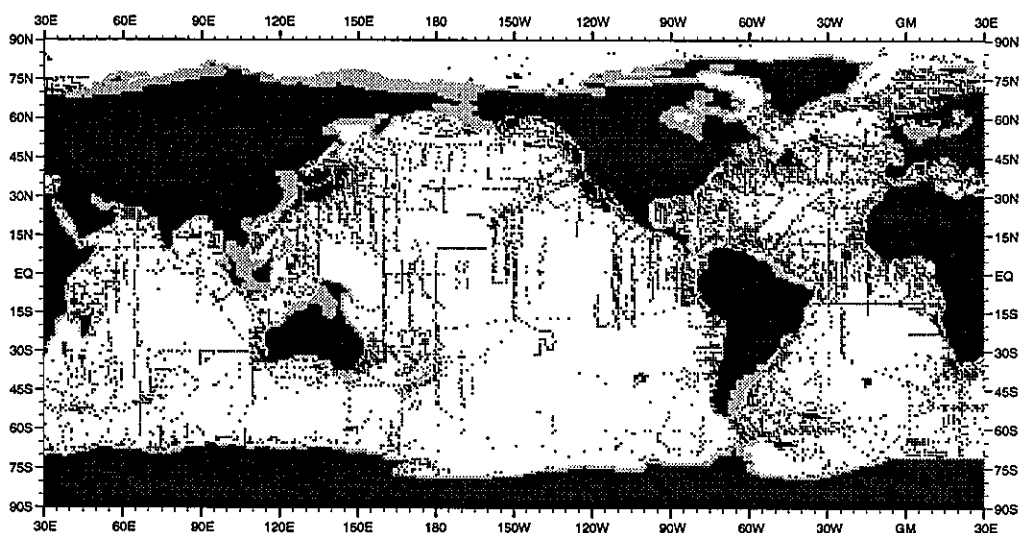


Fig. 18 March distribution of salinity observations at 125 m depth

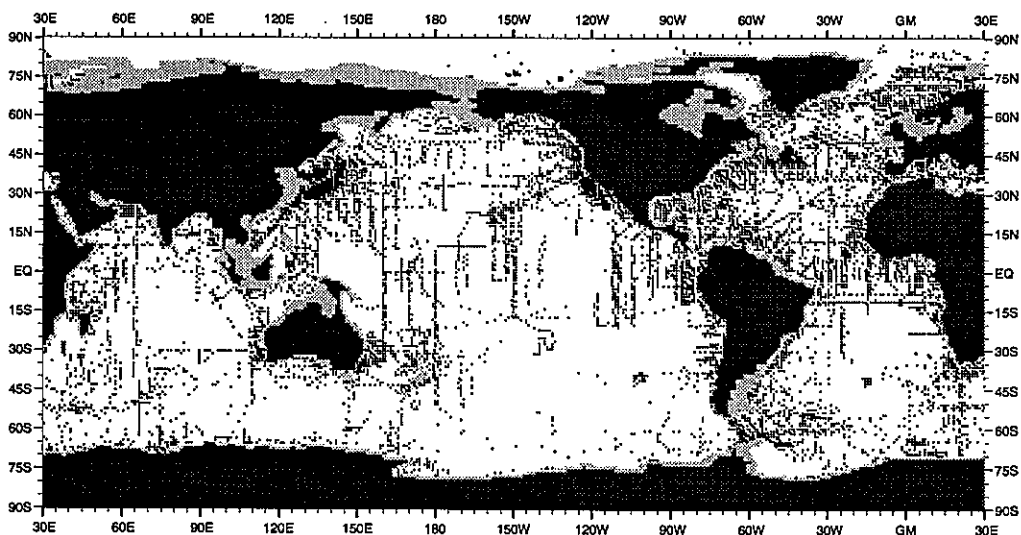


Fig. 19 March distribution of salinity observations at 250 m depth

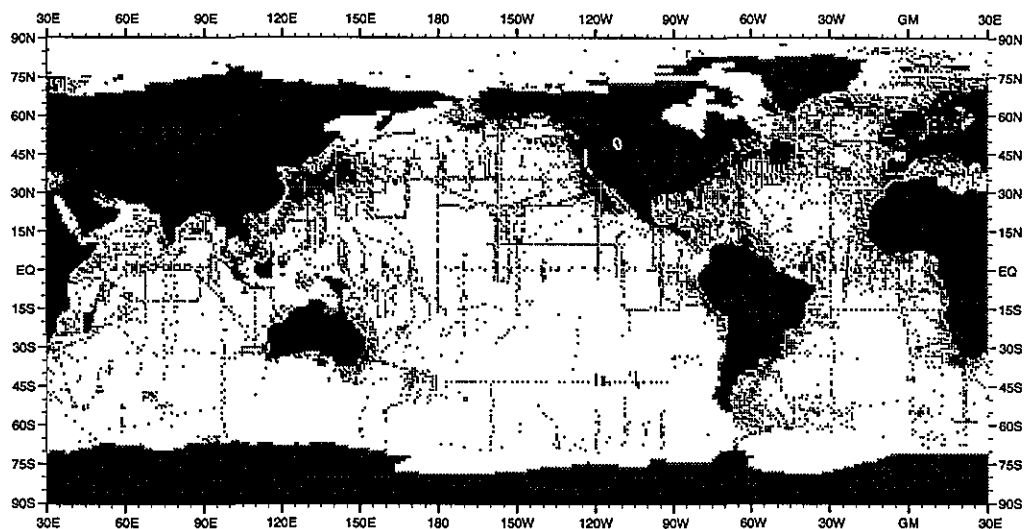


Fig. I10 April distribution of salinity observations at the surface

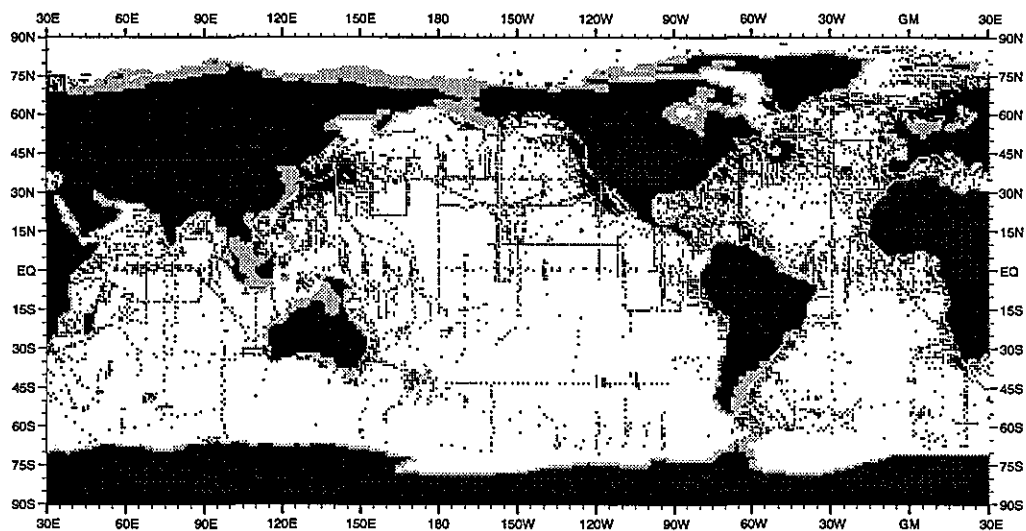


Fig. I11 April distribution of salinity observations at 125 m depth

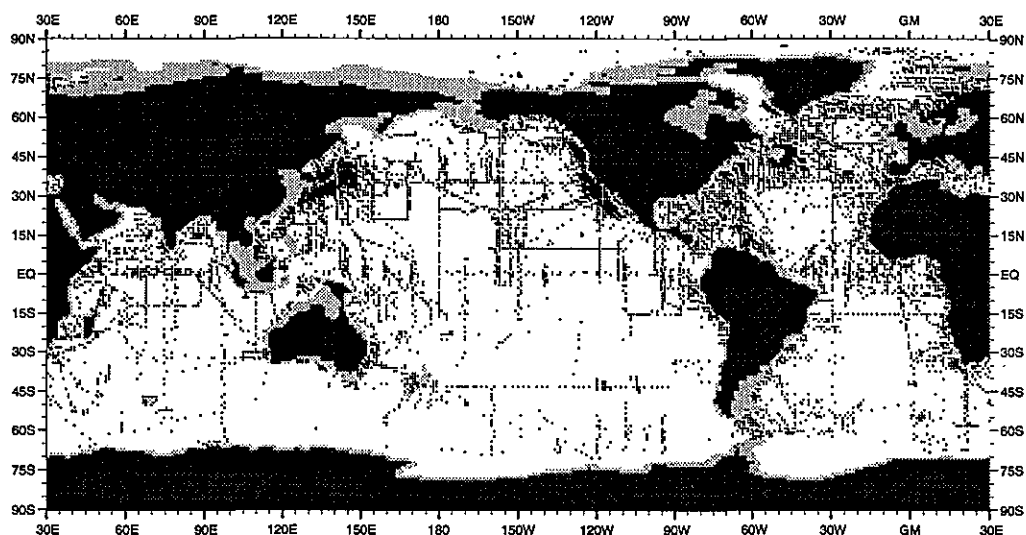


Fig. I12 April distribution of salinity observations at 250 m depth

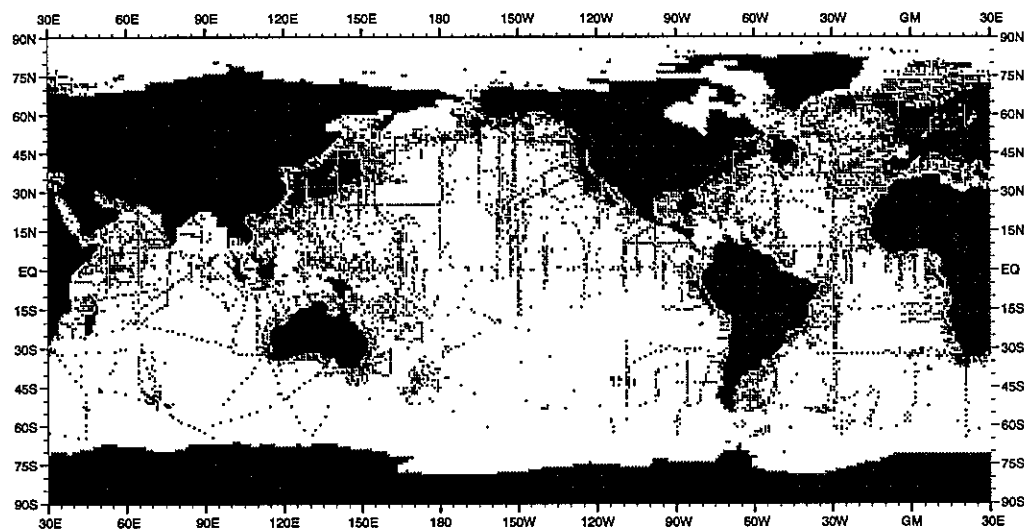


Fig. I13 May distribution of salinity observations at the surface

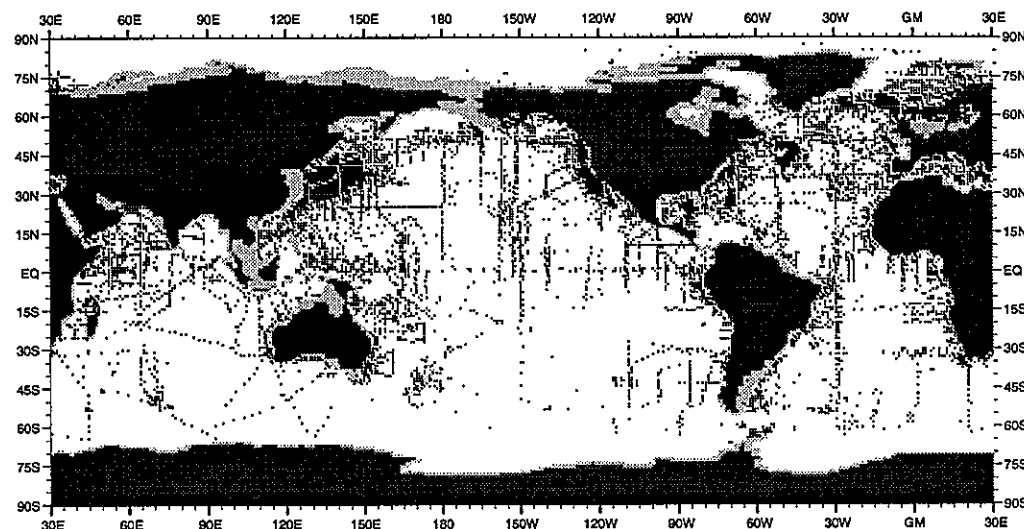


Fig. I14 May distribution of salinity observations at 125 m depth

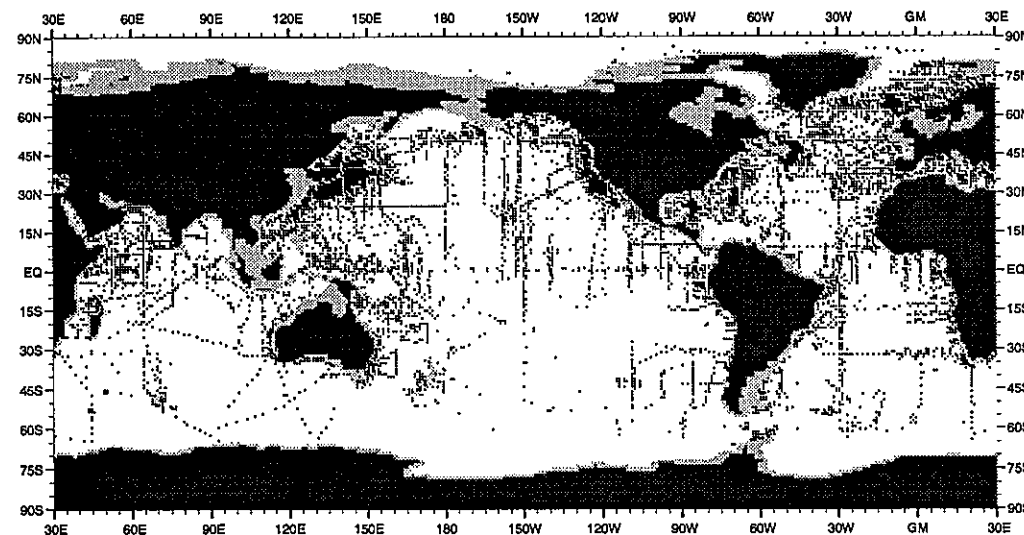


Fig. I15 May distribution of salinity observations at 250 m depth



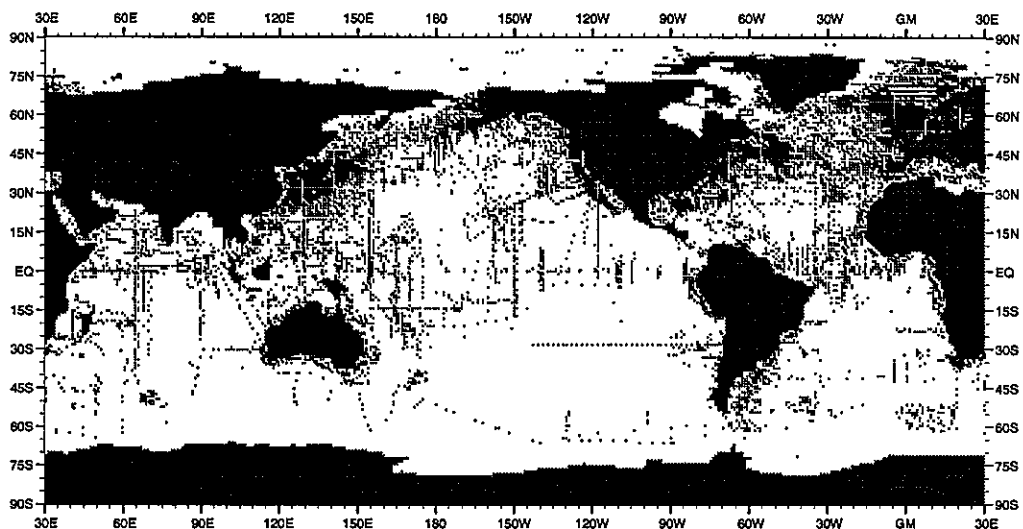


Fig. I16 June distribution of salinity observations at the surface

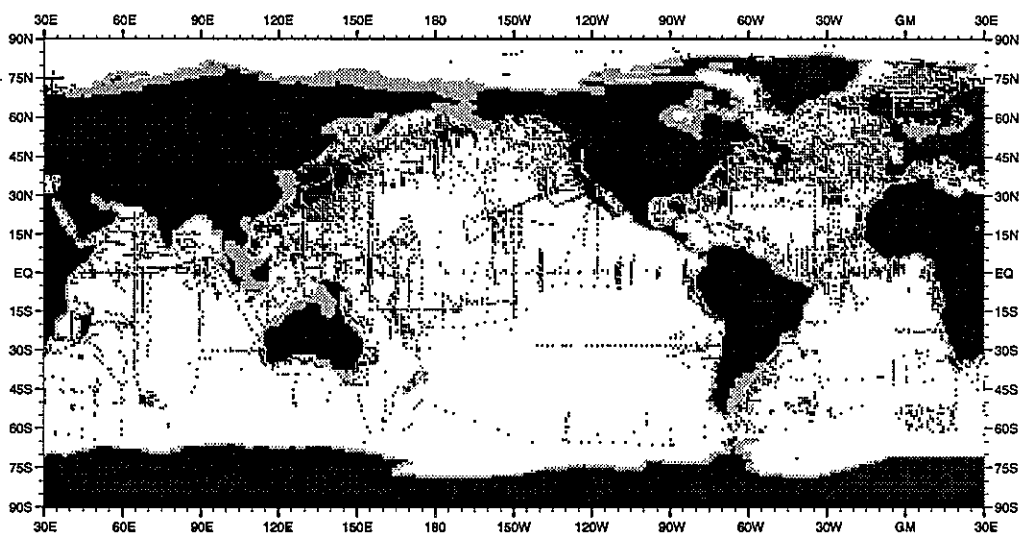


Fig. I17 June distribution of salinity observations at 125 m depth

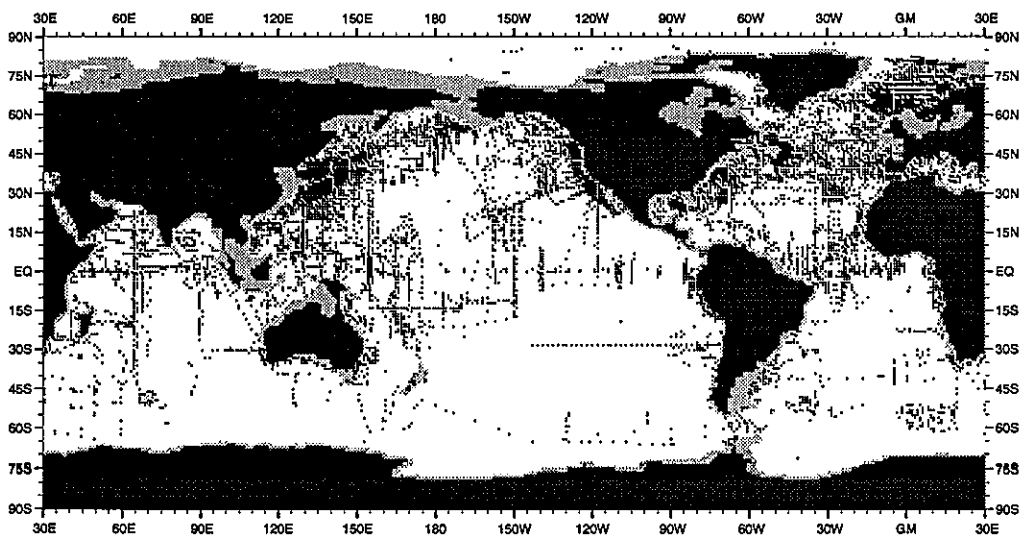


Fig. I18 June distribution of salinity observations at 250 m depth

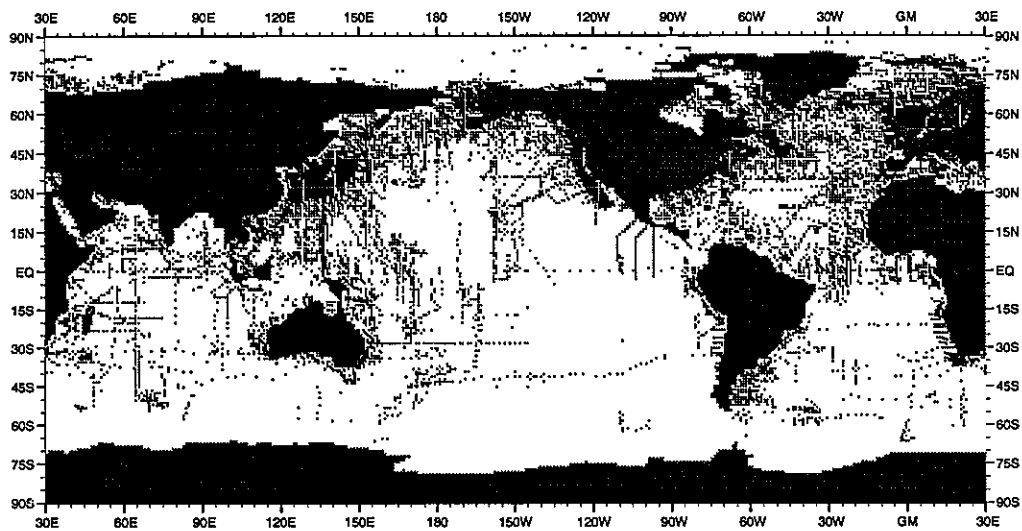


Fig. 119 July distribution of salinity observations at the surface

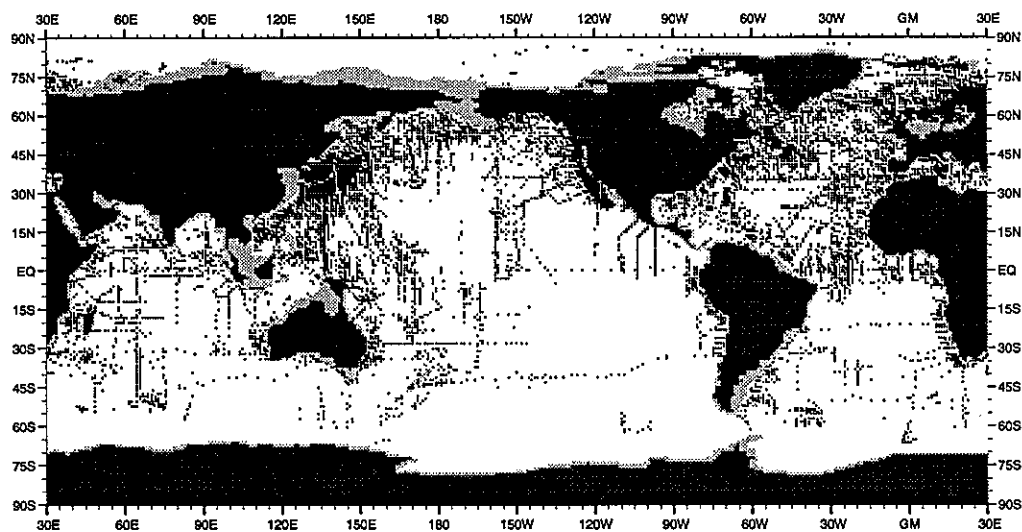


Fig. 120 July distribution of salinity observations at 125 m depth

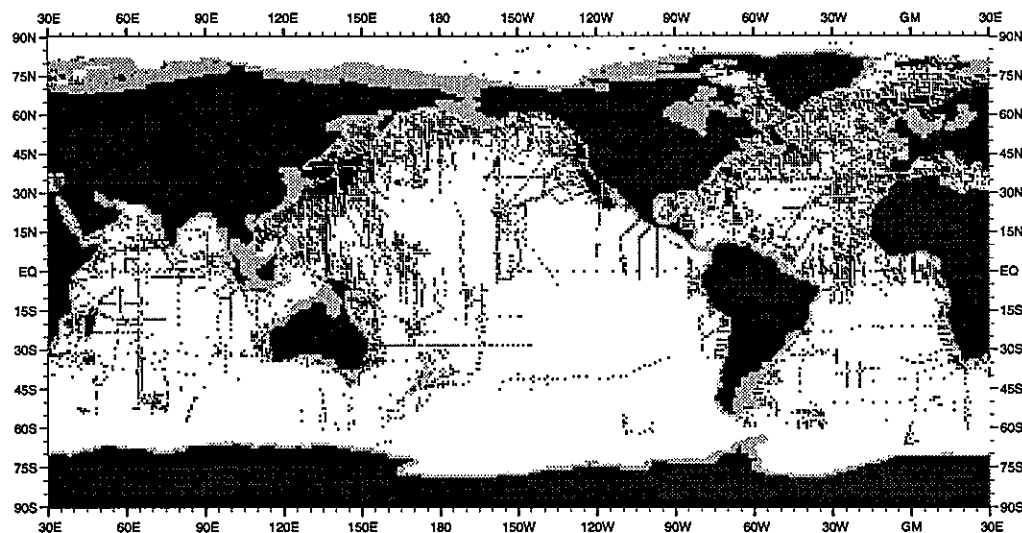


Fig. 121 July distribution of salinity observations at 250 m depth

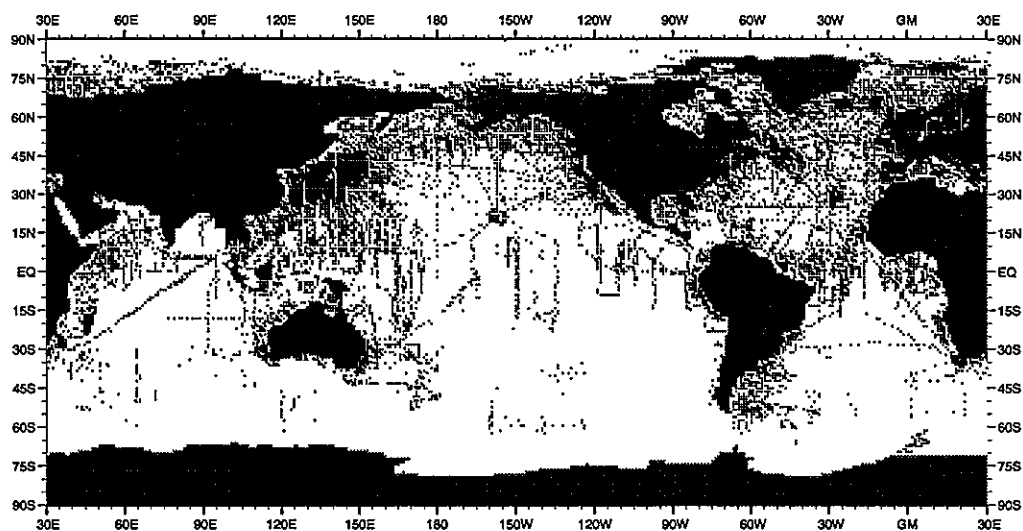


Fig. I22 August distribution of salinity observations at the surface

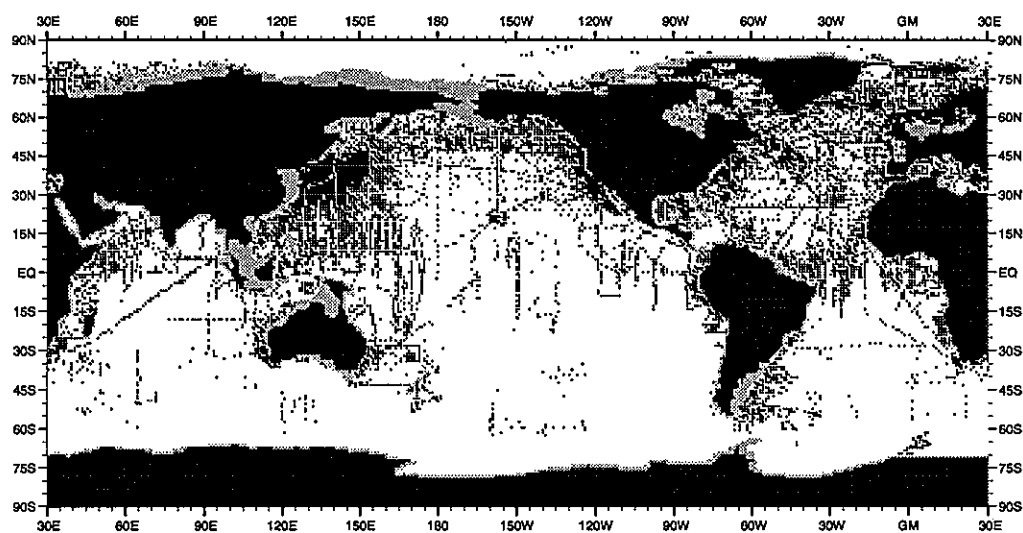


Fig. I23 August distribution of salinity observations at 125 m depth

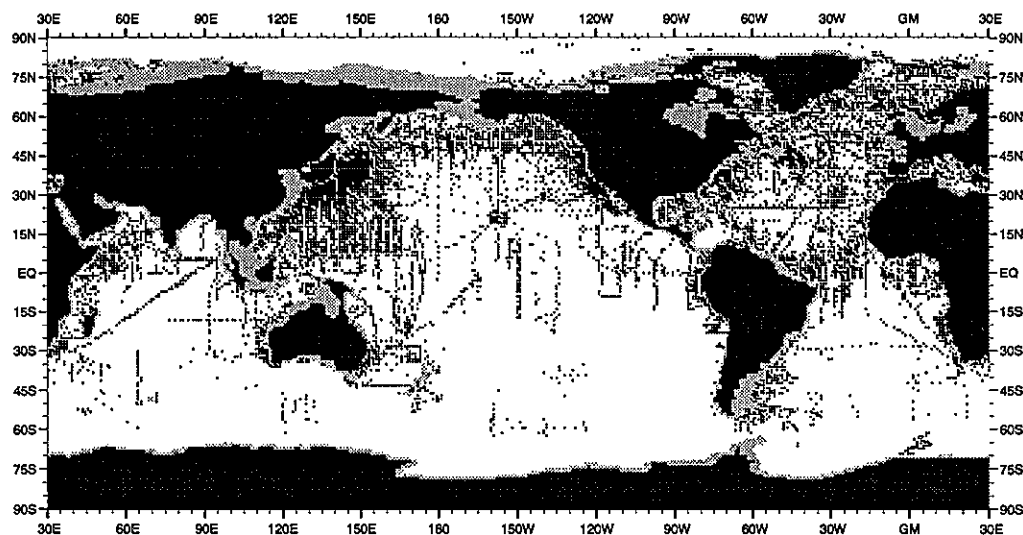


Fig. I24 August distribution of salinity observations at 250 m depth

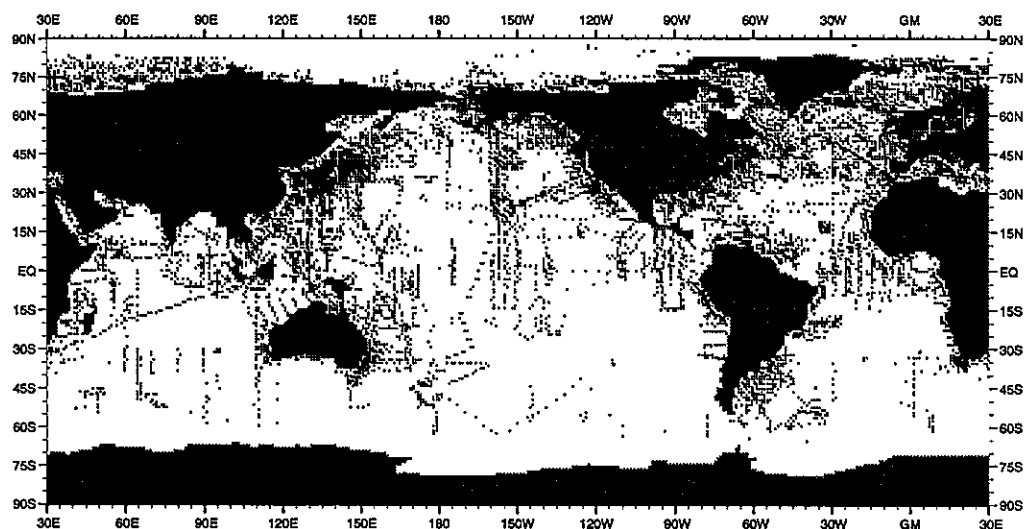


Fig. I25 September distribution of salinity observations at the surface

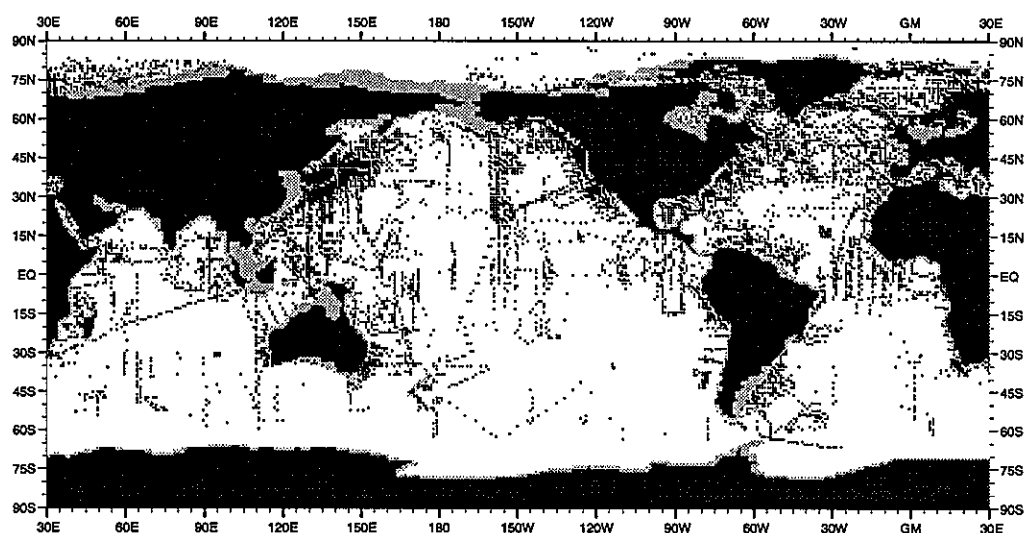


Fig. I26 September distribution of salinity observations at 125 m depth

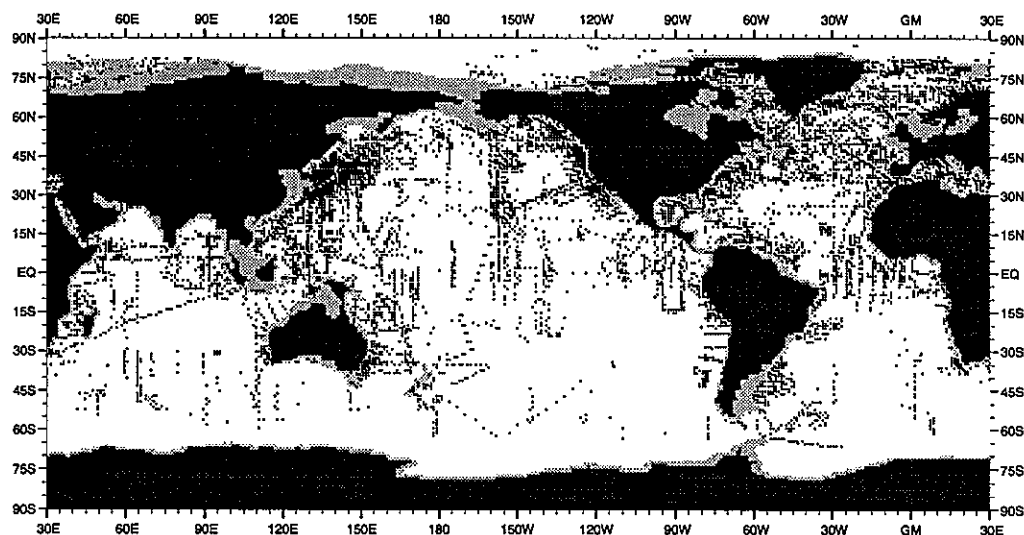


Fig. I27 September distribution of salinity observations at 250 m depth

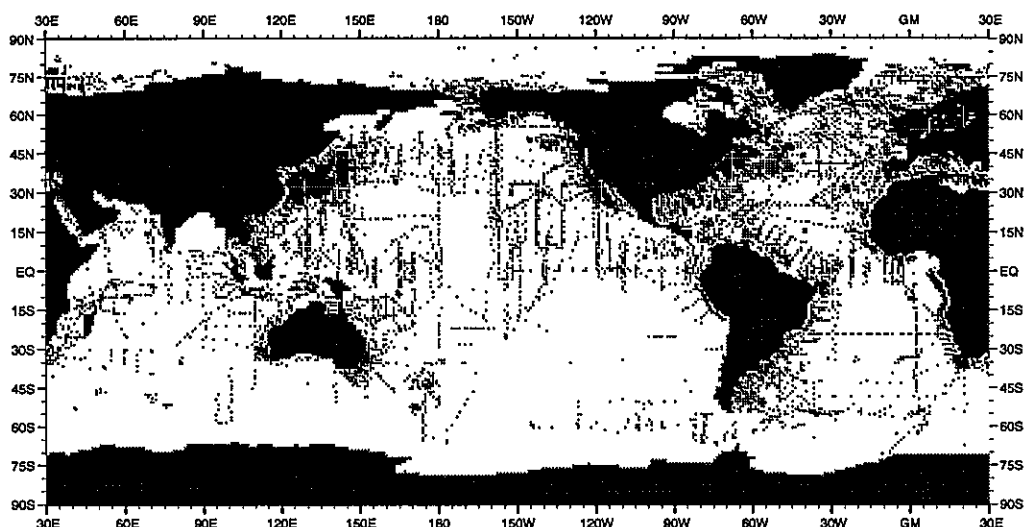


Fig. I28 October distribution of salinity observations at the surface

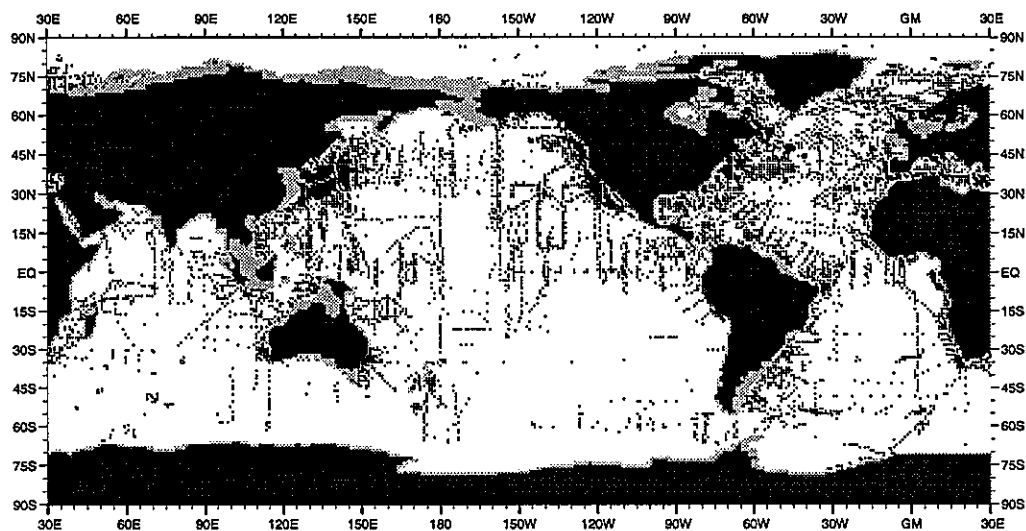


Fig. I29 October distribution of salinity observations at 125 m depth

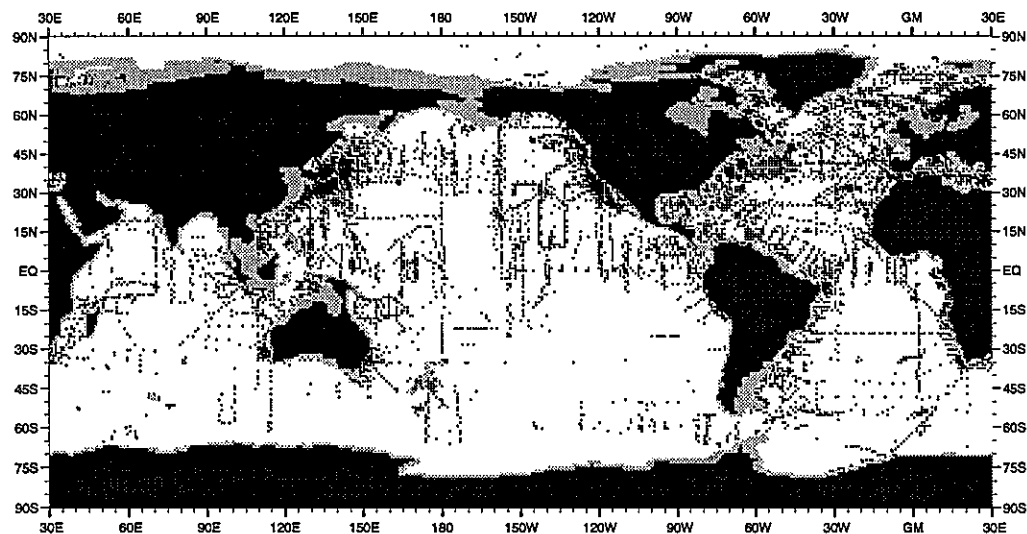


Fig. I30 October distribution of salinity observations at 250 m depth

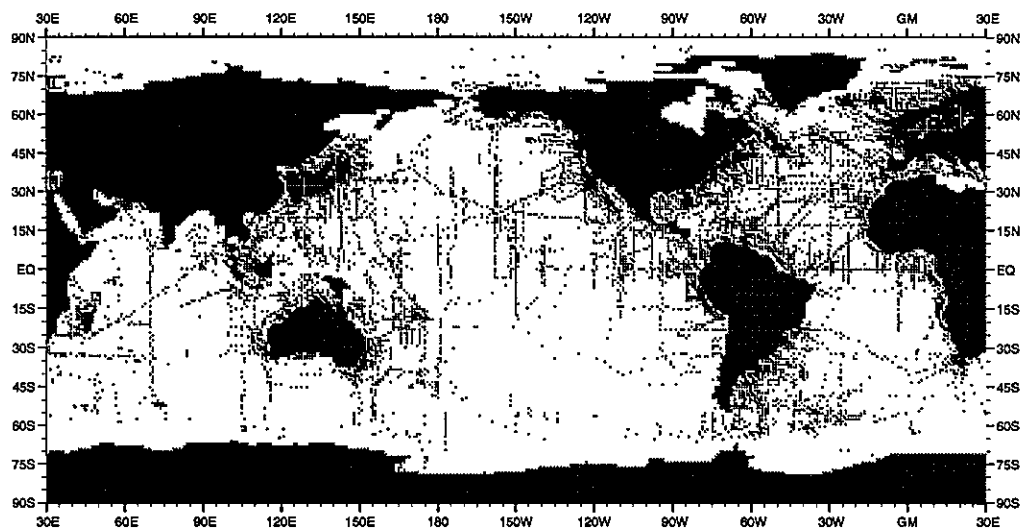


Fig. I31 November distribution of salinity observations at the surface

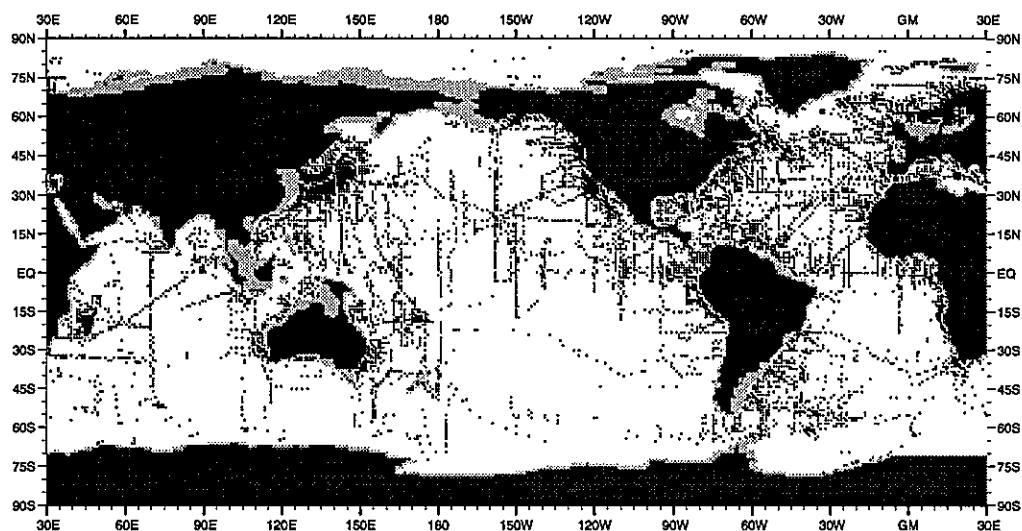


Fig. I32 November distribution of salinity observations at 125 m depth

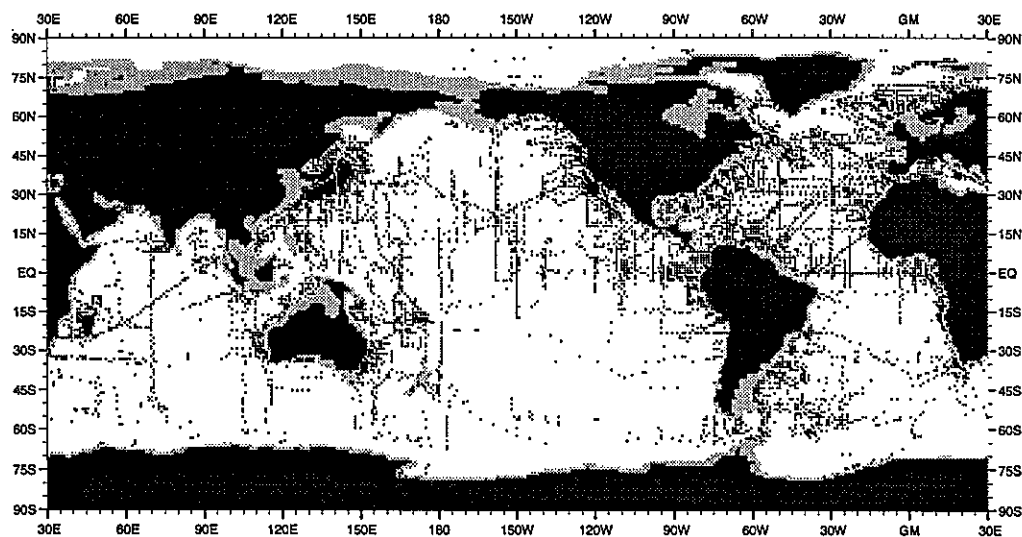


Fig. I33 November distribution of salinity observations at 250 m depth

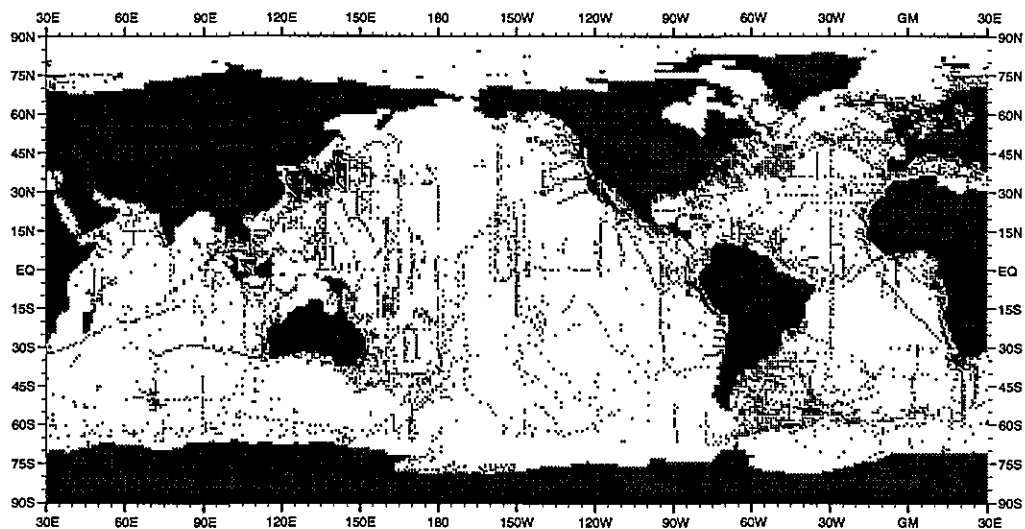


Fig. I34 December distribution of salinity observations at the surface

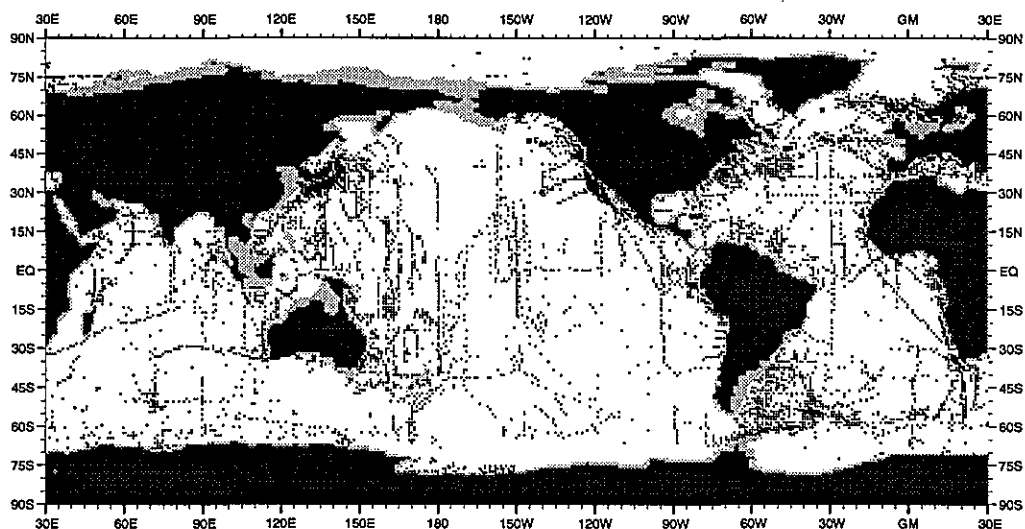


Fig. I35 December distribution of salinity observations at 125 m depth

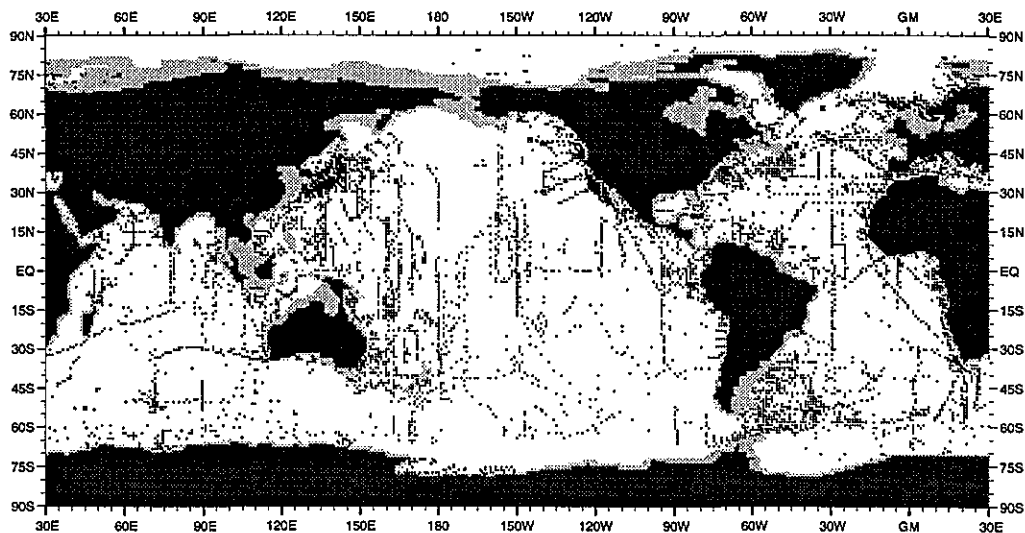


Fig. I36 December distribution of salinity observations at 250 m depth

ISBN 0-16-043200-6



9 780160 432002